UNIVERSITY OF HAWAII
LIBRARY
SEP 11 1957

ADVANCES IN PHYSICS

A QUARTERLY SUPPLEMENT
of the
PHILOSOPHICAL MAGAZINE

EDITOR
PROFESSOR N. F. MOTT, M.A., D.Sc., F.R.S.

EDITORIAL BOARD
SIR GEORGE THOMSON, M.A., D.Sc., F.R.S.
PROFESSOR A. M. TYNDALL, C.B.E., D.Sc., F.R.S.
SIR LAWRENCE BRAGG, O.B.E., M.C., M.A., D.Sc., F.R.S.

VOLUME 6 JULY 1957 NUMBER 23

PRICE per part £1
PRICE per annum £3 15*s*. 0*d*. post free

PRINTED AND PUBLISHED BY TAYLOR & FRANCIS LTD
RED LION COURT, FLEET ST., LONDON E.C.4

C1
A36

Physics in Medicine and Biology

The Journal of the Hospital Physicists' Association
published in association with the Philosophical Magazine

Editor:
J. E. Roberts, D.Sc.

Consultant Editor:
Professor N. F. Mott, F.R.S.

Editorial Board:
W. A. Langmead, M.Sc.
J. S. Mitchell, C.B.E., F.R.S.
J. Rotblat, D.Sc.
D. A. McDonald, D.M.
G. J. Neary, Ph.D.
F. W. Spiers, D.Sc.
J. F. Tait, Ph.D.

Contents of April, 1957

The Investigation of Haemoglobin and Myoglobin Derivatives by Electron Resonance. By J. E. Bennett, J. F. Gibson, D. J. E. Ingram, Department of Electronics, University of Southampton and Thelma M. Haughton, G. A. Kerkut and K. A. Munday, Department of Physiology, University of Southampton

An Approach to an Analysis of the Arterial Pulse Wave. II. Fluid Oscillations in an Elastic Pipe. By M. G. Taylor, M.D., Physiology Department, St. Bartholomew's Hospital Medical College, London

Average Energy of Allowed Beta-particle Spectra. By R. Loevinger, Ph.D., The André Meyer Department of Physics, The Mount Sinai Hospital, New York 29, N.Y.

The Effects of Degraded Radiation in Thyroid Uptake Measurements. By J. I. Trombka and Fearghus O'Foghludha, From the Medical Division, Oak Ridge Institute of Nuclear Studies, Oak Ridge, Tennessee, under contract with the United States Atomic Energy Commission

The Variation of Scattered X-Rays with Density in an Irradiated Body. By J. E. O'Connor, M.Sc., Saint Luke's Hospital, Dublin

Whole Body X-irradiation of Experimental Animals. A short summary of the methods used at the M.R.C. Radiobiological Research Unit, A.E.R.E., Harwell, between 1949–1956. By M. J. Corp, M.S.R., M.R.C. Radiobiological Research Unit, A.E.R.E., Harwell

Subscription price per volume £3 10s. post free, ***payable in advance***
4 parts per volume—£1 per part

Printed and Published by
TAYLOR & FRANCIS LTD

RED LION COURT, FLEET STREET, LONDON, E.C.4

Orders originating in U.S.A. and Canada should be sent to the
Academic Press Inc., 111 Fifth Avenue, New York, 3, N.Y., U.S.A.

Journal of Electronics and Control

A Philosophical Magazine Associated Journal

Devoted to Electron Sciences

Editor:
J. Thomson, M.A., D.Sc., M.I.E.E., F.Inst.P.

Consultant Editor:
Professor N. F. Mott, F.R.S.

Editorial Board:
Professor P. Aigrain (France)
Professor H. B. G. Casimir (Holland)
Dr. W. Klein (Germany)
Dr. R. Kompfner (U.S.A.)

Contents of July, 1957

A Small Amplitude Theory for Magnetrons. By O. Bunemann, Manchester University C.V.D. Group

Perturbation Analysis of Stationary Dense Electron Flow and a Space-Charge-Limited Triode. By G. A. Stuart, Ferranti Ltd. and B. Meltzer, University of Edinburgh

Space Charge Neutralization by Ions in Linear Flow Electron Beams. By N. C. Barford, Imperial College of Science and Technology, London University

Space-Charge in the Relativistic Magnetron. By Louis Gold, Lincoln Laboratory, Massachusetts Institute of Technology, Lexington, Massachusetts

Kinetic Theory of Space-Charge. I. Cut-off Character of the Static Magnetron. By Louis Gold, Lincoln Laboratory, Massachusetts Institute of Technology, Lexington, Massachusetts

Control Section

Price per part £1 5s.

Price per volume £7 post free, *payable in advance.*

6 monthly issues per volume.

Printed and Published by

TAYLOR & FRANCIS LTD

RED LION COURT, FLEET STREET, LONDON, E.C.4

Orders originating in U.S.A. and Canada should be sent to the
Academic Press Inc., 111 Fifth Avenue, New York, 3, N.Y., U.S.A.

The Philosophical Magazine

First Published in 1798

Editor :
Professor N. F. Mott, M.A., D.Sc., F.R.S.

Editorial Board :
Sir George Thomson, M.A., D.Sc., F.R.S.
Professor A. M. Tyndall, C.B.E., D.Sc., F.R.S.
Sir Lawrence Bragg, O.B.E., M.C., M.A., D.Sc., F.R.S.

Contents of July, 1957

Crossing Symmetry and the Relativistic Equation for two Fermions. By S. F. Edwards and P. T. Matthews, Department of Mathematical Physics, University of Birmingham

Remarks on Crossing Symmetry. By S. F. Edwards, Department of Mathematical Physics, University of Birmingham, England and P. T. Matthews, Department of Physics, University of Rochester, Rochester, New York

The Thermal Instability of a Rotating Fluid Sphere Heated Within. By S. Chandrasekhar, F.R.S., University of Chicago

The Etching of Diamonds by Low Pressure Oxygen. By M. Omar and M. Kenawi, Physics Department, A'in Shams University, Cairo

The Kinetics of Colour Centre Formation in Quartz. By E. G. S. Paige, Royal Radar Establishment, Gt. Malvern, Worcs.

Observations on the Magnetic Transition in Hematite at $-15°\text{C}$. By G. Haigh, Department of Physics, Imperial College of Science and Technology, London

Observations on Extensive Air Showers—III: The Distribution of Charged Particles. By T. E. Cranshaw, W. Galbraith and N. A. Porter, Atomic Energy Research Establishment, Harwell

Observations on Extensive Air Showers—IV: The Lateral Distribution of Penetrating Particles. By N. A. Porter, T. E. Cranshaw and W. Galbraith, Atomic Energy Research Establishment, Harwell

Fusion Induced by Mu-Mesons. By T. H. R. Skyrme, Atomic Energy Research Establishment, Harwell, Didcot, Berks.

The Production of Intense Cold Neutron Beams. By I. Butterworth, P. A. Egelstaff, H. London and F. J. Webb, Atomic Energy Research Establishment, Harwell

The Thermal and Magnetic Properties of Ytterbium Ethyl Sulphate between $20°\text{K}$ and $1°\text{K}$. By A. H. Cooke, F. R. McKim, H. Meyer and W. P. Wolf, The Clarendon Laboratory, Oxford University

Price per part £1 5s.
Price per annum £13 10s. post free, *payable in advance.*

Printed and Published by
TAYLOR & FRANCIS LTD
RED LION COURT, FLEET STREET, LONDON, E.C.4

Journal of Fluid Mechanics

Editor:
Dr. G. K. Batchelor, F.R.S.
Cavendish Laboratory, University of Cambridge, Cambridge, England

Assistant Editors:
Dr. T. B. Benjamin, Dr. I. Proudman

Associate Editors:
Professor G. F. Carrier
Pierce Hall, Harvard University, Cambridge 38, Massachusetts, U.S.A.
Dr. W. C. Griffith
Research and Development Laboratory, Missile Systems Division, Lockheed Aircraft Corporation, Palo Alto, California, U.S.A.
Professor M. J. Lighthill
Department of Mathematics, The University, Manchester, England

Contents of August, 1957

The Production of Uniform Shear Flow in a Wind Tunnel. By P. R. Owen and H. K. Zienkiewicz, Mechanics of Fluids Department, University of Manchester

An Exact Solution for Progressive Capillary Waves of Arbitrary Amplitude. By G. D. Crapper, Department of Mathematics, University of Manchester

The Flow past a Rapidly Rotating Circular Cylinder in a Uniform Stream. By D. W. Moore, Jesus College, Cambridge

Experiments on the Onset of Wave Formation on a Film of Water flowing down a Vertical Plane. By A. M. Binnie, Trinity College, Cambridge

Wave Formation in Laminar Flow down an Inclined Plane. By T. Brooke Benjamin, Department of Engineering, University of Cambridge

A Note on the Application of the Supersonic Area Rule to the Determination of the Wave Drag of Rectangular Wings. By R. C. Lock, Aerodynamics Division, National Physical Laboratory, Teddington

Experiments on Convection of Isolated Masses of Buoyant Fluid. By R. S. Scorer, Department of Meteorology, Imperial College, London

The Vorticity Jump across a Gasdynamic Discontinuity. By Wallace D. Hayes. Department of Aeronautical Engineering, Princeton University, and the Ramo-Wooldridge Corporation

The Collision of two Ionized Streams. By F. D. Kahn, Department of Astronomy, Physical Laboratories, University of Manchester

Price per part £1
Price per volume £5 10s. (6 parts per volume) post free

Printed and Published by
TAYLOR & FRANCIS LTD
RED LION COURT, FLEET STREET, LONDON, E.C.4

Orders originating in U.S.A. and Canada should be sent to the
Academic Press Inc., 111 Fifth Avenue, New York, 3, N.Y., U.S.A.

CONTENTS

Studies of Remanent Magnetism and Viscous Magnetism in the Basalts of Iceland. By Ari Brynjólfsson, Institut für Geophysik der Universitat, Göttingen 247

Palaeomagnetic Study on a Quaternary Volcanic Region in Japan. By T. Nagata, S. Akimoto, S. Uyeda, Y. Shimizu, M. Ozima and K. Kobayashi, Geophysical Institute, University of Tokyo, Japan 255

Magnetic Interaction between Ferromagnetic Minerals Contained in Rocks. By T. Nagata, S. Uyeda and M. Ozima, Geophysical Institute, Tokyo University 264

Magnetic Properties of Ferromagnetic Oxide Minerals as a Basis of Rock-Magnetism. By S. Akimoto, Geophysical Institute, Tokyo University 288

The Problem of Reversed Magnetizations and its Study by Magnetic Methods. By J. H. Parry, Physics Department, King's College, Newcastle-upon-Tyne 299

Some Field and Laboratory Studies of the Depositional Remanence of Recent Sediments. By D. H. Griffiths, R. F. King and A. E. Wright, Department of Geology, University of Birmingham . 306

Remanent Magnetism of the Russell Belt of Gneisses, Northwest Adirondack Mountains, New York. By J. R. Balsley and A. F. Buddington, U.S. Geological Survey, Washington 25, D.C. . . 317

Reflection Microscopy of Ferromagnetic Minerals. By A. P. Millman, Department of Mining Geology, Imperial College, London . . 323

Crystallization Magnetization. By Richard R. Doell, Department of Geology and Geophysics, Massachusetts Institute of Technology, Cambridge, Mass. 327

Remarks relative to Maxwell's Formula for the Magnetic Susceptibility of Disseminated Materials. By L. B. Slichter, Institute of Geophysics, University of California, Los Angeles, California . 333

Chemistry and Magnetic Properties of some Ferrimagnetic Oxides like those occurring in Nature. By E. W. Gorter, Philips Research Laboratories, N.V. Philips' Gloeilampenfabrieken, Eindhoven-Netherlands 336

The Role of Magnetostriction in Rock Magnetism. By John W. Graham, Carnegie Institution of Washington, Department of Terrestrial Magnetism, Washington 15, D.C. 362

ADVANCES IN PHYSICS

A QUARTERLY SUPPLEMENT
of the
PHILOSOPHICAL MAGAZINE

VOLUME 6 JULY 1957 NUMBER 23

Studies of Remanent Magnetism and Viscous Magnetism in the Basalts of Iceland

By ARI BRYNJÓLFSSON
Institut für Geophysik der Universitat, Göttingen

§ 1. INTRODUCTION

THE paper gives a brief description of the instrument which the author constructed for measuring the direction and intensity of the magnetic moments. It gives further the most important results of the studies of demagnetization in an alternating field, and of the investigation of viscous magnetization. The paper describes also an investigation of the secular variation in Iceland during the last 5000 years. Finally it describes the results of the investigation of an area between normally and reversely magnetized zones, that is, it describes how the direction of magnetization changes continuously from reversed to normal.

§ 2. THE INSTRUMENT

Basalts are somewhat inhomogeneously magnetized. Koenigsberger (1932) showed that when he cut a 4 by 4 by 4 cm sample into eight 2 by 2 by 2 cm samples, the spread in the direction of magnetization of the smaller samples was very great (sometimes it amounted to as much as 15°). Therefore it is of interest to make measurements on large samples ; at the same time the method must be such that we measure the vectorial sum of the individual magnetic moments in the sample. That means the output must be proportional to

$$\iiint \boldsymbol{\mu}(x, y, z)\, dx\, dy\, dz$$

integrated over the entire sample ; where $\boldsymbol{\mu}$ is the magnetic moment per unit volume.

The instrument which we constructed fulfilled this requirement and with it we can perform measurements on any sample smaller than about 1200 cm^3.

The instrument is an induction instrument. The sample rotates with a frequency of 5 c.p.s. The induced current is commutated and then measured with a galvanometer. The sensitivity is 10^{-7} e.m.u./g., it is limited by the commutator noise. The specimen is fixed in a Cardan-suspension. This device makes it possible to install the specimen with its direction of magnetization accurately parallel to the axis of rotation. In this way the direction of magnetization is easily determined with a 0·1° accuracy (*zero-method*). The constant earth-field is reduced by 1/100 or to 0·005 Oersted by means of mu-metal screens. The mu-metal screen, a condenser in the circuit and the stand, that is a good conductor, reduce the fluctuations by more than 1/600. The fluctuations are also reduced by the commutator.

The instrument is portable.

§ 3. DEMAGNETIZATION

Preliminary studies indicated that partial demagnetization is of great interest, as the intensity of the normally magnetized basalts decreased for every increase of the demagnetizing field ; while the intensity of reversely magnetized samples of basalt *increased* as they were partially demagnetized in alternating field smaller than 30–50 Oe. For greater demagnetization fields, the intensity decreased as for normally magnetized basalts. Further preliminary studies showed that the viscous magnetization was removed by a partial demagnetization of the sample (Brynjólfsson 1956).

We represent the demagnetization effect by means of negative differential demagnetization curves. That means the differential quotient

$$(-dI/dH_{\max})$$

is plotted as a function of $H_{\max}$. Here I is the intensity of the magnetization of the sample and $H_{\max}$ the maximal demagnetization field.

From fig. 1 we see that the differential demagnetization curves are very different for different samples.

Curves one and two belong to postglacial basalts (which are, of course, normally magnetized), curve three to a normally magnetized tertiary basalt, and curves four and five to a reversely magnetized tertiary basalt. It is especially interesting that with reversely magnetized basalt, the intensity always increases at the beginning. (Experimental result I.) When the sample is strongly magnetized, the effect is often compensated by the ordinary decrease by demagnetization.

The average of many (14) differential demagnetization curves for postglacial basalts is nearly constant. It decreases just a little at the end. (Experimental result II.)

The amount of the decrease of the intensity depends on the angle between the direction of the magnetization of the sample, and the direction of the alternating field, as follows. (Experimental result III.)

When the postglacial basalt sample is demagnetized in all directions with $H_{\max}=140$ Oe, the intensity decreases from 100 to 57, i.e. if $I^0=100$ we have $I_*^{140}=57$, a change of $43\% \pm 1{\cdot}2\%$. The decrease of the intensity fluctuates between 63% and 9%, and the circle of confidence for each sample is 12°. When the sample is demagnetized in all directions perpendicular to its direction of magnetization, the intensity decreases from 100 to 66·6, i.e. if $I^0=100$ $I_\perp^{140}=66{\cdot}6$. This can be done by rotating the sample about the axis defined by its direction of magnetization, with a demagnetizing field perpendicular to this axis. If we next rotate a new sample about an axis perpendicular to its direction of magnetization, keeping the direction of the demagnetizing field constant, and therefore demagnetizing in all directions in a plane perpendicular to the preceding plane containing the magnetization vector of the sample, the intensity decreases from 100 to 59·6, i.e. if $I^0=100$ we have $I_\pm^{140}=59{\cdot}6$. If both of these operations are performed on the same sample, thereby demagnetizing in all directions, the intensity decreases from 100 to 57, as previously stated.

Fig. 1

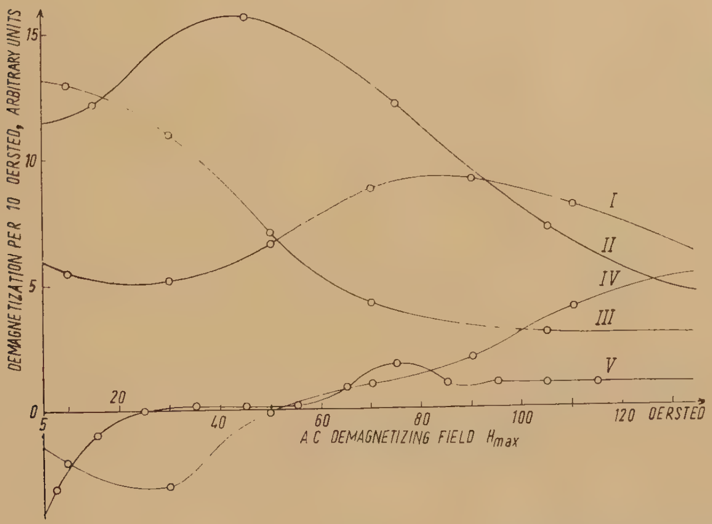

The experimental results II and III of differential demagnetization together with the experimental results of Schmucker (1956) which show that the thermo-remanent magnetization is proportional to the external field (when the external field is lower than about 10 Oe)—coupled further with the hypothesis that the sample contains many grains or domains which can be magnetized in *two anti-parallel directions only*, and that the probabilities for this direction of easy magnetization to be in one or another direction are equal—make it possible to calculate how the amount of demagnetization depends on the direction of $H_{\max}$.

The values calculated in this manner are in accordance with the experimental ones. If $I^0 = 100$, then the values of I_*^{140}, $I_\pm^{140}$ and $I_\perp^{140}$ are as follows :

	Experimental values	Calculated values
I_*^{140}	57·0	(57)
$I_\pm^{140}$	59·6	60·6
$I_\perp^{140}$	66·6	67·0

I.e. we can explain the experimental results when we assume that there only exist two directions of easy magnetization in each grain ; on the other hand the experimental results are in contradiction to the hypotheses that there exist many more directions of easy magetization in each grain. Further as we have the good agreement between the experimental and the calculated values, we must assume that the anisotropy in each grain is very strong.

Fig. 2

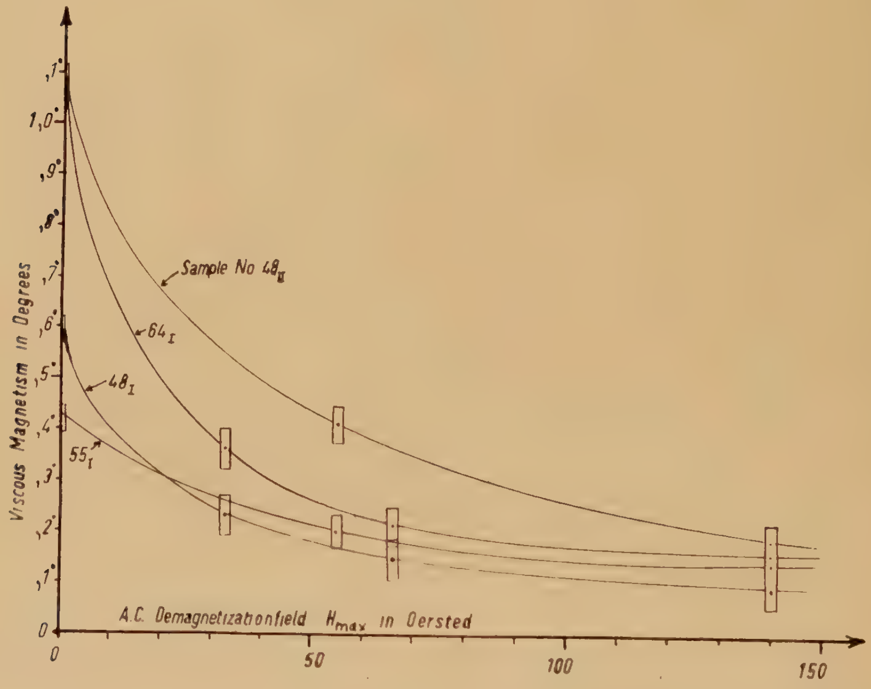

§ 4. Viscous Magnetism

As we can measure the change of direction of the magnetic moment very accurately, we can easily investigate the viscous magnetization.

At the beginning, we demagnetize the sample in all directions with 140 Oe and determine the direction of the magnetic moment with 5′

accuracy. Then we fix the sample with its direction of magnetization at a right angle to the direction of the earth field. The viscous magnetization is then proportional to the change in direction. This change after some months amounts to 1° to 10° which is large compared with 5′.

It is now of great interest that the *viscous magnetization is mostly removed when the sample is partly demagnetized in alternating fields* ($H_{\text{max}}=ca.$ 100 Oe). (Experimental result IV.)

Figure 2 illustrates how strongly the viscous magnetism is reduced by partial demagnetization.

The ordinate shows the amount of viscous magnetization and the abscissa the maximal demagnetization field H_{max}.

The laboratory investigation of viscous magnetism thus indicates that in case of reversely magnetized basalts the increase of intensity on demagnetization with $H_{\text{max}}=ca.$ 40 Oe is due to the removal of the viscous magnetism. (Experimental result V.) This then indicates that in the case of tertiary basalts the viscous magnetism (caused by the present normal field) amounts to 5×10^{-4} to 5×10^{-5} e.m.u./g. In the case of weakly magnetized samples this is a very serious effect. It is then of great interest to us that this viscous magnetism can be removed (mostly) by partial demagnetization with $H_{\text{max}}=100$ Oe. (The sample can be cleaned.)

In the theory of viscous magnetization worked out mainly by Street and Woolley (1949), Street, Woolley and Phillips (1954) and Street, Woolley and Smith (1952) and, in a different way, by Néel (1949, 1950, 1951, 1952) the viscous magnetism is thought of as caused by the thermal fluctuations. Thus the thermal fluctuations can bring a domain from one state to another ; the thermal fluctuations deform the domains and, as the magnetic state depends on the form of and strains in the grains, there exists a coupling between the thermal fluctuations and the magnetic state.

The influence of thermal fluctuations is described by the Maxwell–Boltzmann term $\exp\{-(E/kT)\}$.

If we assume with Street and Woolley that the energy E is nearly equal to $I_s \,.\, v \,.\, H_c$, we can find the volume v of the domains from the form of demagnetization curves of the viscous magnetization. This gives a diameter for the domains equal to or greater than 2×10^{-6} cm. (Experimental result VI.)

If we use Néel's expression for E, we find almost the same volume for the domains. That is, the investigation of viscous magnetism indicates that the *diameter of the smallest domains is about* 2×10^{-6} *cm.*

§ 5. POSTGLACIAL BASALTS

Twenty-five postglacial lavas were investigated. The intensity of magnetization I_r in lava-flows, which cooled down after A.D. 500, fluctuated between $1{\cdot}2\times10^{-2}$ and $1{\cdot}1\times10^{-3}$ e.m.u./g. with a mean of $5{\cdot}1\times10^{-3}$ e.m.u./g. (Experimental result VII.) The intensity in the older flows was about 20% smaller.

Figure 3 shows the secular variation in Iceland. (Experimental result VIII.) The points represent the dipoles that correspond to the direction of magnetization (in Iceland). The positive numbers at the points indicate the age A.D. Those with minus indicate the age B.C. A line across the circle of confidence shows that the age of the corresponding flow is between A.D. 300 and about A.D. 900. A cross in the circle of confidence indicates that the age of the corresponding flow is between 1000 B.C. to about A.D. 200. These points between 1000 B.C. and about A.D. 200 all show very easterly declination. Although the field in Iceland alone does not define the dipole very accurately, the results indicate that the south pole of the whole field must have been somewhere in the neighbourhood of northern Norway or Novaja Zemlja, U.S.S.R. If this is right, *the ancient Greeks should have seen the northern light much more frequently than they are seen in that region today.* This is in accordance with Aristoteles' exhaustive description in his book "Meteorologia", Chapter IV and V.

Fig. 3

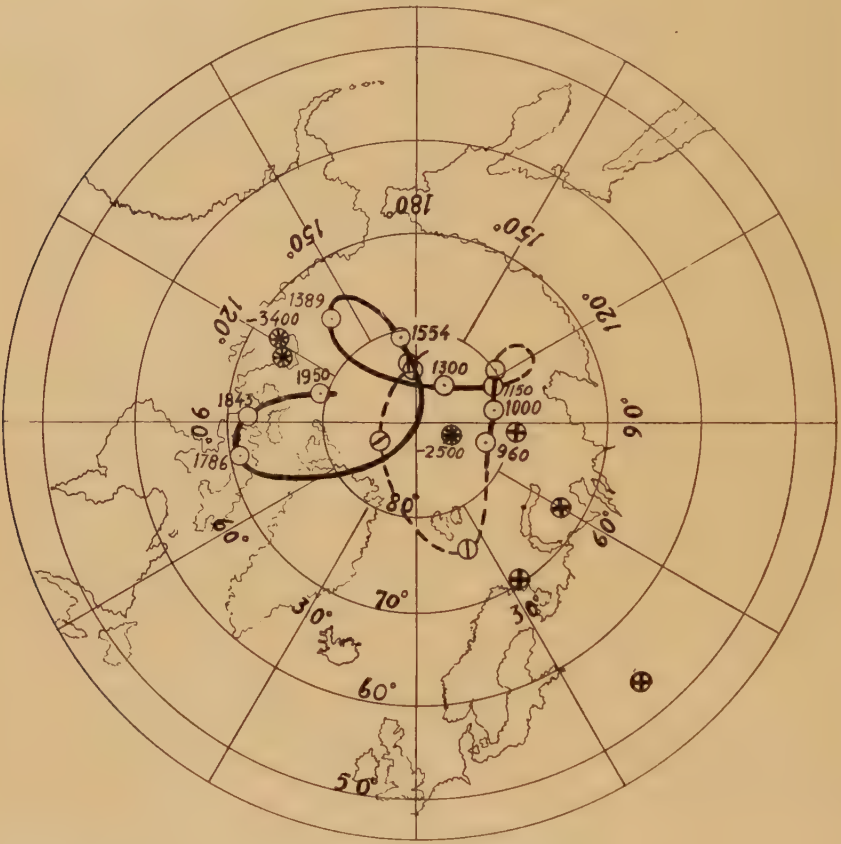

We see that the secular variations are very great. We also see that the mean direction of the field corresponds to a magnetic south pole in the neighbourhood of the geographic north pole and not with the present magnetic south pole. Thus, these measurements indicate *that even during the last* 5000 *years, the mean dipole field is that corresponding to the magnetic pole coincident with the geographic pole and not corresponding to the dipole of today.* (Experimental result IX.) This is an interesting result as the magnetic direction in Iceland is a sensitive indicator for which of the *two* directions is the more significant.

Fig. 4

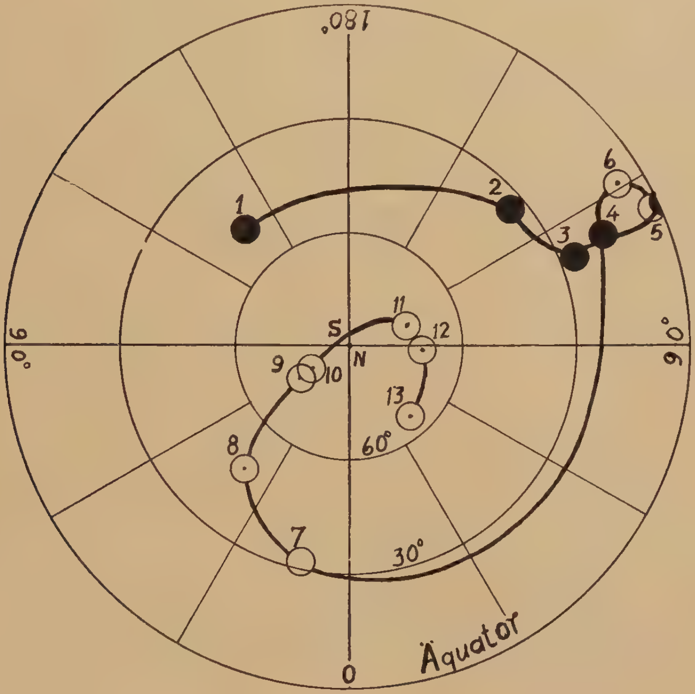

§ 6. TERTIARY BASALTS

It was found that *the direction of magnetization in each lava was much more homogeneous after a partial demagnetization of the sample in alternating field with maximal amplitude* $H_{\max} = 140$ Oe, *than before the demagnetization.* (Experimental result X.) This was most clearly seen with weakly magnetized basalts. On partial demagnetization, the weakly demagnetized samples changed their direction much more than the strongly magnetized samples in the same lava. During the demagnetization all the samples from a single lava changed their direction in the same way (not randomly). *At low demagnetization fields* (*ca.* 50 Oe) *the direction always changed away from the direction of the present earth field at the location of the sample* *in nature.* (Experimental result XI.) *This change again indicates that a viscous magnetization caused by the earth field is removed by demagnetization.*

As a result of special studies of the tertiary basalts, I will here mention the result of an investigation of an area between normally and reversely magnetized lava-groups. This result shows that *the direction of magnetization changes gradually from reversed to normal.* (Experimental result XII.) In fig. 4 the full points represent the magnetic south pole on the southern hemisphere, the empty circles the magnetic south pole on the northern hemisphere. Each point belongs to one lava and the successive points to successive lava flows. It is clearly seen that the change is gradual from the southern hemisphere, over the equator, and to the geographic north pole. The clockwise traces of the variation remind one of the present clockwise traces of the secular variation. Perhaps this similarity indicates that the reversal of the field took place during a period of 1000–3000 years. (Experimental result XIII.) It is difficult to understand how such changes could be caused by some self-reversal during the cooling process or during the time passed, as we would then expect random variations in the direction of magnetism. These lavas were all weakly magnetized. *The fine-structure of these changes* was only obtained after the demagnetization (before the partially demagnetization the circle of confidence is greater than after it). The intensity is about five times smaller than is otherwise the case in tertiary basalts.

ACKNOWLEDGMENTS

Acknowledgment is made to the Research Council of Iceland, the University of Iceland and the Alexander von Humboldt-Stiftung in Germany for a grant-in-aid for this research.

The author wishes to express his thanks to Director Th. Sigurgeirsson and to the geologists in Iceland for their help and interest in this work.

The author is deeply grateful to Professor J. Bartels and other members of the Geophysikalisches Institut in Göttingen for encouragement and suggestions.

REFERENCES

BRYNJÓLFSSON, A., 1956, *Naturwiss.*, **43**, 154.

KOENIGSBERGER, J., 1932, *Beitr. Geophys.*, **35**, 207.

NÉEL, L., 1949, *Ann. Geophys.*, **5**, 99; 1950, *J. phys. Radium*, **11**, 49; 1951, *Ibid.*, **12**, 339; 1952, *Ibid.*, **13**, 249.

PHILLIPS, J. H., STREET, R., and WOOLLEY, J. C., 1955, *Proc. phys. Soc. Lond.* B, **68**, 345.

SCHMUCKER, U., 1956, *Dissertation* (Göttingen: Mat. Nat. Fak.).

STREET, R., and WOOLLEY, J. C., 1949, *Proc. phys. Soc. Lond.* A, **62**, 562; 1950, *Ibid.*, B, **63**, 509.

STREET, R., WOOLLEY, J. C., and PHILLIPS, J. H., 1954, *Phil. Mag.*, **45**, 505.

STREET, R., WOOLLEY, J. C., and SMITH, P. B., 1952, *Proc. phys. Soc. Lond.* B, **65**, 679.

Palaeomagnetic Study on a Quaternary Volcanic Region in Japan

By T. Nagata, S. Akimoto, S. Uyeda,
Y. Shimizu, M. Ozima and K. Kobayashi

Geophysical Institute, University of Tokyo, Japan

Recent studies in palaeomagnetism have indicated that at some epoch or epochs in the late Tertiary or the early Quaternary ages the direction of the main geomagnetic field may have been opposite to that observed at the present time. Since 1954, a palaeomagnetic research has been conducted on the North-Izu and Hakone volcanic region (fig. 1), with the purpose of examining the above possibility.

In this region, there are four major strato-volcanoes and several small ones (fig. 2). The geology of this region has been thoroughly studied by H. Kuno†, under whose directions all the rock specimens have been sampled. The ages and order of eruption of these volcanoes are as follows:

(1) Usami Volcano : older Pleistocene
(2) Taga Volcano
(3) Yugawara Volcano
(4) Hakone Volcano : from middle to younger Pleistocene
(5) Omuro-yama Volcano Group : from younger Pleistocene to Holocene.

A complete succession of lavas from these volcanoes has been obtained by Kuno.

The number of localities so far sampled are 58, and at each locality 4–7 oriented rock specimens were collected. The ages of the samples range from the very beginning of the Pleistocene to the Holocene.

The directions and the intensities of the natural remanent magnetism of each specimen were measured, for the most part by an astatic magnetometer, although those of few specimens with weak remanent magnetization were measured by a spinner type magnetometer.

In table 1, the directions and the intensities of magnetization of the collected samples are listed in the chronological order as established by Kuno. The error in direction for each locality was estimated by Fisher's method (1953), and is expressed in the table as the radius of the 95% circle of confidence, while the values of the intensity are the averages of the 4–7 specimens.

---

† Professor, Department of Geology, Tokyo University.

Table 1

1	2	3	4	5	6 Direction		
Age	Name†	Sample Numbers	Classification of Rocks	Localities	D	I	Error‡ 5%
Quaternary	ÔMURO-YAMA VOLCANO GROUP						
	Ômuro volc.	27	Andesite	North-West of Ippekiko	10°	14°	14°
	Zyobosi volc.	25	Andesite	Near Sakasagawa	-9	47	7
	Umenokidaira volc.	26	Andesite	East of Zyoyama	-9	39	6
	CENTRAL CONE OF HAKONE VOLCANO						
	CC_9						
	CC_8	3	Andesite	Rokudozizo	-6	38	23
	CC_7	4	Andesite	Motohakone	-15	44	22
	CC_6						
	CC_5	2	Andesite	Asinoyu	-4	56	20
	CC_3						
	CC_2						
	CC_1	6	Pumice	Takanosu-yama	-11	82	19
	YOUNG SOMMA OF HAKONE VOLCANO						
	YS_5	50	Andesite	Byôbuyama	2	33	15
	YS_3	1	Andesite	Ôhiradai	-20	51	73
	OLD SOMMA OF HAKONE VOLCANO						
	O_{20}	9	Andesite Aphyric	Manazuru	3	52	10
	O_{18}	11	Andesite	Hayakawa	-12	60	18
	O_{12}	57	Andesite	Siraisityôba	8	44	7
	O_{11}	10	Andesite	Nebukawa	-9	55	10
	O_5	51	Andesite	Sukumogawa	22	47	16
	OS_1	13	Aggromerate basalt	Sengokubara	-40	38	18
	OS_1	14	Aggromerate basalt	Sengokubara	3	65	16
	O_2	52	Andesite	Hatazyuku	-21	47	21
	YUGAWARA VOLCANO						
	YV_2						
	YV_1	8	Andesite	Yugawara	-3	46	7
	D_2	16	Pyrox. dacite	Akanezaki	-25	50	7
	TAGA VOLCANO						
	TV_5	17	Basalt	Aziro-Usami	-34	54	5
	TV_4	49	Andesite	Kameisitôge	-46	39	12
	TV_4	53	Andesite	Taga-oku (1)	-6	57	17
	TV_2	54	Andesite aggromerate	Taga-oku (2)	11	49	13
	TV_1	15	And. tuff breccia	Uomizaki	-15	57	9
Quaternary	USAMI VOLCANO						
	UV	42	Andesite	Near Ito	-48	48	19
	UV	43	Andesite	Near Ito	-24	43	28
	UV	41	Andesite	Near Ito	-26	56	21
	UV	40	Andesite	Near Ito	-32	70	6
	UV	18	Andesite	Usami Tunnel	151	-46	12
	UV	45	Andesite	Usami Tunnel	150	-41	7
	UV	47	Andesite	Usami Tunnel	144	-3	44
	UV	48	Andesite	Usami Tunnel	151	-30	13
	UV	32	Andesite	Southern cliff of Sukumo yama	114	-62	21
	UV	33	Andesite	Southern cliff of Sukumo yama	-137	-71	31
	UV	34	Andesite	Southern cliff of Sukumo yama	97	-53	38
	UV	35	Andesite	Southern cliff of Sukumo yama	73	-18	15
	UV	36	Andesite	Southern cliff of Sukumo yama	-144	-43	20
	UV	28	Andesite	Northern cliff of Zyoyama	163	21	24
	UV	23	Andesite	Sakasagawa	-7	53	8
	UV	20	Andesite	Siohukizaki Beach	-29	63	7
	UV	21	Andesite	Siohukisaki Beach	-32	63	19
	UV	22	Andesite	Siohukizaki Beach	-31	66	7
	Zyo formation	29	Shale	Near Zyo	-15	51	16
Tertiary	AZIRO BASALT GROUP						
	B_{4a}	12	Olivine-augite basalt	Aziro	-27	54	49

7 Direction of the Centred Dipole		8 J_n 10^3 e.m.u./gr	9 J_n/J_{T_c}	10 $(J_n)T$	11 $(J_{T_c})T$	12 $(J_n)\tilde{H}$	13 $(J_{T_c})\tilde{H}$	14 $J_s(T)$	15 T_c	16 Reliability§
78°N	80°W	6·42								
80 N	0	1·27								
76 N	14 W	1·32								
75 N	22 W	3·15		#	#	#	#	#	#	#
75 N	7 E	1·33	0·74 #	#	#	#	#	#	#	#
87 N	80 E	1·85	1·03 #	#	#	#	#	#	#	#
50 N	134 E	2·73	0·45 △	#	#	#	#	#	#	#
73 N	46 W	0·38								
75 N	38 E	0·59	0·25 △	△	△	△	△	#	#	△
87 N	90 W	0·88	0·38 △	△	△	#	#	△	#	△
81 N	86 E	1·35	1·32 #	#	#	#	#	#	#	#
80 N	72 W	0·76								
84 N	60 E	0·92	0·59 #	△	△	#	#	△	#	#
73 N	112 W	1·02								
57 N	33 E	5·22	0·55 #	#		#	#		#	#
78 N	144 E	2·03	0·80 #	#	#	#	△		#	#
75 N	28 E	0·63								
82 N	24 W	1·27	0·70 #	#	#	#	#	△	#	#
72 N	42 E	1·69	2·45 △	#		#	#		#	△
68 N	55 E	2·70	1·2 #	△	#	#	#		#	#
54 N	39 E	3·78								
86 N	97 E	1·77								
82 N	98 E	0·47								
79 N	65 E	0·80	0·17 ×	#		#	△		#	△
54 N	51 E	0·62								
70 N	26 E	0·70	0·63 #	△	△			△	△	△
73 N	62 E	0·41								
61 N	108 E	0·49								
68 S	146 W	2·58	2·4 △	#	#	#	#	#	#	#
65 S	155 W	3·69	0·64 #	#	#					
47 S	175 W	0·67								
61 S	169 W	3·89								
43 S	104 W	4·86								
58 S	3 W	6·29								
25 S	107 W	1·70								
11 N	113 W	2·92								
62 S	117 W	9·18								
41 S	157 E	0·14	0·10 ×	#	#	#	#	△	#	△
85 N	33 E	0·59								
56 N	86 E	0·94	0·33 △	#	#	#	#	#	#	#
67 N	83 E	1·12	#	#	#	#	#	#	#	#
66 N	93 E	1·06	×	#	△	#	#		#	△
79 N	33 E	0·46								
71 N	36 E	4·43	0·89 #	#	#	△	△		#	#

---

† The symbols are due to Kuno's nomenclature.
‡ The error angles for 5% are calculated by Fisher's method.
§ Reliability for palaeomagnetic purpose.

As we have discussed previously, the palaeomagnetic study by means of the natural remanent magnetism of an igneous rock is possible when and only when the direction of the natural remanent magnetism is known to have remained invariable throughout the time since the rock was formed. From the present knowledge, the above condition may be regarded as satisfied when the natural remanent magnetism concerned is proved to be the stable T.R.M. (thermo-remanent magnetism) of a stable titano-magnetite phase, produced when the rock cooled at the time of its formation. Therefore, we have proposed that a set of practical tests should be applied on the rock specimen, when one wants to use its natural remanent magnetism for the palaeomagnetic purpose. The details of these tests have been described in our previous paper (1954), but since the criteria for reliability which we quoted there were essentially qualitative in nature,

Fig. 1

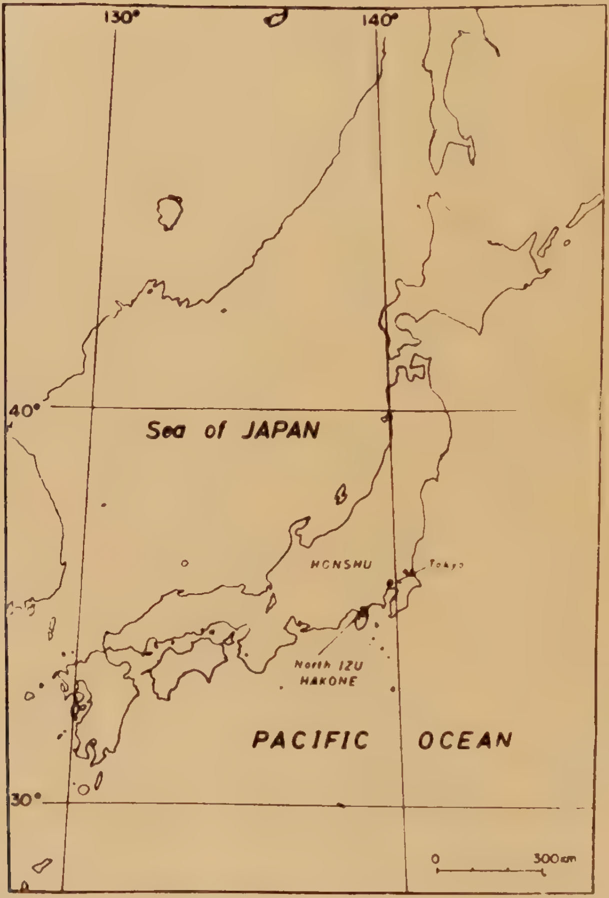

Map of the Japanese Islands, indicating the locality of the *North Izu and Hakone* volcanic region.

Fig. 3*a*

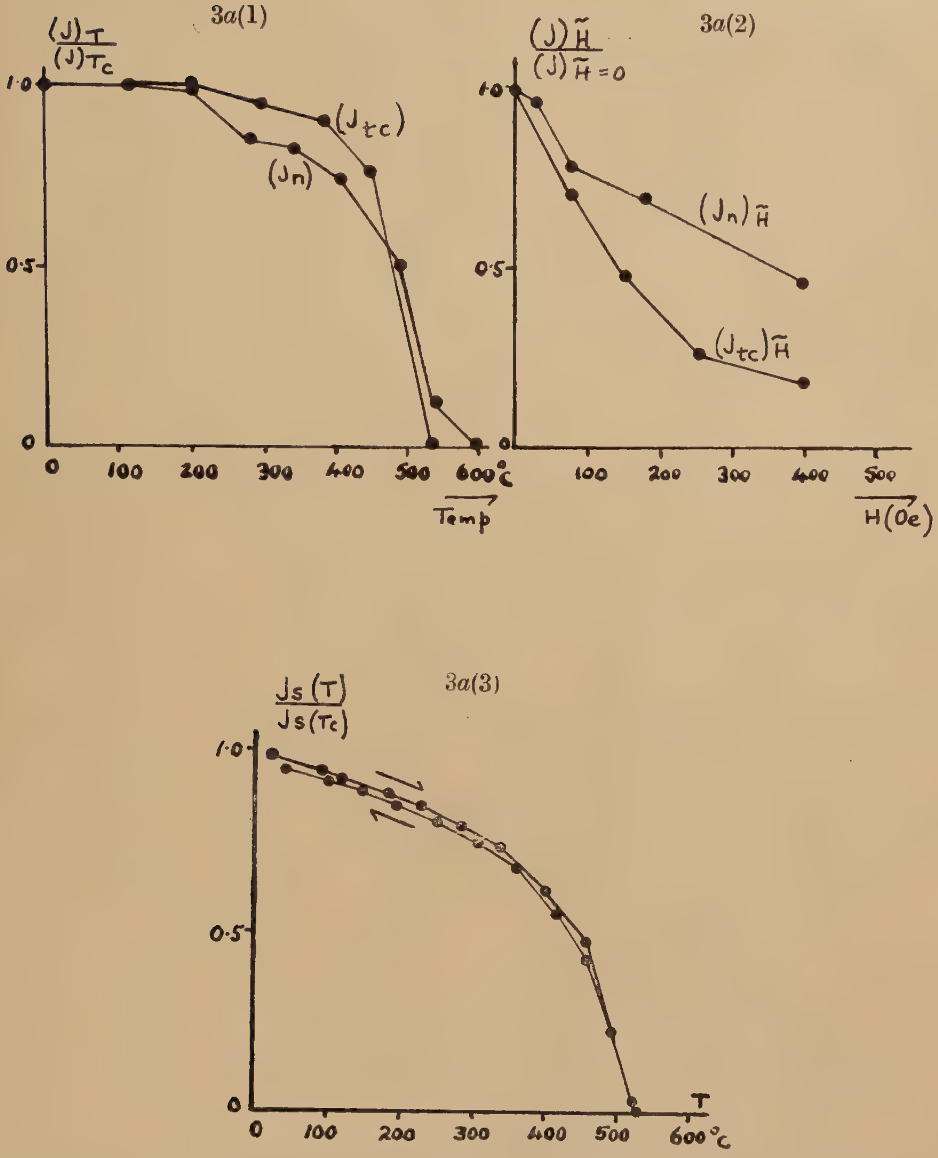

Example of the tests for the reliability of natural remanent magnetism.

Sample : No. 4, CC_7, Andesite.
J_n : normal direction.
Test (1) J_n/J_{T_c} 0·74
(2) see fig. 3*a*(1)
(3) see fig. 3*a*(2)
(4) T_c 520°c
(5) see fig. 3*a*(3)

Fig. 3*b*

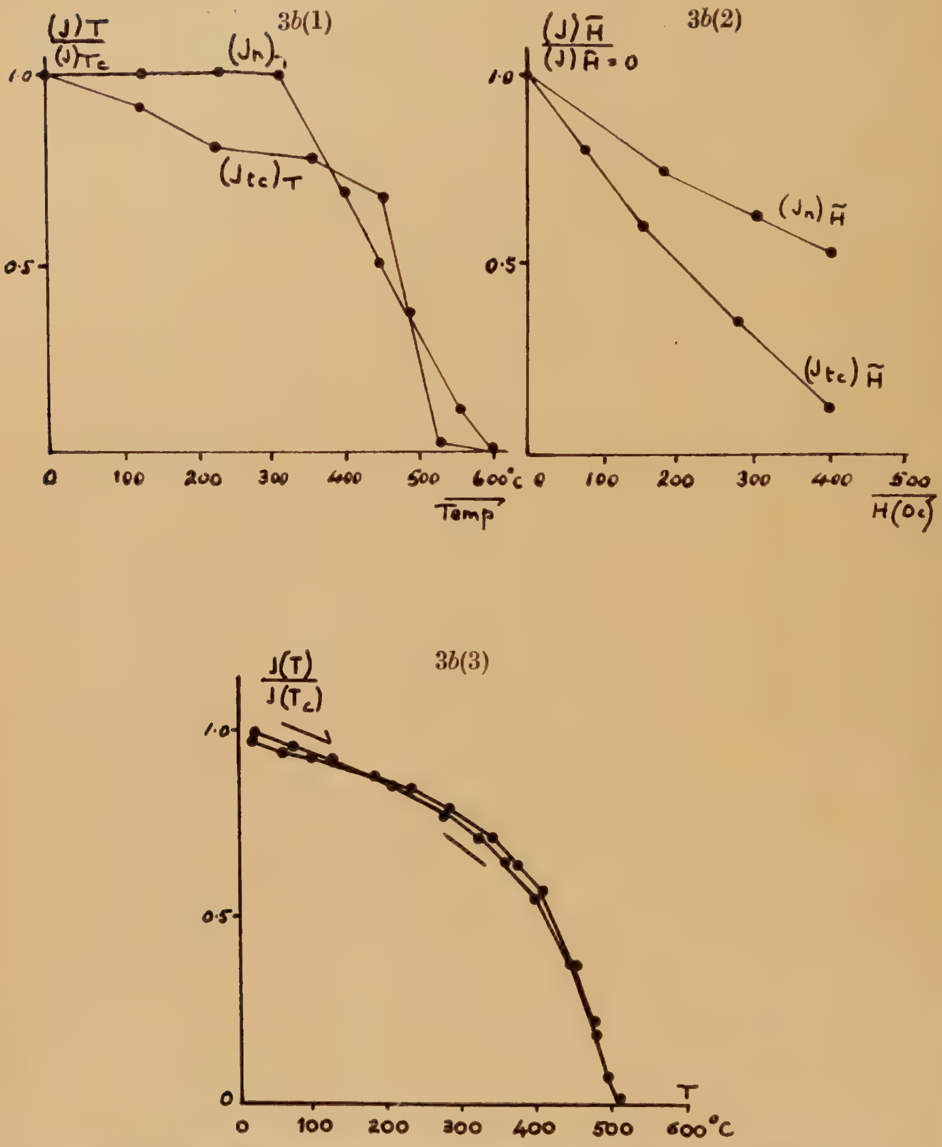

Example of tests for the reliability of natural remanent magnetism.

Sample : No. 18, UV, Andesite.
J_n : reverse direction.
Test (1) J_n/J_{T_c} 2·4
(2) see fig. 3*b*(1)
(3) see fig. 3*b*(2)
(4) T_c 510°c
(5) see fig. 3*b*(3)

we have refined them by adding some rather more quantitative conditions in the present Report. Thus in table 1, columns 9 to 11, we use the symbols, ♯, △, ×, to indicate 'adoptable', 'somewhat dubious' and 'rejectable' respectively, on the following basis :

(1) The ratio $J_n(T_0)/J_{T_c}(T_0)$ should be nearly equal to unity.
♯——$0{\cdot}5 < J_n/J_{T_c} < 1{\cdot}5$
△——$0{\cdot}2 < J_n/J_{T_c} < 0{\cdot}5$, or $1{\cdot}5 < J_n/J_{T_c} < 2{\cdot}5$
×——otherwise.

(2) The modes of $J_n - T$ and $J_{T_c} - T$ should be similar.

(3) The modes of $(J_n)\tilde{H}$ and $(J_{T_c})\tilde{H}$ should be similar.

(4) Contained ferromagnetic mineral should exclusively be a single-phased Ti-poor titano–magnetite with a single high T_c.
♯——$T_c > 400°\text{c}$
△——$400°\text{c} > T_c > 300°\text{c}$
×——$300°\text{c} > T_c$.

(5) $J_s(T)$-curve measured in vacuum should be 'reversible'.

Some of the results of the above tests are illustrated in fig. 3.

The extent of the secular variation of the geomagnetic field during the whole Quaternary age, estimated from the remanent magnetization of rocks which were considered to be suitable for palaeomagnetic study, is shown in fig. 4. The values of declination and inclination listed in table 2 represent the estimated average value of the geomagnetic field during the active period of each volcano. The estimated positions of the geomagnetic north pole during the whole Quaternary age are plotted in fig. 5.

Table 2

Number	Volcanic activity	D_0	I_0	Error angle for			Position of the calculated magnetic pole (in geographical coordinates)
				$p=0{\cdot}05$	$p=0{\cdot}10$	$P=0{\cdot}50$	
8	OV	−3°	44°	14°	11°	5°	81°N 32°W
7	CC	−9	55	23	19	9	86 N 65 E
6	YS	−7	43	34	11	8	79 N 13 W
	Erosion						
5	OS	−11	53	11	9	5	83 N 50 E
	YV	−3	46	—	—	—	82 N 30 W
4	TV	−19	55	20	17	8	78 N 62 E
3	UV_3	−33	55	15	13	6	70 N 61 E
2	UV_2	144	−43	29	23	13	64 S 145 W
1	UV_1	−27	63	12	10	5	72 N 86 E

It will be noticed that the reversals of the natural remanent magnetism are found exclusively in the lava flows occurring at the middle horizon of the lava sequence of the Usami Volcano. If the activity of this volcano

Fig. 4

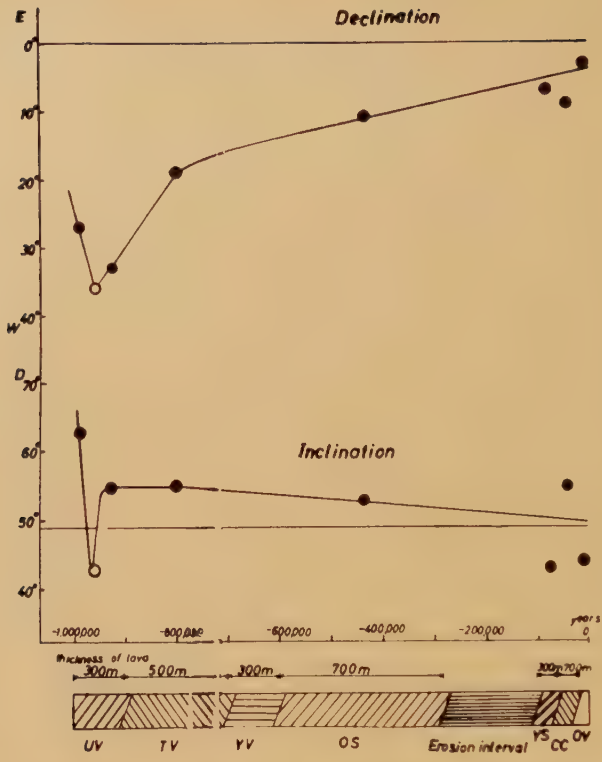

Change of the estimated direction of the geomagnetic field during the whole Quaternary age in *North-Izu and Hakone* volcanic region, Japan.

Fig. 5

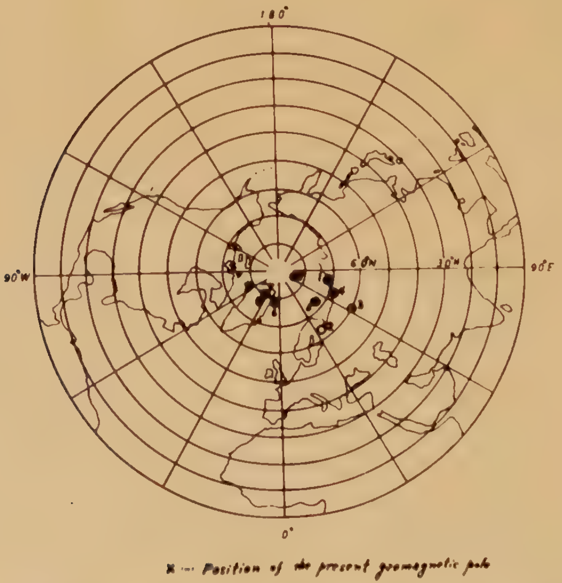

The estimated positions of the geomagnetic north pole during the whole Quaternary age (see table 2).

lasted for 100 000 years[†], the duration of the reversal of the geomagnetic field must have been shorter than this.

The conclusions drawn from the above data are as follows :

(1) On smoothing out the fluctuations whose periods are shorter than the period of each volcanic activity, the position of north pole of the geomagnetic centred dipole can be estimated to have shifted from 72°N, 86°E to 81°N, 32°W, during the whole Quaternary age.

(2) A period when the total reversal of the geomagnetic field may have taken place has been found at a time in the earliest Quaternary ; namely, the middle period of the formation of the Usami Volcano.

Further work to make the present research more complete is now being carried on (Nagata *et al.* 1957).

REFERENCES

FISHER, R. A., 1953, *Proc. Roy. Soc.* A, **217,** 295.
NAGATA, T., *et al.*, 1954, *J. Geomag. Geoelect.*, VI, No. 4.
NAGATA, T., AKIMOTO, S., UYEDA, S., SHIMIZU, Y., OZIMA, M., KOBAYASHI, K., and KUNO, H., 1957, *J. Geomag. Geoelect.*, **9,** No. 1.

[†] The three volcanoes, Usami, Taga and Yugawara, were erupted during the earlier half of the Pleistocene (approximately a million years ago). Therefore the Usamo Volcano is assumed to have been erupted for a period corresponding to one-third of 500 000 years.

Magnetic Interaction between Ferromagnetic Minerals Contained in Rocks

By T. Nagata, S. Uyeda and M. Ozima
Geophysical Institute, Tokyo University

§ 1. Introduction

When more than two ferromagnetic minerals are present in rocks, it is generally to be expected that some magnetic interaction exists between them, especially in the course of the development of the thermo-remanent magnetism (TRM). In recent years, the role played by such magnetic interaction in rock-magnetism has been attracting the interest of a number of investigators (Néel 1951, Graham 1953, Grabovsky and Pushkov 1954, Parry 1954). The general interest shown in this matter is related to the important nature of its function in the field of palaeomagnetism (Nagata *et al.* 1954).

The most typical example of the phenomena caused by the magnetic interaction is the Haruna-type reverse thermo-remanent magnetism (RTRM), of which we have previously conducted fairly detailed studies (Nagata 1952, 1953 a, Nagata *et al.* 1952, 1953 a, b, Uyeda 1955). The results of the magnetic, chemical, crystallographic and microscopic examinations of the grains responsible for the production of the RTRM of the Haruna rock indicated no evidence of the existence of the titanomagnetite (Ti–Mt) phase in these grains. Rather, the data showed that these grains are composed of two solid solutions of the ilmenite–hematite series, namely the ferromagnetic ilmenites, one of which is intergrown with the other as fine lamellae. Therefore, it was concluded that although this rock's main ferromagnetic mineral is the Ti–Mt, the RTRM characteristics in this case are to be entirely attributed to the ferromagnetic ilmenites contained therein.

Other examples of the phenomena caused by the magnetic interaction are the anomalous increase (AI) phenomenon of TRM of some Ti–Mt such as that of the Niisima iron sand, also studied by us in detail (Nagata 1953 b, Nagata and Ozima 1955) and the reversal of natural remanence of some of the Ti–Mt samples reported by Kawai *et al.* (1954 a, b, 1956). The reverse natural remanence of the Adirondack rocks found by Balsley and Buddington (1954) may also be an example of magnetic interaction.

The possibility of producing the RTRM and the AI phenomenon by the coexistence of two ferromagnetic minerals was also examined theoretically

(Uyeda 1955)†, and it was shown that these phenomena can be explained in terms of the magnetic interaction between two ferromagnetic minerals forming an intergrowth of fine lamellae, which can be revealed by a high power microscope.

Since the characteristics of the magnetic interaction were expected to depend on the magnetic properties of the participating materials, and on their state of coexistence, we have tried, in the present work, to realize as many combinations of the minerals as possible by applying the heat treatment to several natural ferromagnetic ilmenites, and to the Ti–Mt from the Niisima Island, Japan. The ferromagnetic ilmenites were adopted as the specimens for our study because some of them show the RTRM, while the Ti–Mt of Niisima was adopted because it was known to show the AI phenomenon.

We will briefly describe, §§ 2–3, the results of the experiments conducted on the ferromagnetic ilmenites, and discuss some general conclusions derived from these results, concerning the role played by magnetic interaction in the magnetism of rocks. As the examples of the conclusions in § 3, the AI phenomenon of TRM of the Ti–Mt (§ 4), and the mode of thermal change of the coercive force of some specimens composed of two ferromagnetic minerals (§ 5), will be described.

§ 2. Effect of Heat Treatments on the TRM of Ferromagnetic Ilmenites

The chemical, crystallographic and magnetic properties of the ferromagnetic ilmenites used in the present study are shown in table 1 and fig. 1. In fig. 1, the empirical relations between the chemical composition, the crystallographic parameters, and the Curie point, are also shown for the series ilmenite–hematite and magnetite–ulvöspinel. These relations, established by Akimoto (1955) and Nagata and Akimoto (1956), were used in the present work to estimate the chemical composition and the Curie point of the individual coexisting solid solutions on these joins, contained in the samples, from the x-ray data.

---

† Generally, the magnetization (J) of a system composed of two constituents A and B, with the Curie points T_{cA} and T_{cB}, where $T_{cA} > T_{cB}$, at a temperature T is expressed as,

$$J(T) = J_A(T) + J_B(T)$$

where the suffices A and B denote the quantities of the two constituents. In the process of cooling in a weak magnetic field (H_{ex}) from a temperature higher than T_{cA}, the B-constituent is magnetized at $T \leqslant T_{cB}$ by not only H_{ex} but also by some magnetic field of interaction due to the already magnetized A-constituent, i.e. the effective magnetic field determining the direction and the intensity of J_B should be expressed as,

$$H_{\mathrm{eff}} = H_{\mathrm{ex}} - NJA(T),$$

where N denotes the coefficient of magnetic interaction between the two constituents. Hence, the problem is to evaluate N for various configurations of the A- and B-constituents. If N is large enough to make $H_{\mathrm{eff}} < 0$, $J_B(T)$ becomes also negative, and if, moreover, $|J_A(T)| < |J_B(T)|$, the *RTRM* is produced.

The mineral samples, packed in an open quartz tube with an asbestos plug, or in a sealed evacuated (10^{-3} mm Hg) quartz tube, were inserted in an electric furnace whose temperature had attained a designated value. After being kept in the furnace for a measured length of time they were removed and allowed to cool. The duration of each heat treatment was 10 minutes in most cases.

Fig. 1

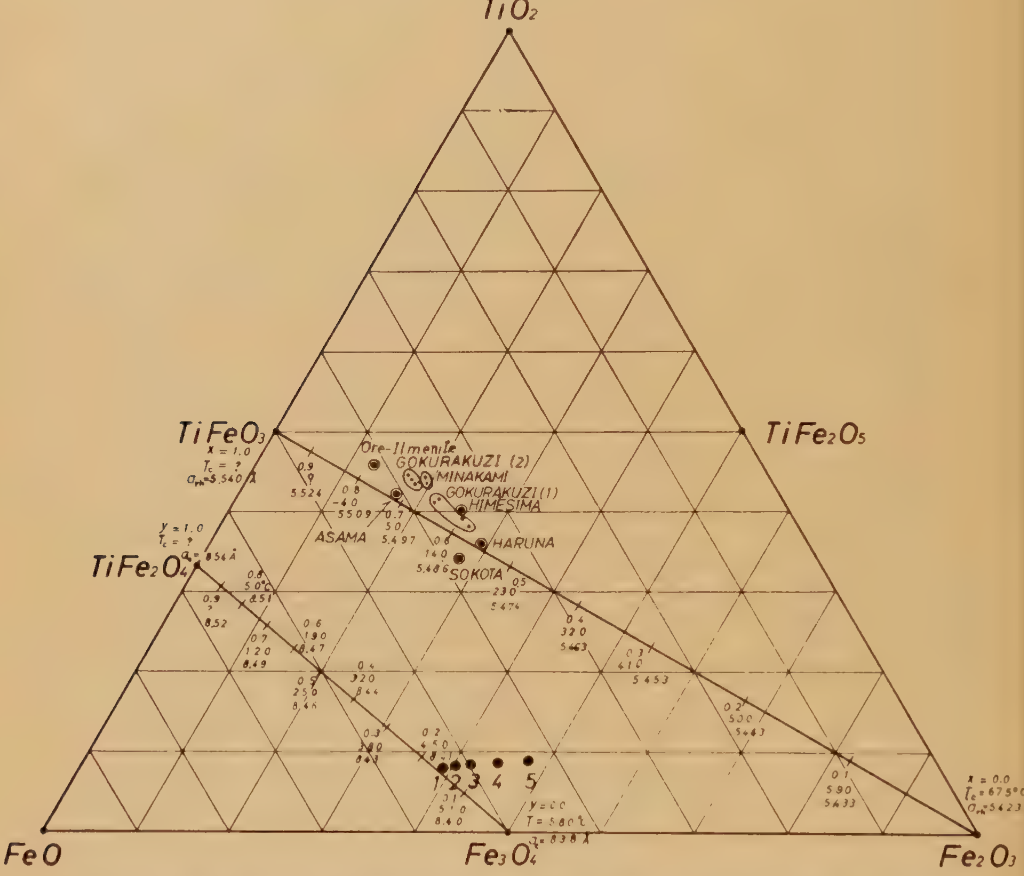

Chemical composition of the ferromagnetic ilmenites examined and the relations between the chemical composition, the Curie point and the lattice parameter of the joins ilmenite–hematite and magnetite–ulvöspinel. The full circles near the magnetite–ulvöspinel join are the Niisima titanomagnetite samples (§ 4) :

1 original sample
2 heat treated at 550°c for 2 hours in air
3 heat treated at 550°c for 10 hours in air
4 heat treated at 550°c for 23 hours in air
5 heat treated at 650°c for 12 hours in air.

Table 1. Properties of the Ferromagnetic Ilmenite–Hematite Series

Locality	Rock	T_s°c†	Chemical composition‡			a_{rh}	α_{rh}§	T_c°c‖	$I_s(T_0)$
			FeO	Fe_2O_3	TiO_2				
						Å			emu/gr
Haruna	dacite pumice	250~230	34·30	29·36	36·34	5·478	55° 02″	260	23
Sokota	iron sand	300~20	38·00	27·79	34·21	5·483	55 01	250	26
Himesima	hornblende mica andesite	300~20	35·53	20·70	43·77	5·489	54 36	190	29
Gokurakuzi (1)	iron sand	150~130	37·18	21·49	41·32	5·487	55 00	130	30
Gokurakuzi (2)	iron sand	70~50	38·47	17·48	44·05	5·494	54 57	70	24
Asama	dacite pumice	300~20	40·66	16·97	42·37	5·498	54 56	100	18
Minakami	rhyolite tuff	40~25	36·68	18·80	44·52	5·501	54 55	55	12
Thailand	ore-ilmenite	—	41·14	12·46	46·40	5·516	54 52	20	6

† T_s denotes the thermomagnetic separation temperature.
‡ In molecular per cent.
§ a_{rh} and α_{rh} are the rhombohedral crystal parameters.
‖ T_c denotes the Curie point.

The TRM was produced in the geomagnetic field during the process of cooling from the furnace temperature. The variation of the TRM thus produced is illustrated in figs. 2 (*a*) to (*g*). In these figures, the abscissa

Fig. 2 (*a*)

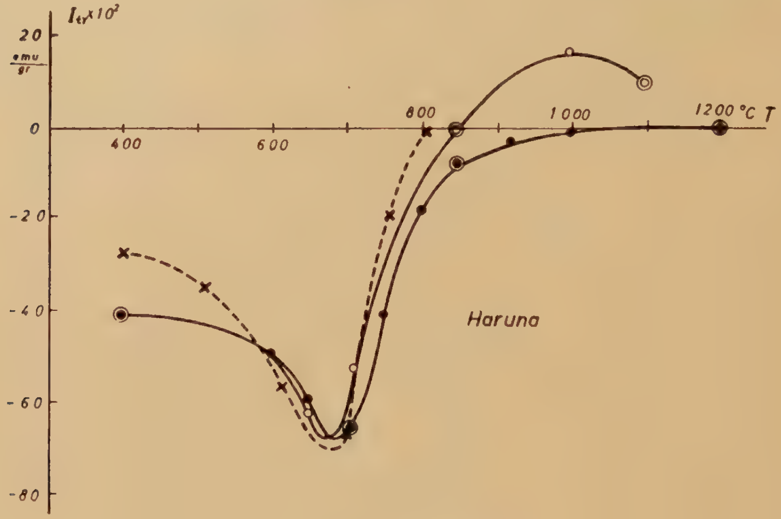

For caption see page 272.

Fig. 2 (*b*)

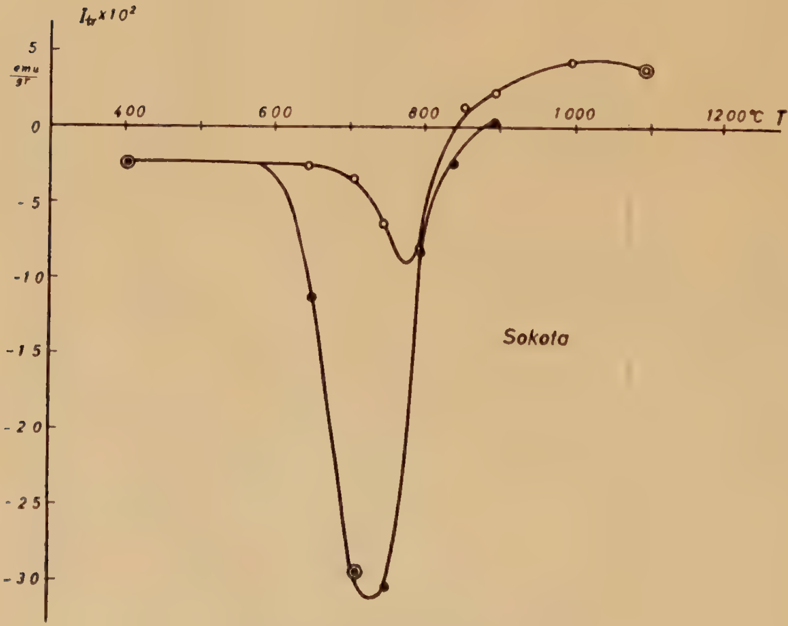

For caption see page 272.

Fig. 2 (*c*)

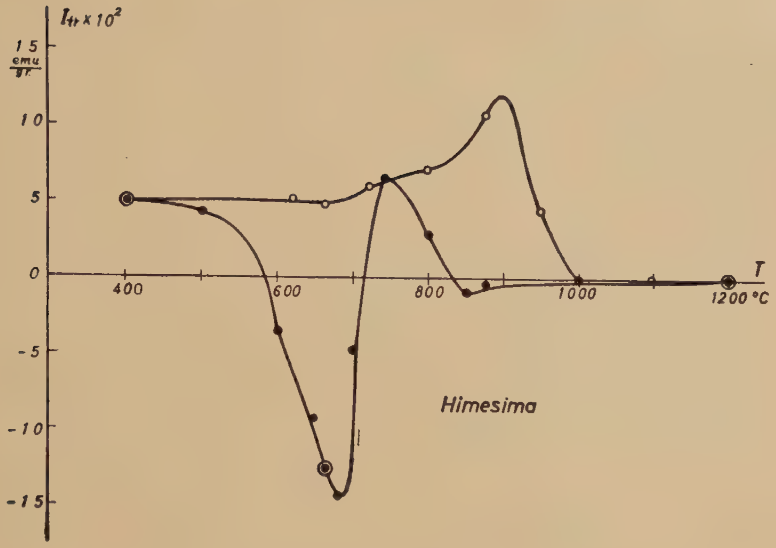

For caption see page 272.

Fig. 2 (*d*)

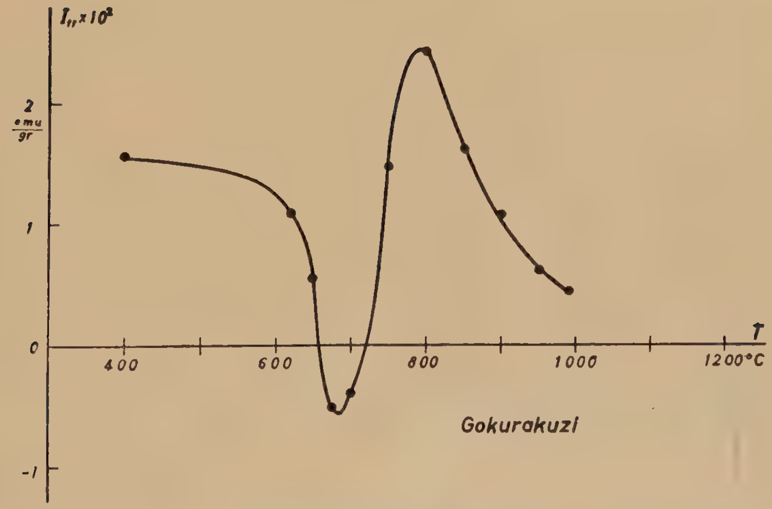

For caption see page 272.

Fig. 2 (d_1)

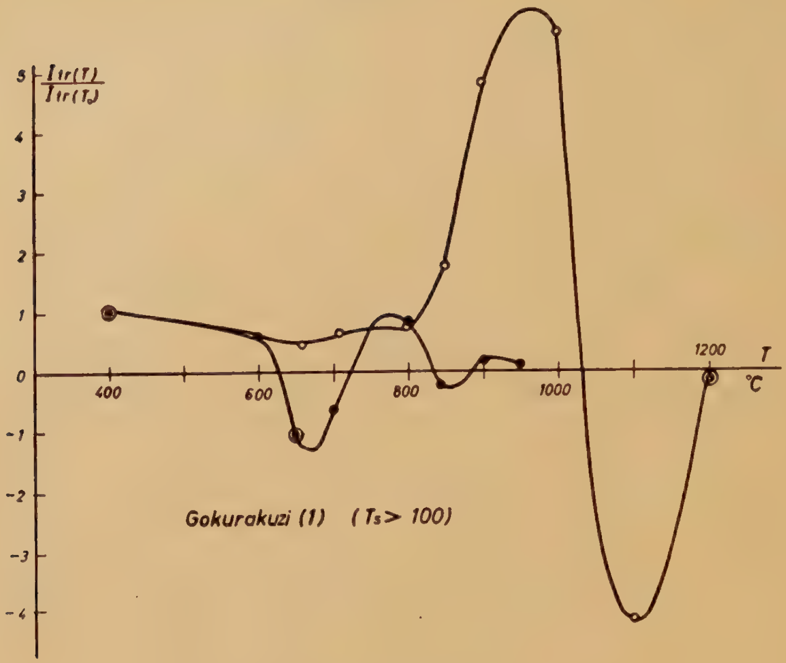

For caption see page 272.

Fig. 2 (d_2)

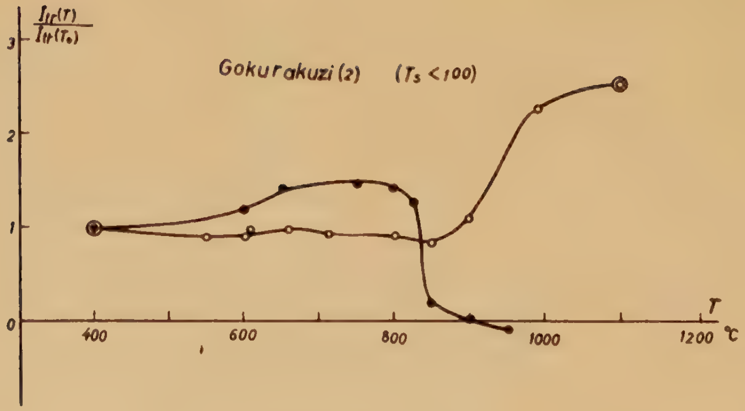

For caption see page 272.

Fig. 2 (*e*)

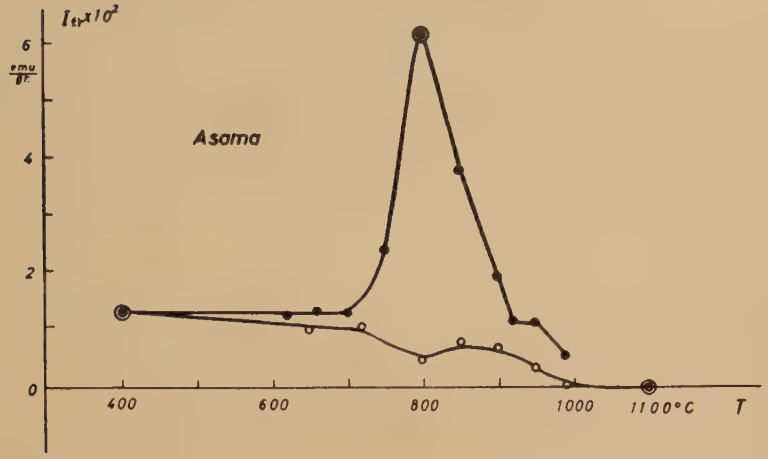

For caption see page 272.

Fig. 2 (*f*)

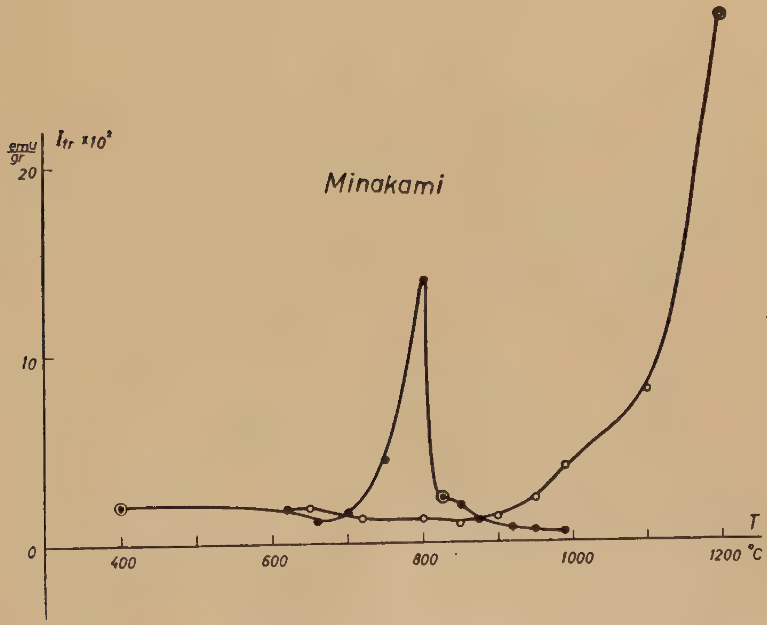

For caption see page 272.

shows the furnace temperature, and the full and hollow circles represent the intensities of the TRM of the samples heat treated in air and in the evacuated sealed tubes respectively. The double circles stand for the samples on which at least one of the chemical, crystallographic, thermomagnetic and microscopic examinations were performed. In fig. 2 (*a*), the cross marks show the TRM, after heat treatment repeated several times, in an open-air tube at different temperatures.

Fig. 2 (*g*)

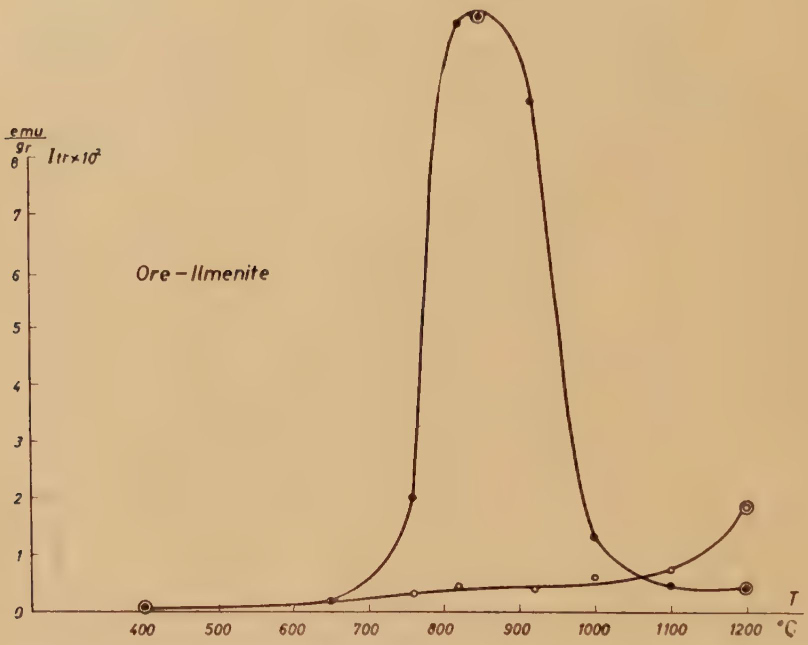

The variation of TRM of the ferromagnetic ilmenites due to heat treatment at T°c (abscissa) for 10 minutes in an open-air tube (full circles) and in an evacuated sealed tube (hollow circles). Double circles stand for the samples on which X-ray, chemical and microscopic analyses were conducted.

Although the curves in these figures seem to be rather complicated, it may be possible to summarize their principal features. To do this, it will be convenient to classify the samples into the following three groups according to their Curie points (T_c) :

(*a*) high T_c group : Haruna and Sokota samples,

(*b*) intermediate T_c group : Himesima and Gokurakuzi (1) samples,

(*c*) low T_c group : Gokurakuzi (2), Minakami, Asama and the ore-ilmenite samples.

2.1. *Effect of Heat Treatment in an Open-Air Tube on TRM*

(1) When the treatment temperature is 600°c–700°c, samples of the high T_c group, which have the RTRM characteristics in the original state, reveal a marked intensification of the RTRM (Nagata and Uyeda, 1956) (figs. 2 (*a*) and (*b*). Samples of the intermediate T_c group, which have only normal TRM in the original state, acquire the RTRM characteristics (figs. 2 (*c*), (*d*), (d_1). Samples of the low T_c group, having no RTRM in the original state, do not acquire the RTRM characteristics (figs. 2 (d_2), (*e*), (*f*) and (*g*)).

(2) When the treatment temperature is 750°c–850°c, samples of the high T_c group show a continuous decrease in the RTRM (figs. 2 (*a*) and (*b*)). Samples of the intermediate T_c group, which acquired the RTRM in (1), again show the normal TRM (figs. 2, (*c*), (*d*) and (d_1)). Samples of the low T_c group reveal a very remarkable intensification in the normal TRM (figs. 2 (d_2), (*e*), (*f*) and (*g*)).

(3) When the treatment temperature exceeds 850°c, the TRM of all the samples diminishes to nearly zero and their ferromagnetic nature also decreases.

Thus, heat treatment in an open-air tube can have two different effects ; it can intensify or produce RTRM when samples with relatively high Curie points are treated at about 600°c–700°c, or it can intensify the normal TRM found in the samples with relatively low Curie point, when the latter are treated at temperatures of about 750°c–850°c. The samples of the intermediate T_c group can be considered as being subject to both of these two effects, as shown by figs. 2 (*d*), (d_1) and (d_2).

2.2. *Effect of Heat Treatment in an Evacuated Sealed Tube on TRM*

(1) When the treatment temperature is 600°c–700°c, samples of the high T_c group again reveal an intensification of the RTRM, but the intensification of the RTRM of the Sokota sample is much less than that in the case of treatment in an open-air tube (figs. 2 (*a*) and (*b*)). Samples of the intermediate T_c group do not acquire the RTRM characteristics, in complete contrast to the case of treatment in an open-air tube (figs. 2 (*c*) and (d_1)). Samples of the low T_c group show no appreciable change in the TRM (figs. 2, (d_2), (*e*), (*f*) and (*g*)).

(2) When the treatment temperature exceeds 700°c, the features are rather complicated. Samples of the high T_c group show an initial increase in the normal TRM, but when the treatment temperature is raised further the TRM begins to decrease (figs. 2 (*a*) and (*b*)). Samples of the intermediate T_c group show the same feature as the high T_c group, but the Gokurakuzi (1) sample suddenly shows (fig. 2 (d_1)) RTRM when the treatment temperature reaches 1100°c, this being a new type of RTRM, having a somewhat different mechanism from that of the Haruna-type RTRM, the magnetic interaction being between the ferromagnetic

ilmenite and the Ti–Mt produced by the reduction of the original sample. Samples of the low T_c group show a steady increase in the normal TRM with the exception of the Asama sample (figs. 2 (d_2), (e), (f) and (g)).

The effect of the heat treatment in a sealed evacuated tube seems to be less systematically related to the Curie point of the sample than in the case of the treatment in the open-air tube. In the following discussion, it will be shown how these features may be explained by the magnetic interaction between coexisting minerals.

§ 3. Interpretation of the Results

To interpret the various phenomena described above in terms of magnetic interaction, chemical, crystallographic, magnetic and microscopic examinations of some of the treated samples were made. Figures

Fig. 3 (*a*)

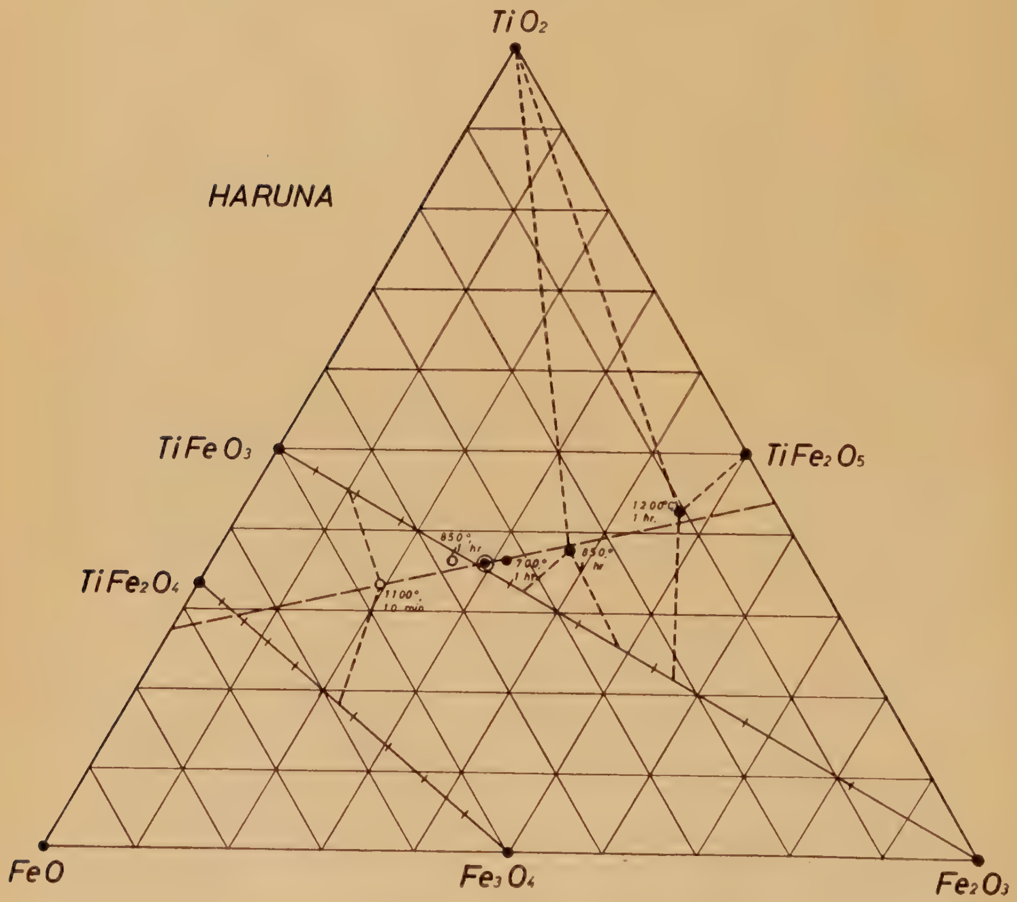

For caption see page 278.

3 (*a*) to (*e*) show the results. In these figures, the full and the hollow circles represent the chemical composition of the samples heat treated in open-air and evacuated sealed tubes respectively, and the treatment temperature and the duration of the treatment are attached to each circle. Double circles stand for the original samples. The chemical composition of the individual solid solutions contained was estimated from the x-ray data on the basis of the relations in fig. 1. It was verified that the Curie points measured directly by the thermomagnetic study are in good agreement with those estimated from the relations in fig. 1. It is clear in these figures that oxidation and reduction took place during the heat treatments, bringing about various combinations of ferromagnetic and

Fig. 3 (*b*)

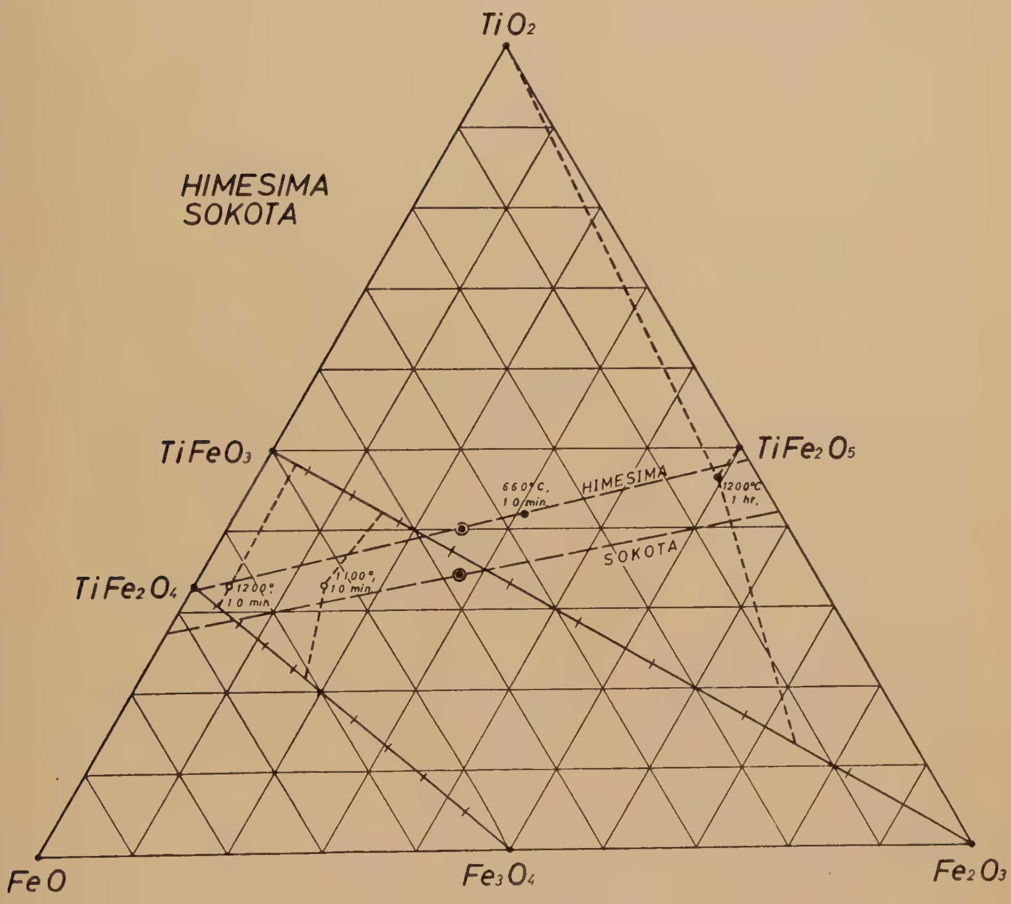

For caption see page 278.

non-ferromagnetic minerals in the samples of which the TRM characteristics were examined.†

The main conclusions of the roles of the magnetic interaction, obtained through these experiments, are as follows.

Fig. 3 (*c*)

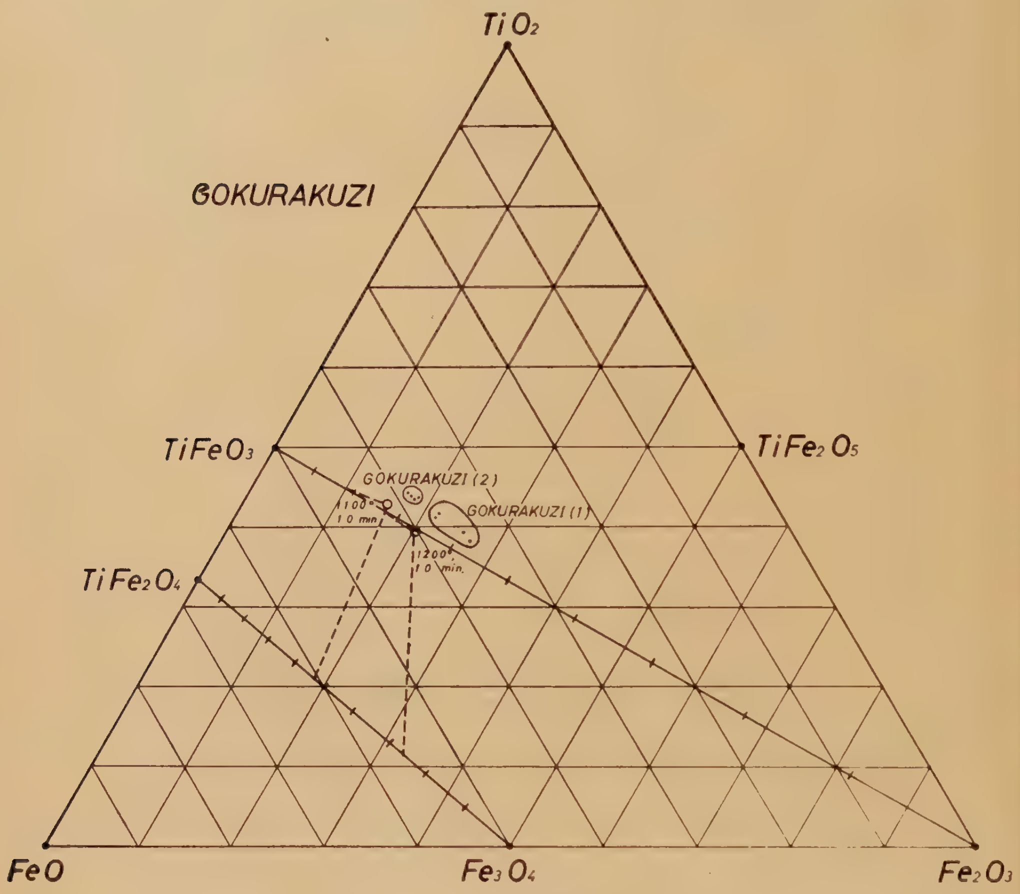

For caption see page 278.

Case (1)

When two ferromagnetic minerals coexist within a grain in the form of an alternately laminated structure, the magnetic interaction acts negatively. The most typical example of this case is the Haruna-type RTRM.

---

† It will be noticed that the oxidation of these samples proceeds in two steps: the first, called oxidation of the first degree, takes place below 850°c and produces some rutile and titan–hematite, while the chemical composition of the remaining ferromagnetic ilmenite itself is moved toward that of the hematite; the second one, called oxidation of the second degree, takes place when the temperature exceeds 850°c, and produces some pseudo-brookite in addition to the rutile and titan–hematite. This is in agreement with the result reported by Curnow and Parry (1956).

in which the participating minerals seem both to be ferromagnetic ilmenites with different but very closely related properties (Uyeda 1955). As stated already, the RTRM of the Haruna and Sokota samples is increased remarkably while the Himesima and Gokurakuzi samples acquire the Haruna-type RTRM through the heat treatment in an open-air tube at 600°c–700°c for 10 minutes. Plates 1, 2, 3 and 4 are the photomicrographs of the polished surfaces of the heat treated Haruna, Sokota, Himesima and Gokurakuzi samples, showing the RTRM. The occurrence of the ferromagnetic ilmenites with different but similar properties within a grain is presumed to be caused by a 'partial exsolution' (Uyeda 1956). The hypothesis of the partial exsolution will be explained, taking the Haruna sample as the example, as follows. Figure 4 is the probable phase relationship

Fig. 3 (*d*)

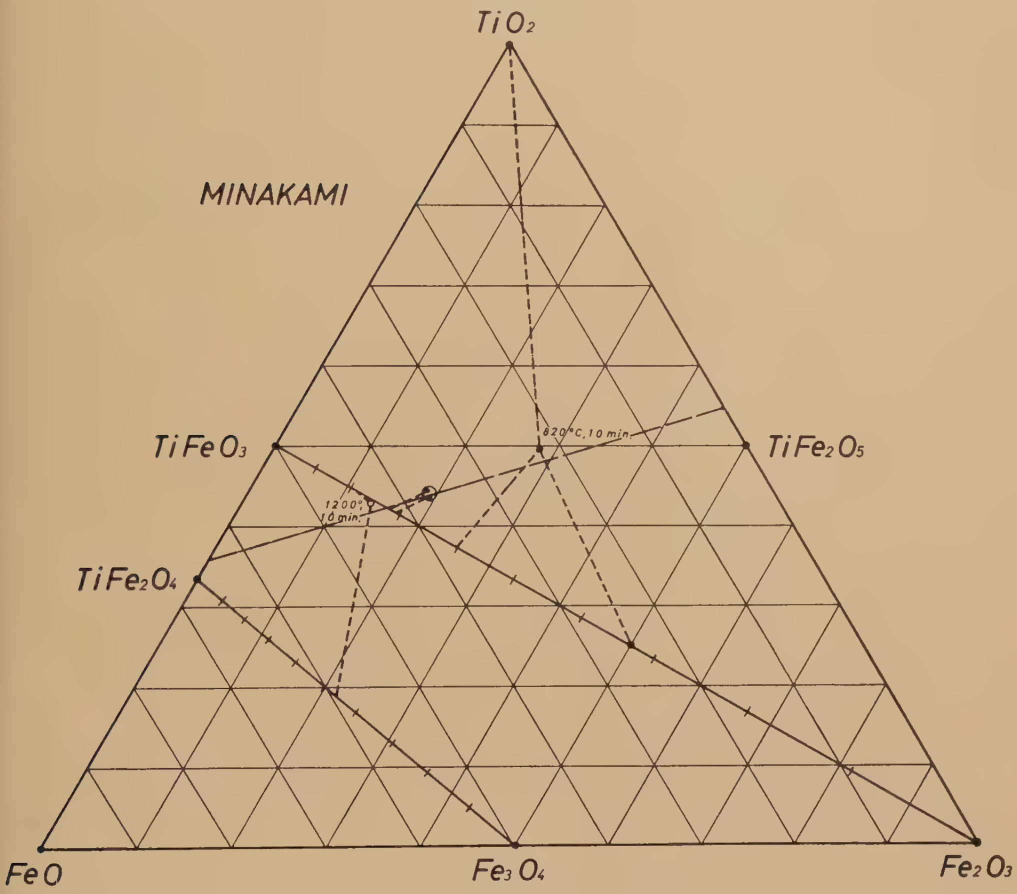

For caption see page 278.

of the ilmenite–hematite system (Nicholls (1955)),† where the vertical line H^A represents the composition of the Haruna sample in its original state. According to Kuno (1954), the mother rocks of the ferromagnetic ilmenites examined here are volcanic in origin and their crystallization temperature should range between 800°c–900°c approximately. Now, we assume it to be about 900°c. Therefore, the mineral at the crystallization temperature would have exsolved into F_1 and T_1. During the subsequent cooling, the exsolution should have proceeded along F_1I and T_1H.

Fig. 3 (*e*)

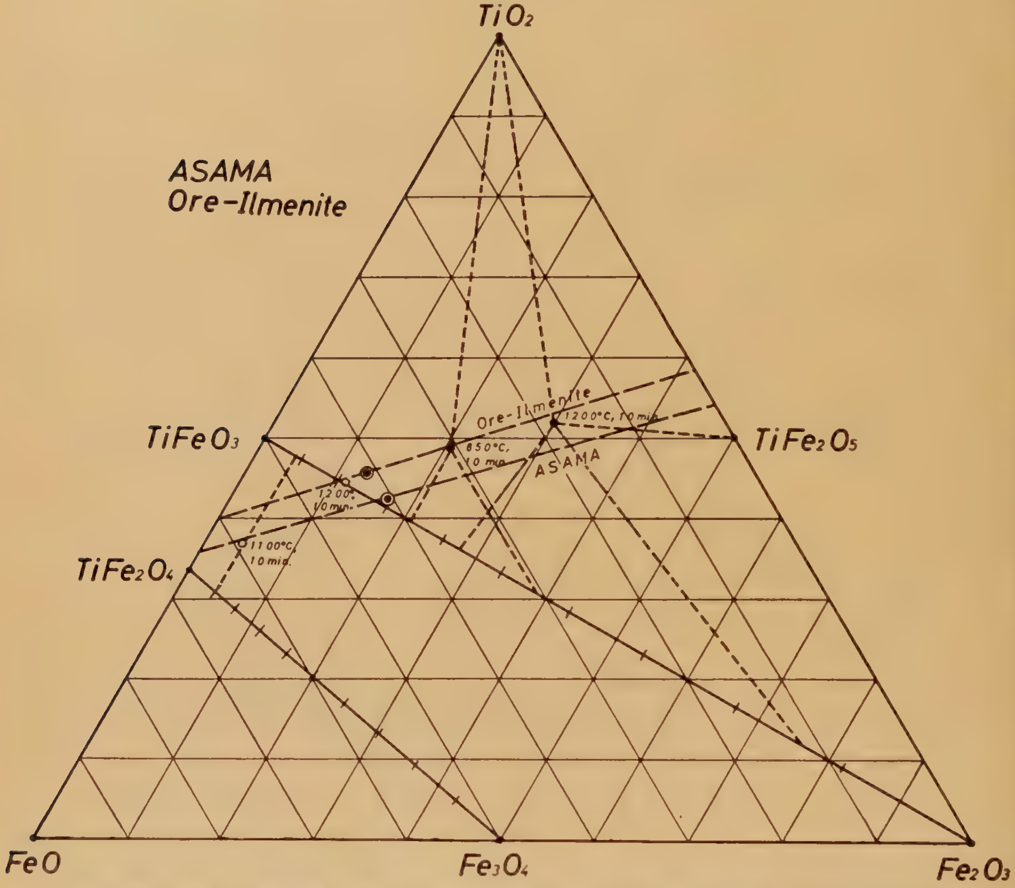

The results of chemical and crystallographic analyses on the ferromagnetic ilmenites heat treated in an open-air tube (full circles) and in an evacuated sealed tube (hollow circles). The double circles and the small full circles (figs. 3 (*c*) and (*d*)) represent the original samples and the broken lines show the theoretical oxidation-reduction lines. The dotted lines are the results of x-ray analysis.

---

† In fig. 4, the broken line indicates the boundary between the ferromagnetic (left) and the non-ferromagnetic or parasitically ferromagnetic (right) regions.

But, as the cooling rate of such volcanic rocks is believed to be very high, the exsolution at each temperature level may have always been incomplete. If such a partial exsolution has actually taken place, the Haruna sample should contain, in each grain, many ferromagnetic ilmenites with nearly

Fig. 4

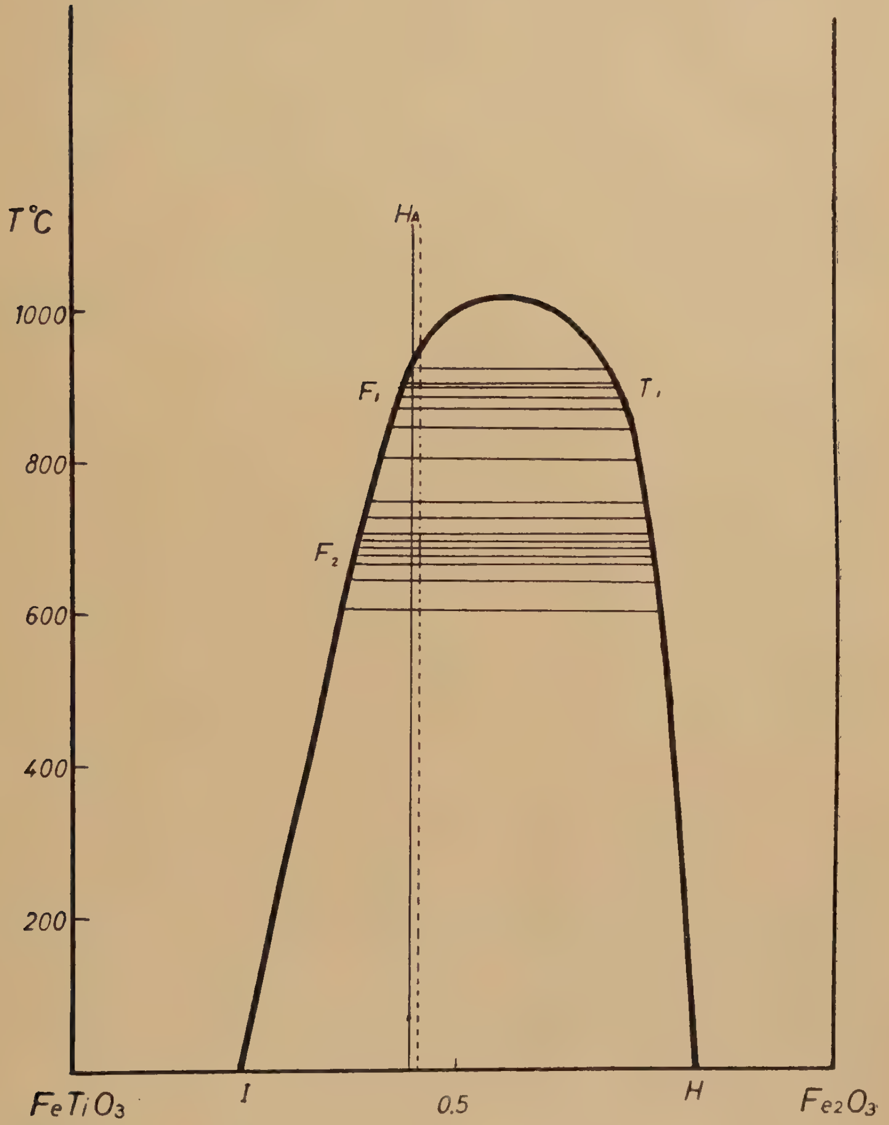

Probable form of the phase relationship of the system ilmenite–hematite, illustrating the coexisting phases in the Haruna sample. The vertical dotted line indicates the boundary between the ferromagnetic and non-ferromagnetic or parasitically ferromagnetic regions.

continuous chemical composition. However, it would be highly probable that in the process of total cooling, there was a temperature level where the exsolution was most effective. If such was the case, the components of the Haruna sample in the present state may be, aside from the small amount of titan–hematites (T_1 and T_2), roughly classified into two parts, F_1 and F_2, as schematically illustrated in fig. 4. We regard these two classes of ferromagnetic ilmenites as the two major ferromagnetic minerals participating in the production of RTRM of the Haruna-type. Now, let us assume that the effective exsolution temperature was 680°c–700°c. Then, when the sample undergoes the heat treatment at these temperatures, the F_2 component should develop at the expense of the F_1 component. If, further, the proportion of F_1 and F_2 after the treatment is nearer to the optimum proportion for producing the RTRM than in the original one, the intensification of RTRM can be explained. It is possible to extend the hypothesis of the partial exsolution to the cases of the intermediate and low T_c groups and explain the various effects of heat treatment mentioned in the previous section, if the little oxidation and reduction taking place during the treatments are taken into account.

An example of RTRM caused by the magnetic interaction between titanomagnetite and the ferromagnetic ilmenite was newly produced in the present study (fig. 2 (d_1)), by heat treating the Gokurakuzi (1) sample at 1100°c in the evacuated sealed tube, and was proved by magnetic and x-ray analyses to have been caused by the magnetic interaction between the Ti–Mt developed by the reduction and the originally existing ferromagnetic ilmenite. Plate 5, the photomicrograph of the polished surface of the Gokurakuzi (1) sample after being heat treated at 1200°c in the evacuated state, shows that the Ti–Mt phase is present as fine lamellae in the host of the ferromagnetic ilmenite. As will be shown later, the anomalous increase phenomenon of TRM can be regarded as an example of Case (1).

Case (2)

When the non-ferromagnetic minerals, such as titan–hematite, rutile, or ilmenite with a Curie point lower than the room temperature, are intergrown in the host of the ferromagnetic mineral, the TRM of the sample is intensified remarkably in the normal direction. The typical examples are the intensification of the TRM due to the heat treatment at 750°c–850°c in an open-air tube (figs. 2 (*c*) to (*g*)), and that of TRM due to the heat treatment at temperatures higher than 800°c in an evacuated sealed tube (figs. 2 (*a*), (*b*), (d_2), (*f*) and (*g*)). In the former cases, the results of the chemical and x-ray analyses of the Haruna, Minakami and the ore-ilmenite samples (figs. 3 (*a*), (*d*) and (*e*)) after the treatment at 820°c–850°c in air showed that the oxidation of the first degree during the treatment produced some titan-hematite and rutile in the samples as mentioned already. The titan–hematite and rutile, developed in the form of a fine intergrowth as shown in Plates 6 and 7, may be expected to act as the non-magnetic inclusions which hinder the free displacement of the magnetic domain walls, so that the coercive force of the sample may be expected to increase. Thus, the observed intensification of the TRM may be related to the increase of the coercive force.†

To verify the above reasoning we made an additional experiment on the Minakami (70°c$>T_s>$50°c) sample; the result of which is shown in fig. 5. Figure 5 shows the relation between the TRM characteristics and the coercive force (H_c) at room temperature (T_0), from which the following relation

$$J_{tr}(T_0)/J_s(T_0) \propto H_c(T_0) \quad . \; . \; . \; . \; . \; . \; . \; . \quad (1)$$

Fig. 5

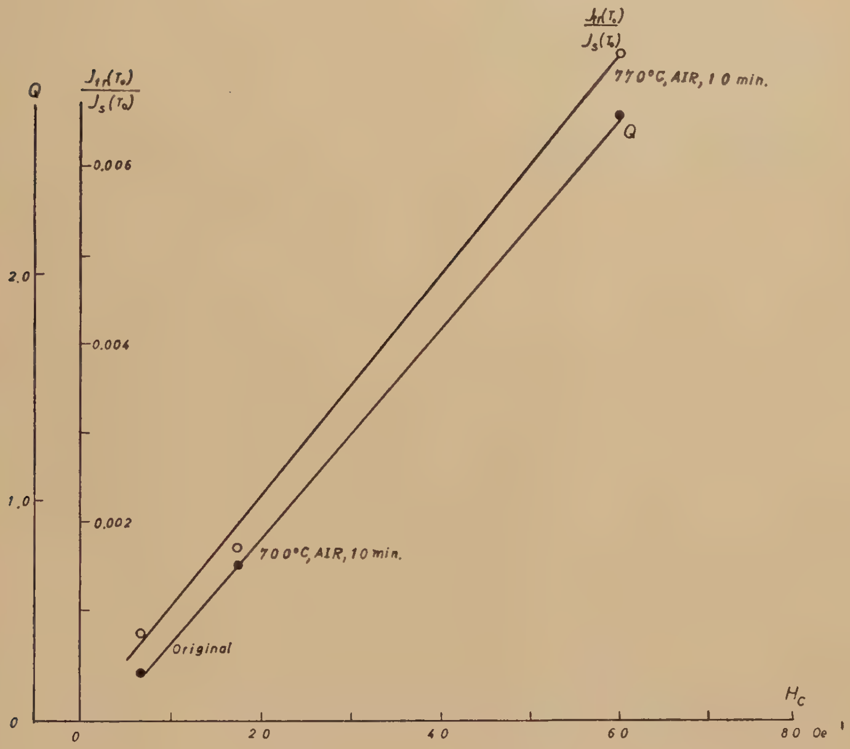

The relation between the TRM and the coercive force. The magnetic field concerned is 2·0 oe. The conditions of the heat treatment are noted near the circles. The sample is ferromagnetic ilmenite of Minakami. Q is the ratio=TRM/reversible magnetization at T_0.

---

† In the case of the samples of the high T_c group such as the Haruna one, the original composition being near the limit of the ferromagnetic region (fig. 4), the remaining 'ferromagnetic ilmenite' part itself becomes non-ferromagnetic by the oxidation. Therefore, their TRM does not increase in the normal direction.

will be obtained, where J_{tr} and J_s denote the intensity of the TRM produced in the geomagnetic field and the saturation magnetization respectively. In a recent paper, Néel (1955) theoretically deduced the relation,

$$J_{tr}(T_0)/J_s(T_0) \propto \sqrt{H_c(T_0)}. \quad . \quad . \quad . \quad . \quad . \quad . \quad (2)$$

In the case considered by Néel, J_s is assumed to vary as $(T-T_c)^{1/2}$, which is nearly true for the magnetite. In the present case of the ferromagnetic ilmenite, however, J_s varies as $(T-T_c)$. Hence, if we accept the linear mode of thermal change of H_c as reported by Nagata and Akimoto (1956), it is readily shown that Néel's reasoning revealed in § 57 of his paper leads to the relation (1) for ferromagnetic ilmenite.

As for the case of the intensification of the TRM by the heat treatment in an evacuated sealed tube, it was verified that the heat treatment produces the Ti–Mt phase in the form of fine lamellae and, at the same time, makes the remaining ilmenite–hematite phase non-ferromagnetic as seen in figs. 3 (*c*) and (*d*) and Plates 8 and 9.

Such an effect of coexistence of the ferro- and non-ferromagnetic minerals may also be regarded as originating from a kind of ‘ magnetic interaction ’. As will be seen in § 5, the abrupt increase of H_c of the samples, composed of two ferromagnetic phases, during heating should be the demonstrative examples of Case (2).

Case (3)

The decrease of the normal TRM revealed in fig. 2 is always proved to be due to the decrease of the ferromagnetism of the sample, although the reason for this decrease, in the case of treatment in the evacuated state (figs. 2 (*c*) and (*e*) and figs. 3 (*b*) and (*e*)), is different from that in the case of treatment in the open-air. The former is due to the lowering of the Curie points due to extreme reduction, while the latter is due to the radical oxidation of the samples.

§ 4. THE ANOMALOUS INCREASE OF TRM

As an example of Case (1) in § 3, where the participating ferromagnetic minerals are both Ti–Mt, we have conducted a detailed study on the anomalous increase (AI) phenomenon of TRM.† Although we have previously found that some Ti–Mt sand derived from biotite rhyolite pumice of Niisima Island shows the AI phenomenon (Nagata 1953 b) we have used, in the present study, a Niisima Ti–Mt which does not show the AI phenomenon in its original state. By using this sample, we were able to observe the mechanism of this phenomenon by the heat treatment more clearly. The thermomagnetic characteristics of the sample before and after the heat treatment at 650°c for 3·5 hours in air are shown in

---

† The intensity of the ordinary TRM undergoes a monotonous decrease when the sample is heated in a non-magnetic space. But the TRM of some Ti–Mt is known to show an increase in the thermal demagnetization. This phenomenon is called the anomalous increase of TRM.

Fig. 6 (*a*)

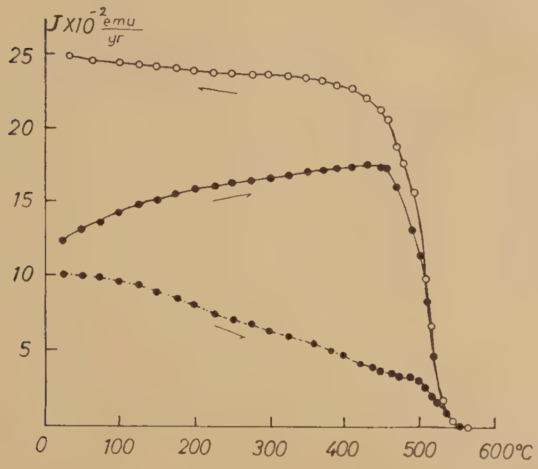

Thermomagnetic characteristics of the original Niisima Ti–Mt sample: full circles: magnetization in the heating process in $H=2{\cdot}0$ oe. Hollow circles: mode of development of TRM in $H=2{\cdot}0$ oe. Broken line: thermal decay of TRM in a non-magnetic space.

Fig. 6 (*b*)

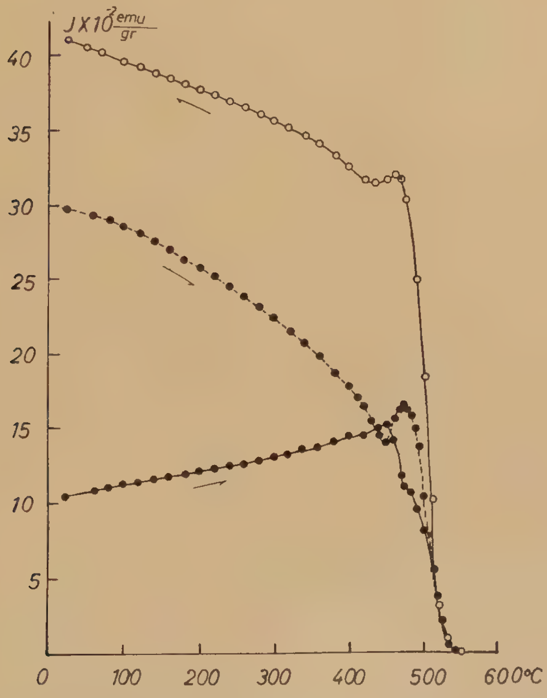

Thermomagnetic characteristics of the Niisima sample heat treated at 650°c for 3·5 hours in air. The thermal decay curve of TRM reveals the anomalous increase at 480°c. Symbols are the same as in fig. 6 (*a*).

figs. 6 (*a*) and (*b*), in which the appearance of the AI due to the treatment is demonstrated. The thermal decay curve of the TRM reveals a marked AI phenomenon at 480°c in fig. 6 (*b*). By the thermal change curve of the reversible magnetization in this figure, two distinct Curie points can be identified at 470°c and 540°c. Figure 7 shows thermal decay of the partial TRM ($J^{505°}_{550°,\, H=2\cdot0\,\mathrm{oe}}$) for the original sample and the samples which underwent the heat treatment for different durations. On the other hand, it was also shown that the similar treatment in an evacuated sealed tube does not produce the AI phenomenon. Judging from these experimental results, it may be concluded that the constituent with a Curie point at 540°c (*H*-constituent) has been developed by the oxidation of the constituent with a lower Curie point (*L*-constituent) in the course of the heat treatment in air, and the coexistence of ferromagnetic minerals thus produced is the origin of the AI phenomenon. When the sample is heat treated in air at 650°c for 12 hours, the AI phenomenon disappears again and its thermomagnetic curve shows that this sample now consists of the *H*-constituent exclusively ; all the *L*-constituent having been oxidized to the *H*-constituent. In fig. 1 and table 2, the chemical composition and the crystal parameter of some typically heat treated samples are listed.† Plates 10, 11 and 12 are the photomicrographs of the polished surfaces of the original and the heat treated samples. All of these data can be regarded as proving the mechanism described above.

Table 2. Properties of the Niisima Samples Examined

Sample	Chemical composition in mol. %			Lattice parameter *a* in Å	Curie point
	FeO	Fe_2O_3	TiO_2		
Original	52·24	39·52	8·24	8·408±0·0009	470°c
Heat treated for 23 hours in air at 550°c	46·70	44·74	8·55	8·395±0·001 8·404±0·002	540°c 470°c
Heat treated for 12 hours in air at 650°c	43·88	47·40	8·71	8·394 8·404 (faint)	540°c

§ 5. THERMAL CHANGE OF COERCIVE FORCE OF FERROMAGNETIC MINERALS COMPOSED OF TWO PHASES

Figure 8 shows the thermal change of the coercive force of the ferromagnetic mineral samples known to be composed of two closely intergrown ferromagnetic minerals. The cross marks represent the $H_c(T)$ of the

---

† It is interesting that the *H*-constituent also belongs to the Ti–Mt phase with the spinel structures, in spite of the fact that the chemical composition deviates considerably from the magnetite–ulvöspinel join (fig. 1 and table 2).

Fig. 7

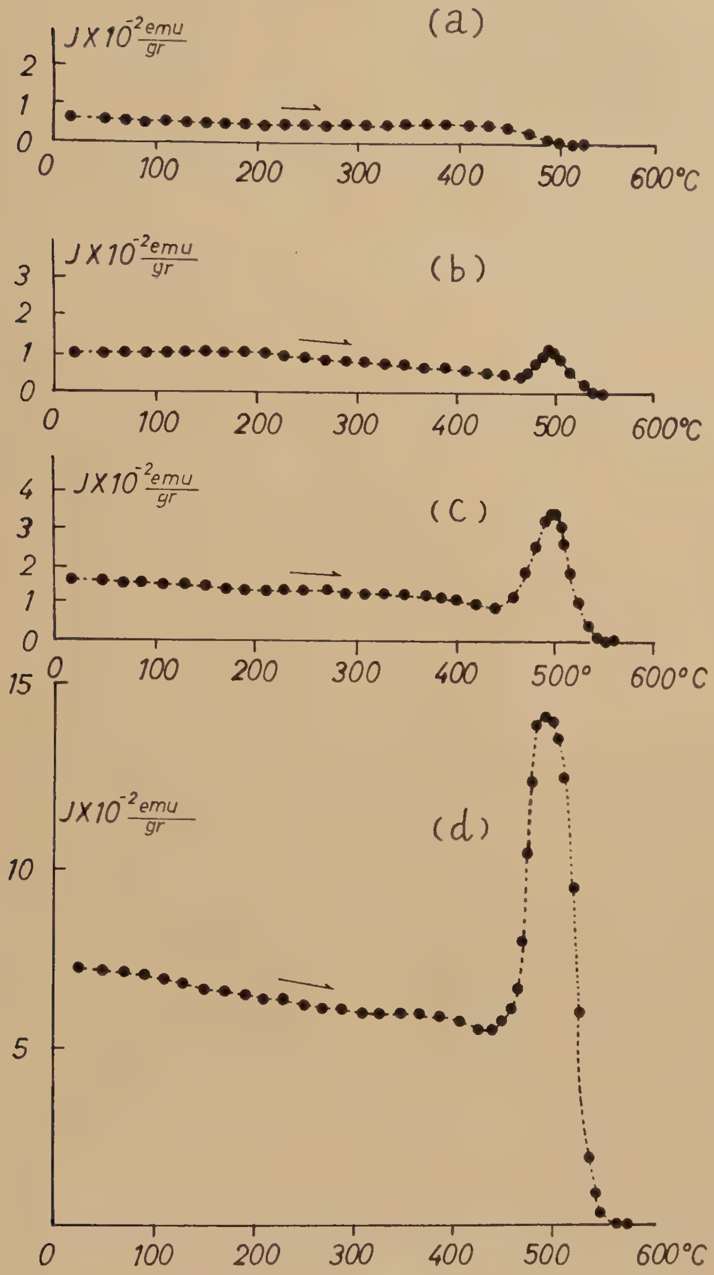

Thermal decay curves of the partial TRM ($J^{505°}_{550°,\ H=2\cdot0\text{ oe}}$) in a non-magnetic space. The amount of the anomalous increase depends on the length of the heat treatment.

(*a*) : original sample of Niisima Ti–Mt,
(*b*) : sample heat treated at 550°c in air for 0·5 hour,
(*c*) : sample heat treated at 550°c in air for 2 hours,
(*d*) : sample heat treated at 550°c in air for 10 hours.

Himesima ferromagnetic ilmenite sample (250°c$>T_s>$230°c) heat treated at 660°c in an open-air tube for 10 minutes to acquire the Haruna-type RTRM (§ 2), and the full circles represent the $H_c(T)$ of the Niisima Ti–Mt sand, heat treated at 650°c in air for 3·5 hours to acquire the capability of showing the anomalous increase of TRM (§ 4). The measurement of the coercive force was conducted by the ballistic method and the maximum external magnetic field furnished by a solenoid-coil was about 750 oe. In this figure, it is clearly observed that the coercive force of both samples abruptly increases at a temperature nearly equal to the lower Curie point of the two phases concerned. This increase in the coercive force may be considered to be due to the fact that, at temperatures higher than the lower Curie point, the phase that is now non-ferromagnetic acts in the same way as the non-magnetic inclusions as in the cases described in Case (2) of § 3.

Fig. 8

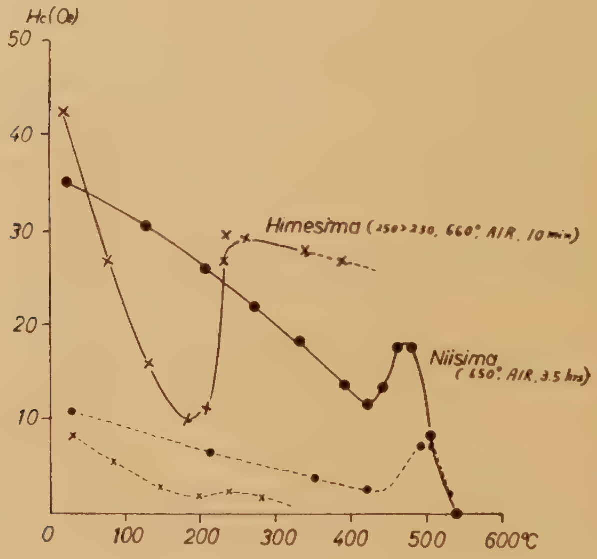

Thermal change of the coercive force.

Cross marks. Himesima ferromagnetic ilmenite (250°c$>T_s>$230°c), heat treated at 660°c in air for 10 minutes to acquire the RTRM characteristics.

Full circles. Niisima titanomagnetite, heat treated at 650°c in air for 3·5 hours to acquire anomalous increase character of TRM.

Corresponding broken lines are the $H_c(T)$ of original samples.

§ 6. Conclusion

The role of magnetic interaction between coexisting minerals in the course of the production of TRM has been examined experimentally on the system FeO–Fe_2O_3–TiO_2. The general conclusions obtained may be summarized as follows :

(1) When two ferromagnetic minerals coexist within a grain in the state of finely laminated structures, the magnetic interaction is negative. Examples of this are furnished by the Haruna-type RTRM, in which the two participating minerals are believed to be both ferromagnetic ilmenites. The reversal of natural remanent magnetism during thermal demagnetization revealed in some titanomagnetites reported by Kawai *et al.*, and the reverse natural remanence of the Adirondack rocks found by Buddington and Balsley may also be included in this case.

(2) When non-ferromagnetic minerals are intergrown with the ferromagnetic ones, both the coercive force and the TRM of the sample are intensified. The increase of the intensity of TRM may be related to the increase of the coercive force in the manner suggested by Néel. An empirical relation,

$$J_{tr}(T_0)/J_s(T_0) \propto H_c(T_0)$$

has been obtained for the heat treated ferromagnetic ilmenite containing titan–hematite and rutile. The abrupt increase in the coercive force of the samples, containing two ferromagnetic minerals, near the lower Curie point was indicated as an example of this case.

These results seem to confirm the validity and the necessity of the tests proposed by us previously for determining whether or not a given rock can be used for palaeomagnetic purposes.

REFERENCES

AKIMOTO, S., 1955, *Japanese J. Geophys.*, **1,** No. 2.

BALSLEY, J. R., and BUDDINGTON, A., 1954, *J. Geomag. Geoelec.*, **6,** 176.

CURNOW, C. E., and PARRY, L. G., 1956, *J. Proc. Roy. Soc. New S. Wales*, **89,** 64.

GRABOVSKY, M. A., and PUSHKOV, A. H., 1954, *Izvest. Akad. Nauk. S.S.S.R.*, ser. Geofiz., No. 4, 320.

GRAHAM, J. W., 1953, *J. Geophys. Res.*, **58,** 243.

KAWAI, N., 1956, *Proc. Japan Acad.*, **32,** 464.

KAWAI, N., and KUME, S., 1956, *Proc. Japan Acad.*, **32,** 459.

KAWAI, N., KUME, S., and SASAJIMA, S., 1954 a, *Proc. Japan Acad.*, **30,** 588 ; 1954 b, *Ibid.*, **30,** 864.

KAWAI, N., KUME, S., and YASUKAWA, K., 1956, *Proc. Japan Acad.*, **32,** 455.

KUNO, H., 1954, *Amer. Miner.*, **39,** 30.

NAGATA, T., 1952, *Nature, Lond.*, **169,** 704 ; 1953 a, *Ibid.*, **172,** 850 ; 1953 b, *Rock Magnetism* (Tokyo : Maruzen Co. Ltd.).

NAGATA, T., and AKIMOTO, S., 1956, *Geofis. pura e appl.*, **34,** 36.

NAGATA, T., AKIMOTO, S., and UYEDA, S., 1953 a, *Nature, Lond.*, **172,** 630 ; 1953 b, *J. Geomag. Geoelec.*, **5,** 168.

NAGATA, T., AKIMOTO, S., UYEDA, S., MOMOSE, K., and ASAMI, E., 1954, *J. Geomag. Geoelec.*, **6,** 182.

NAGATA, T., and OZIMA, M., 1955, *J. Geomag. Geoelec.*, **7,** 105.

NAGATA, T., and UYEDA, S., 1956, *Nature, Lond.*, **177,** 179.

NAGATA, T., UYEDA, S., and AKIMOTO, S., 1952, *J. Geomag. Geoelec.*, **4,** 22.

NAGATA, T., UYEDA, S., AKIMOTO, S., and KAWAI, N., 1952, *J. Geomag. Geoelec.*, **4,** 102.

NÉEL, L., 1951, *Ann. Geophys.*, **7,** 90 ; 1955, *Advanc. Physics*, **4,** 191.

NICHOLLS, G. D., 1955, *Advanc. Physics*, **4,** 113.

PARRY, J. H., 1954, *J. Geomag. Geoelec.*, **6,** 210.

UYEDA, S., 1955, *J. Geomag. Geoelec.*, **7,** 9 ; 1956, *Ibid.*, **8,** 39.

Magnetic Properties of Ferromagnetic Oxide Minerals as a Basis of Rock-Magnetism

By S. Akimoto
Geophysical Institute, Tokyo University

Although a considerable progress has been made both in the understanding of the magnetic behaviour of rocks and in the geophysical application of the magnetization of rocks, the most fundamental problems relating to the magnetic carrier of rocks have been left unsolved for a long time. It is needless to say that the magnetic properties of rocks are due almost

Fig. 1

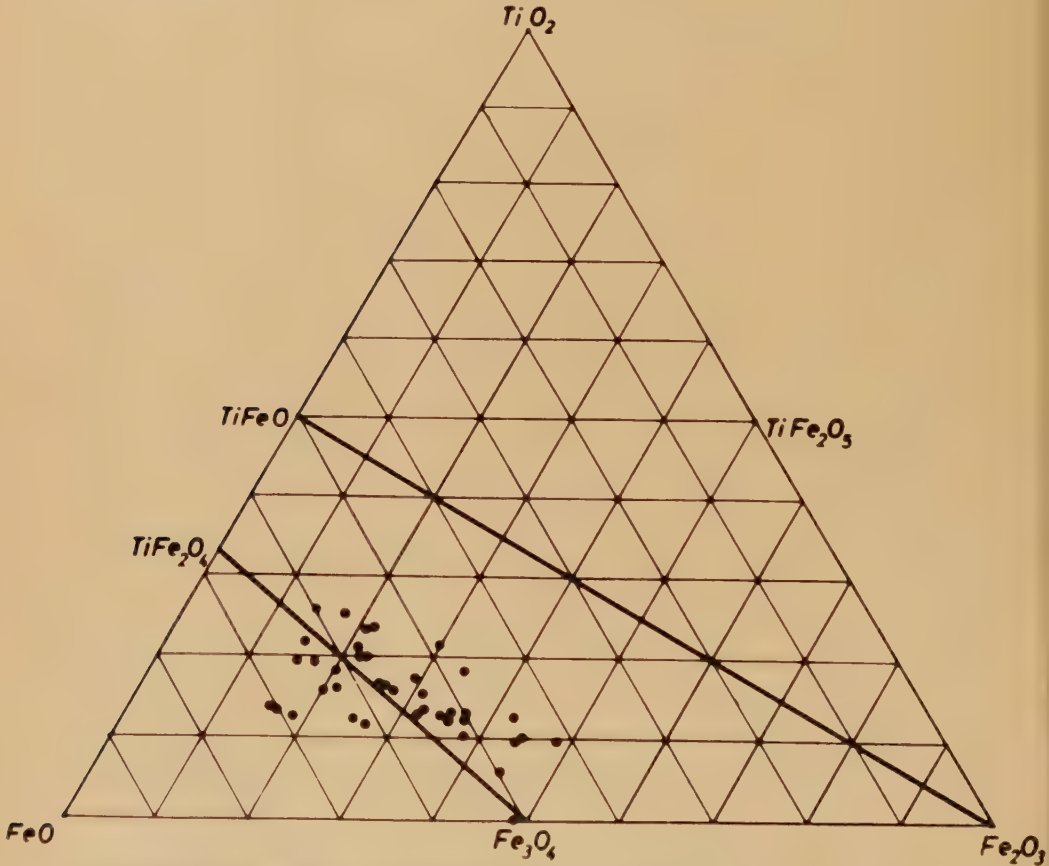

Chemical composition of titanomagnetites represented on a FeO–Fe_2O_3–TiO_2 diagram in mol per cent.

entirely to those of the ferromagnetic minerals scattered with a very small proportion among the practically non-magnetic rock-forming mineral elements. One of the peculiarities by which the problems of the magnetic properties of rocks are distinguished is that the carriers of magnetism are the various more or less pure oxides or sulphide of iron. The ferromagnetic oxide minerals are usually more abundant in rocks, than sulphides, and consequently have a greater influence on the magnetic properties. Hence it seems that one of the most fundamental problems in the study of rock-magnetism is to examine the magnetic properties of ferromagnetic oxide minerals on the basis of the modern physics of matter by taking their crystallographic and chemical properties into consideration.

The ferromagnetic minerals examined in this study are those which are separated from a large number of typical igneous rocks in Japan. The ferromagnetic properties of these rocks could be attributed mostly to the ferromagnetism of titanomagnetites having a spinel type crystal structure. Generally speaking, the ferromagnetism of more than 99% of Japanese igneous rocks at atmospheric temperature comes from that of titanomagnetites, and the remaining 1% or less originates in the ferromagnetic phase of ilmenite–hematite series having a rhombohedral crystal structure.

Expressing the chemical composition of the titanomagnetites specimens on the diagram of the FeO–Fe_2O_3–TiO_2 ternary system shown in fig. 1 it is found that they are distributed around the straight line connecting $TiFe_2O_4$ and Fe_3O_4.

So long as the data examined in the present work are concerned, the calculated content of ulvöspinel ($TiFe_2O_4$) in the titanomagnetite ranges from 0% to about 70%, resulting in the changes in the lattice parameter, intensity of saturation magnetization, and Curie point, in the ranges from 8·38 Å to 8·49 Å, from 93 e.m.u./g to 14 e.m.u./g, and from 580°c to 120°c respectively. The relationships among these quantities are shown in figs. 2, 3, 4, 5 and 6. Here empirical formulae for the relations between chemical composition and lattice parameter, between chemical composition and saturation magnetization, between lattice parameter and Curie point, and between saturation magnetization and Curie point, are given approximately as follows :

$$a - 8{\cdot}38 = \frac{0{\cdot}11}{0{\cdot}7}\,y,$$

$$93 - \sigma_s = \frac{78}{0{\cdot}7}\,y,$$

$$580 - \Theta = \frac{460}{0{\cdot}11}\,(a - 8{\cdot}38),$$

$$580 - \Theta = \frac{460}{78}\,(93 - \sigma_s),$$

where a, y, Θ and σ_s denote respectively the lattice parameter in Å.u., the content of $TiFe_2O_4$ in the assumed solid solution between ulvöspinel and magnetite, the Curie point in °c, and the intensity of saturation magnetization at the atmospheric temperature in e.m.u./g. A series of values of the

Fig. 2

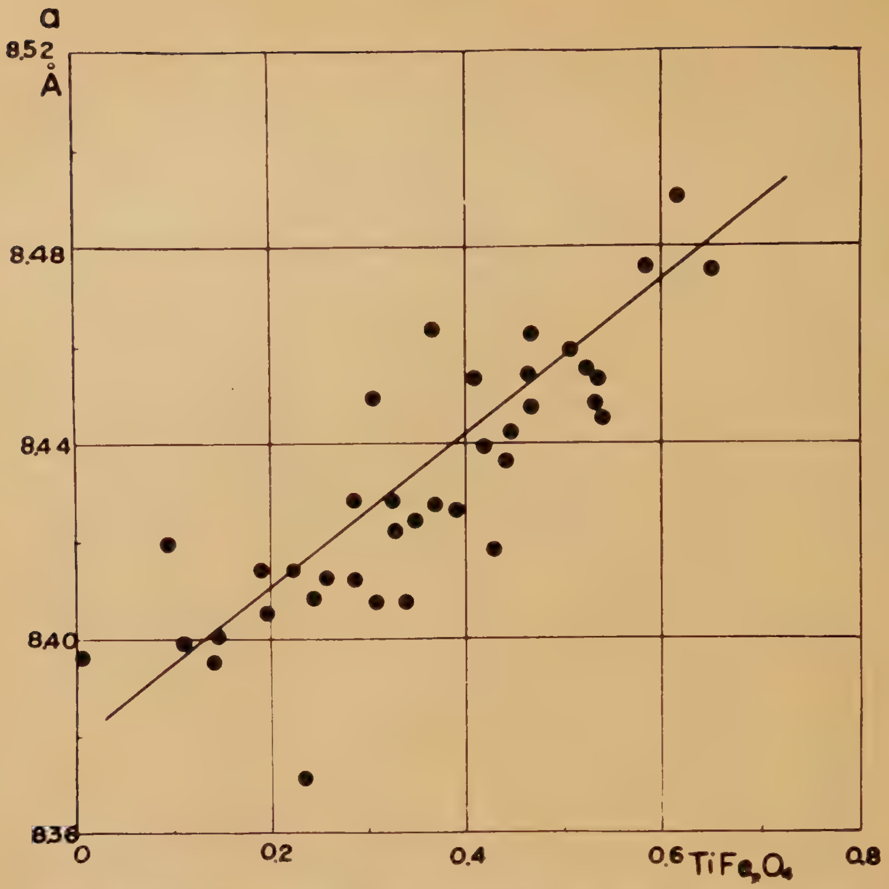

Lattice parameter of titanomagnetites as dependent on the content of $TiFe_2O_4$.

Fig. 3

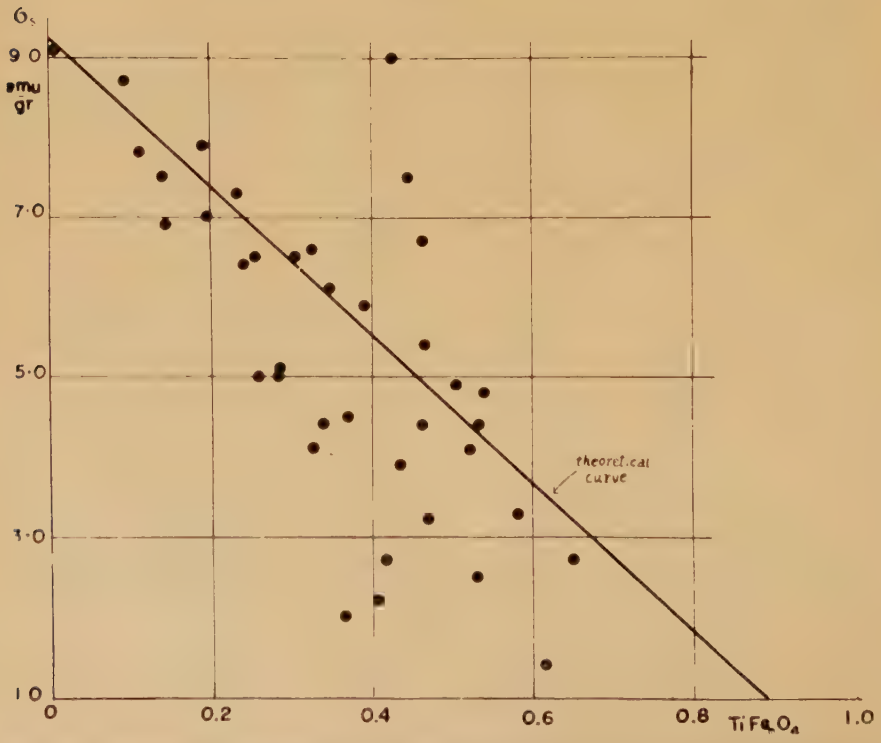

Specific intensity of saturation magnetization of titanomagnetites as dependent on the content of $TiFe_2O_4$.

Fig. 4

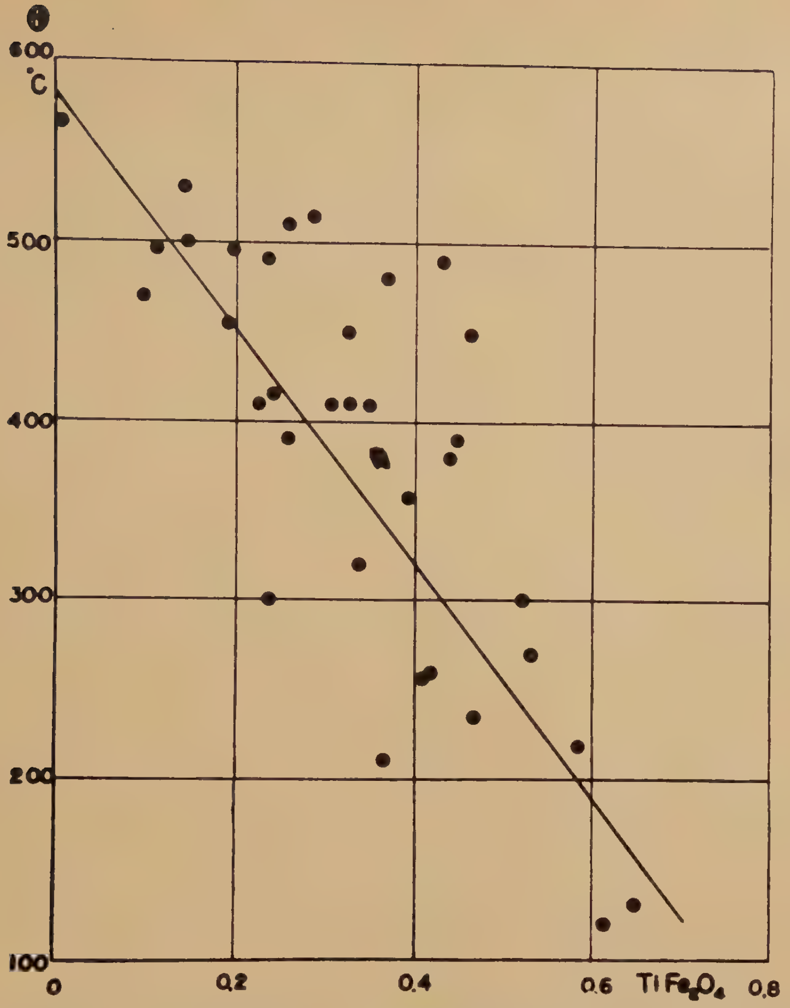

Curie point of titanomagnetites as dependent on the content of $TiFe_2O_4$.

Fig. 5

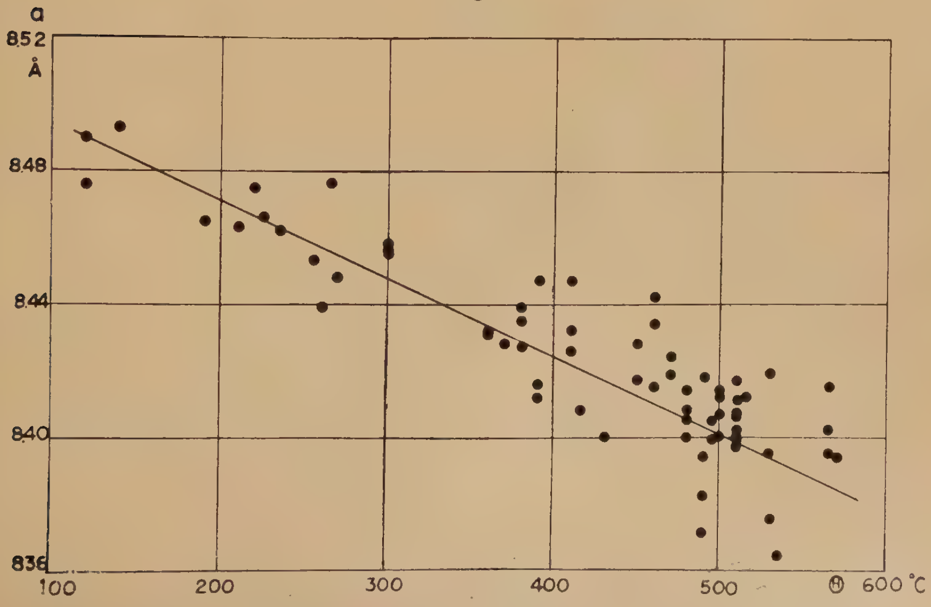

Curie point of titanomagnetites as dependent on lattice constant.

Fig. 6

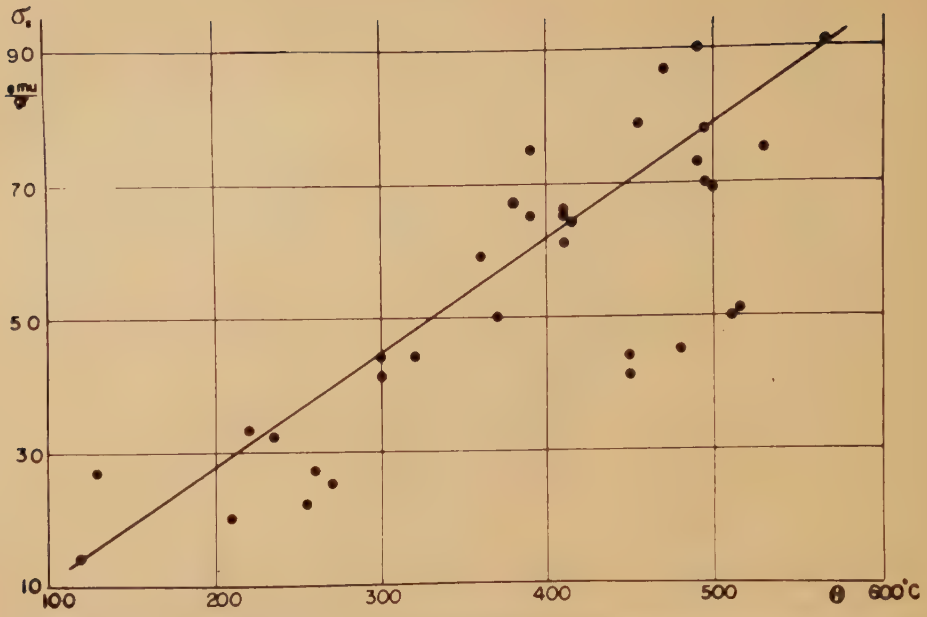

Specific intensity of saturation magnetization of titanomagnetites as dependent on Curie point.

Fig. 7

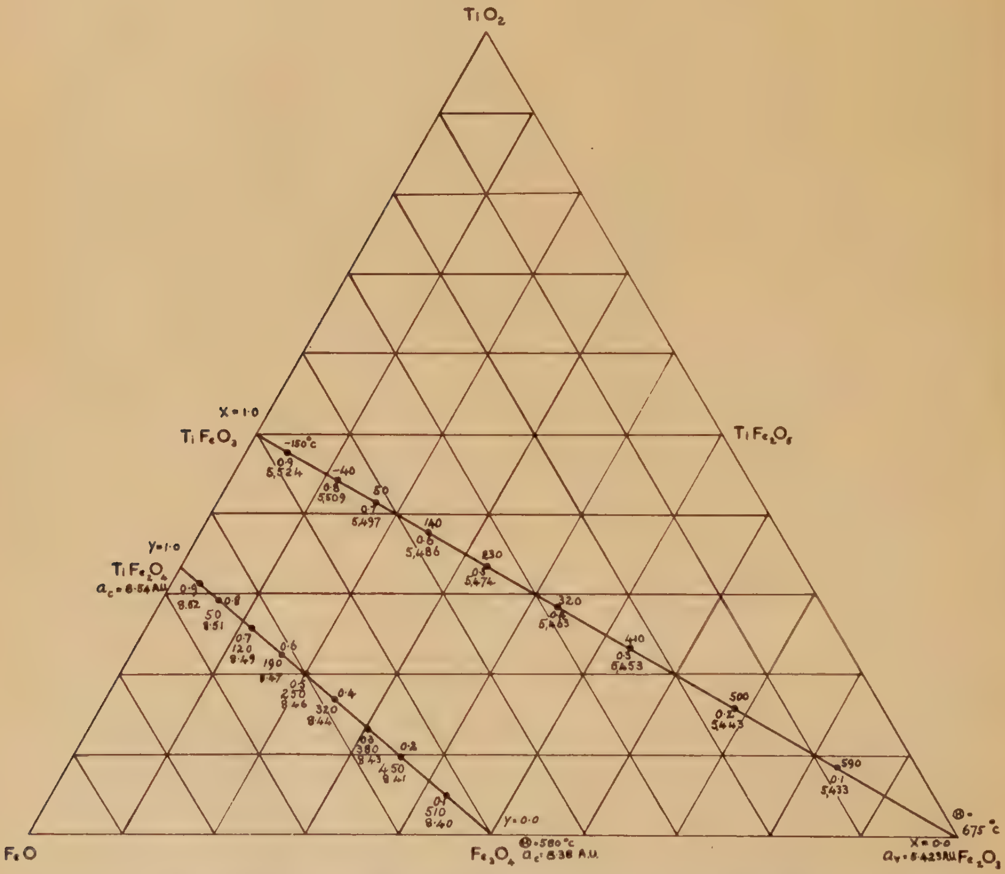

Mutual relations among lattice parameter, Curie point and chemical composition of both titanomagnetites and ilmenite–hematite series minerals, represented on a $FeO–Fe_2O_3–TiO_2$ ternary diagram.

crystal parameter and the Curie point is expressed in figures at the point corresponding to the chemical composition on the $TiFe_2O_4$–Fe_3O_4 line of the FeO–Fe_2O_3–TiO_2 ternary system shown in fig. 7.

The frequency of appearance of titanomagnetites having different contents of ulvöspinel composition, in the Japanese igneous rocks, is graphically illustrated in fig. 8. Thus if in an igneous rock we can determine any one of the following : chemical composition, lattice parameter of crystal, intensity of saturation magnetization or Curie point of the ferromagnetic minerals, we can derive the approximate values of the remaining three.

Fig. 8

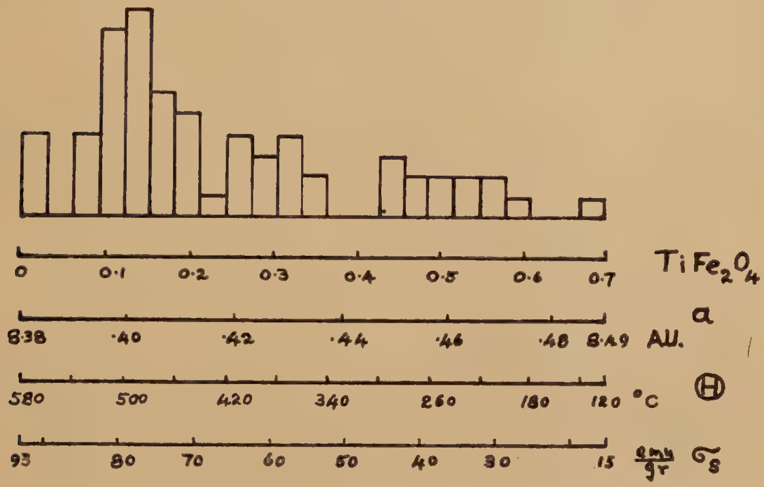

Frequency distribution of titanomagnetites in igneous rocks.

A new discovery in the present study may be the existence of a ferromagnetic phase in the solid solutions between ilmenite and hematite. Since even the small amount of this phase may have a large influence upon the magnetic properties of rocks, especially in the characteristics of thermoremanent magnetism, and since the origin of the ferromagnetism of this Il–Ht series connecting the practically non-magnetic end members must be examined from the view point of ferrimagnetism, the magnetic properties of a large number of natural and synthetic specimens of composition $[x\ TiFeO_3 \,.\, (1-x)\ Fe_2O_3]$ were investigated over the whole range of x. Generally speaking, an ensemble of ferromagnetic minerals in a rock specimen consists of a large number of grains of different composition, with the result that the magnetic properties represent those of the average composition of the ensemble. In the present study, therefore, some of the mineral grains of Il–Ht series separated from each rock specimen were further classified as uniquely as possible with respect to Curie point, with the help of a thermo-magnetic separation method.

The chemical composition of all the specimens examined here are also shown in the FeO–Fe_2O_3–TiO_2 ternary diagram as illustrated in fig. 9, changing continuously along the line connecting the hematite and ilmenite. From the results of chemical and crystallographic analysis and of measurements of various magnetic properties, it was found that the Il–Ht series, $xFeTiO_3(1-x)Fe_2O_3$, at the atmospheric temperature

Fig. 9

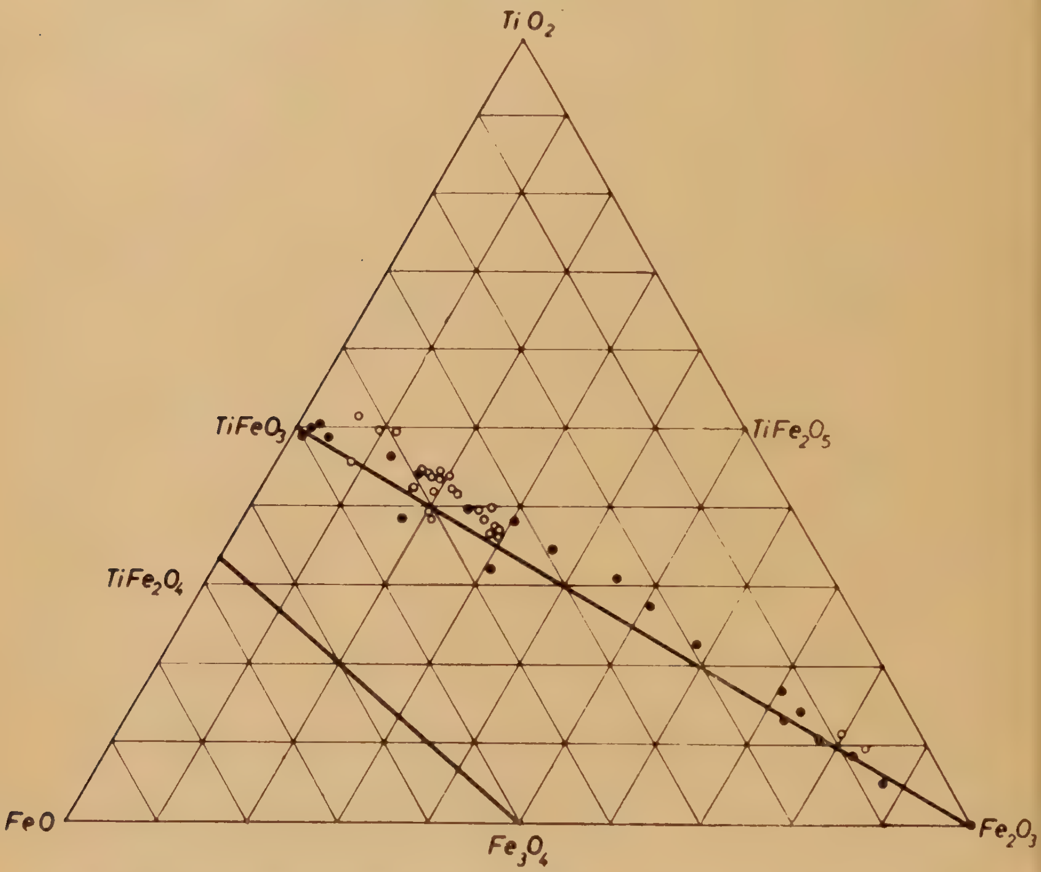

Chemical composition of ilmenite–hematite series minerals represented on a FeO–Fe_2O_3–TiO_2 diagram in mol per cent.
○natural mineral specimens. ●synthetic specimens.

can be classified into three groups: namely (i) feebly ferromagnetic region of $0 < x < 0{\cdot}55$; (ii) ferromagnetic region of $0{\cdot}55 \leq x \leq 0{\cdot}75$; and (iii) paramagnetic region of $0{\cdot}75 \leq x < 1$. An occurrence of ferromagnetism for the specimens of $0{\cdot}75 \leq x \leq 1$ at the lower temperature was further established. The relations between the chemical composition and the lattice parameter and between the chemical composition and Curie point

Fig. 10

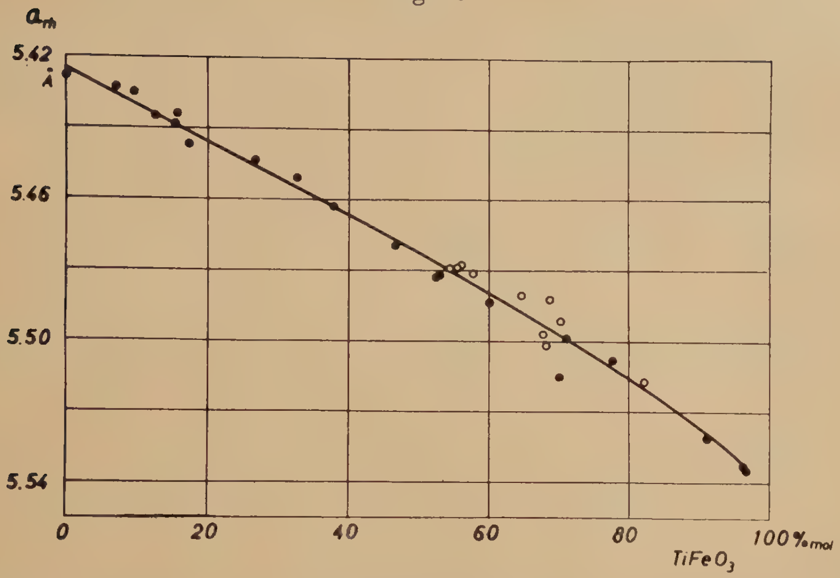

Lattice parameter of ilmenite–hematite series minerals as dependent on the content of $TiFeO_3$.

○ Natural mineral specimens. ● Synthetic specimens.

Fig. 11

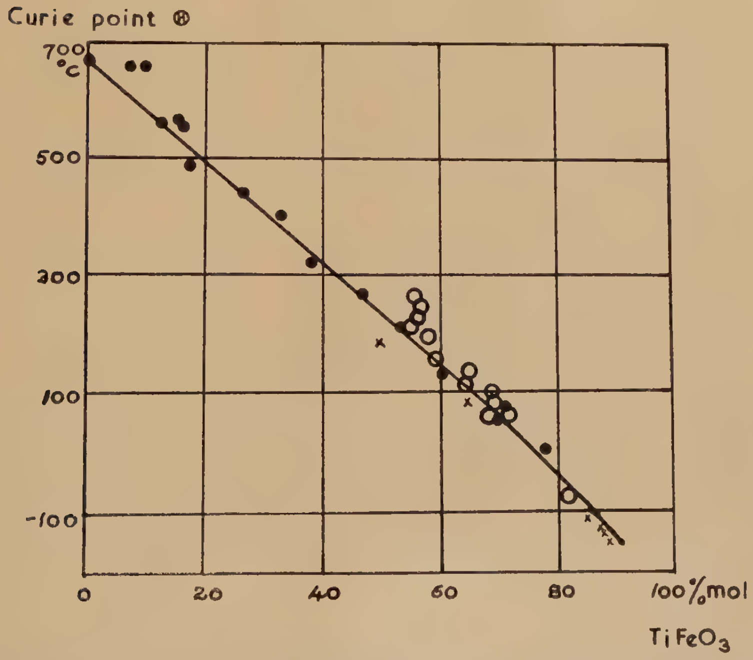

Curie point of ilmenite–hematite series minerals as dependent on the content of $TiFeO_3$.

○ Natural mineral specimens. ● Synthetic specimens.

× Kume's specimen (Kume 1955).

are given in figs. 10 and 11 respectively. These relations are summarized again in fig. 7 where mutual relations among the lattice parameter, the Curie point and the chemical composition are expressed in figures on the $FeTiO_3$–Fe_2O_3 line of the FeO–Fe_2O_3–TiO_2 ternary system.

Assuming that the structure of Il–Ht series in the process of the substitution of $2Fe^{3+}$ by Fe^{2+} and Ti^{4+} is given by

$$\overset{\text{A-site}}{\overrightarrow{(Fe^{3+})}}\ \overset{\text{B-site}}{\overleftarrow{(Fe^{3+})}}\,O_3 \to \overrightarrow{\begin{pmatrix}Fe^{3+}_{1-x}\\ Ti^{4+}_{x}\end{pmatrix}}\overleftarrow{\begin{pmatrix}Fe^{3+}_{1-x}\\ Fe^{2+}_{x}\end{pmatrix}}O_3 \to (Ti^{4+})(Fe^{2+})O_3,$$

the Bohr magneton number, n_B, per one molecule of $xFeTiO_3 \cdot (1-x)Fe_2O_3$, becomes $n_B=4x$. It seems likely however that the above-mentioned

Fig. 12

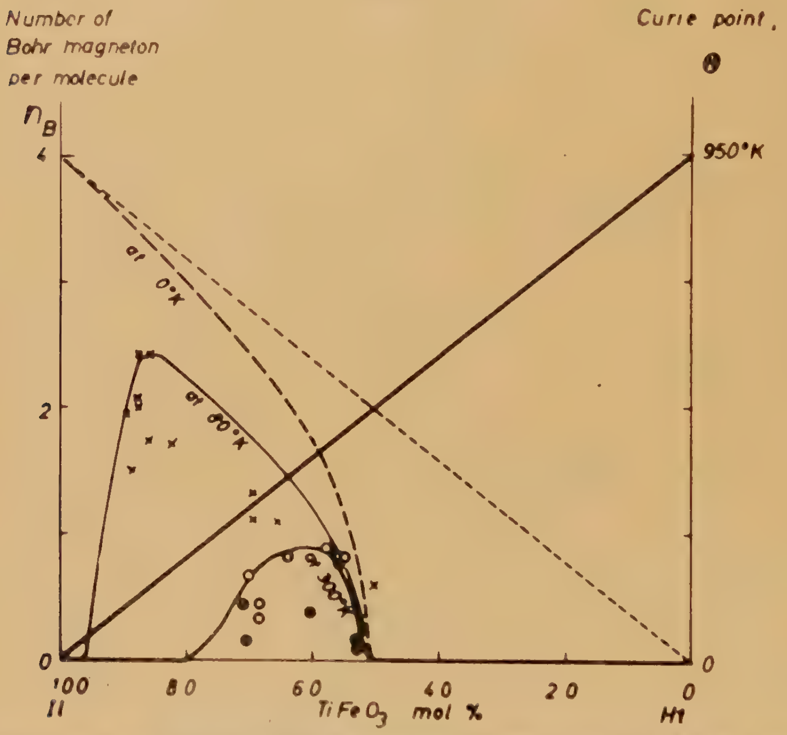

Relations between the intensity of saturation magnetization of the ilmenite–hematite series and the chemical composition at various temperatures.

○ Natural mineral specimens. ● Synthetic specimens.
× Kume's specimen (Kume 1955).

ordering of Ti^{4+} and Fe^{2+} hardly takes place in the range of $0 \leqq x \leqq 0{\cdot}5$ and Ti^{4+} and Fe^{2+} take their positions at random in A and B sub-lattices because the composition is rather near that of hematite, with the result that the Il–Ht series keeps its antiferromagnetic configuration for

$0 \leqslant x \leqslant 0{\cdot}5$, only feeble ferromagnetism appearing owing to disturbances in the antiferromagnetic coupling. On the contrary, the Il–Ht series may approach an ordered state when x becomes larger than 0·5. If we assume the above model as the origin of magnetism, we may write approximately,

$$n_B \simeq 0 \text{ for } 0 < x < 0{\cdot}5$$

$$n_B \leqq 4 \text{ for } 0{\cdot}5 < x < 1.$$

Figure 12 shows the relations between the intensity of saturation magnetization of the Il–Ht series and the chemical composition at various temperatures.

Fig. 13

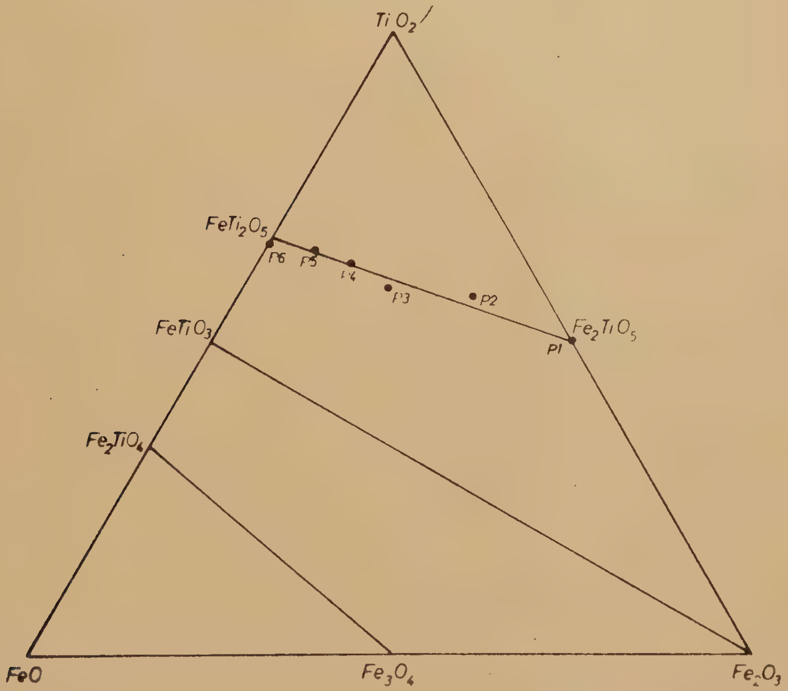

Chemical composition of $TiFe_2O_5$–Ti_2FeO_5 series minerals represented on a FeO–Fe_2O_3–TiO_2 diagram in mol per cent.

In the course of comprehensive research on crystallographic and magnetic properties of FeO–Fe_2O_3–TiO_2 ternary system, we have recently succeeded in synthesis of $TiO_2 . Fe_2O_3$–$2TiO_2 . FeO$ solid solution series, and have examined the magnetic and crystallographic properties of the samples of this series.

The chemical composition of these synthetic $TiO_2 . Fe_2O_3$–$2TiO_2 . FeO$ series solid solutions is illustrated on the diagram of the FeO–Fe_2O_3–TiO_2 ternary system shown in fig. 13. In the x-ray spectrograms of all the specimens, no trace of the ilmenite-hematite series minerals or TiO_2

could be found, but a single phase, the crystal structure of which is very much like that of pseudobrookite, was markedly observed. The crystal structure of this $TiO_2 . Fe_2O_3$–$2TiO_2 . FeO$ series should be regarded as the orthorhombic structure, the parameters *a*, *b*, *c* becoming larger as the $2TiO_2FeO$ content increases. Figure 14 shows the relation between the volume of a unit cell of $TiO_2 . Fe_2O_3$–$2TiO_2 . FeO$ mineral series and the content of $2TiO_2 . FeO$.

Fig. 14

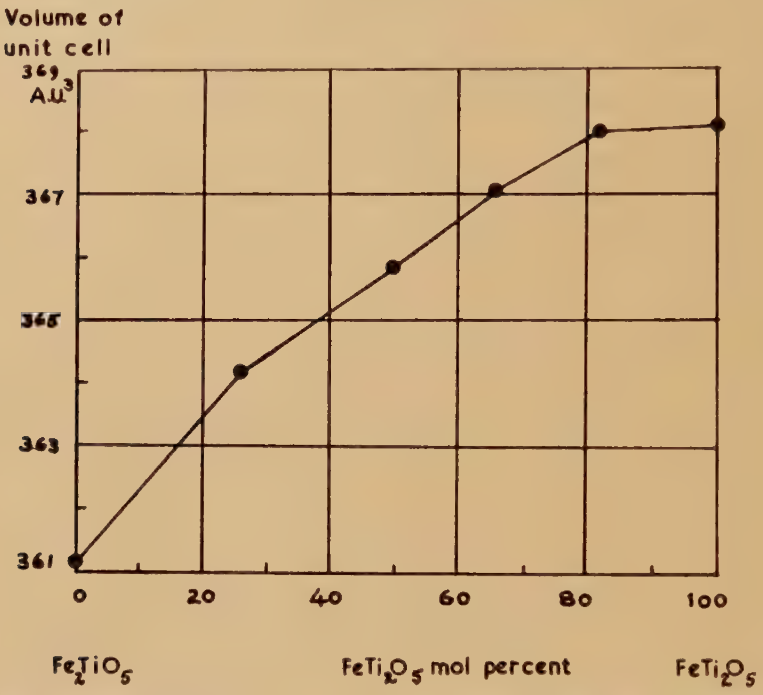

Relation between the volume of a unit cell of $TiFe_2O_5$–Ti_2FeO_5 mineral series and the content of Ti_2FeO_5.

From the measurement of magnetization curve, it seems that these synthetic $Fe_2O_3 . TiO_2$–$2TiO_2 . FeO$ series specimens have a paramagnetic properties at the atmospheric temperature. Hereafter, we must take this new orthorhombic phase into consideration in studying the natural ferromagnetic minerals, especially in interpreting oxidation products of the ilmenite–hematite series minerals or of the titanomagnetites.

REFERENCES

AKIMOTO, S., 1955, *Jap. J. Geophys.*, **1**, No. 2, 1.
NAGATA, T., and AKIMOTO, S., 1956, *Geofis. pura e appl.*, **34**, 36.
Kume, S., 1955, *Proc. Japan Acad.*, **31**, 709.
AKIMOTO, S., NAGATA, T., and KATSURA, T., 1957, *Nature, Lond.*, **179**, 37.

The Problem of Reversed Magnetizations and its Study by Magnetic Methods

By J. H. Parry
Physics Department, King's College, Newcastle-upon-Tyne

The measurement of directions of natural remanent magnetization in rocks and the interpretation of these in terms of the ancient geomagnetic field is the most important part of rock magnetism. It is difficult to conceive of any agency other than the earth's field of sufficient constancy to account for the observed closeness of grouping of the directions within a formation. This close grouping has been found chiefly in red sandstones and plateau lavas neither of which is a common rock ; extension of the work will eventually depend on the use of other rocks. If a lack of consistency appears in the measurements from one formation, experimental work on the magnetic properties is especially necessary. This lack of consistency may be a wide scattering of directions, a planar spread as observed by Runcorn (1956), or a reversal. Questions arise as to why these effects occur, to what they are due, if they do not actually represent ancient field directions, and as to whether, by some physical, chemical, or mathematical means based on a better understanding of the nature and origin of the magnetization, a close consistent grouping can be obtained from them. The answers to these questions will enable unsuitable rocks to be avoided in collections and useful results to be obtained from partially stable rocks, or from rocks with complex magnetizations, such as those with several components of magnetization acquired at different geological periods. As the remanent magnetic properties of a rock depend on the ferromagnetic minerals which it contains, a knowledge of these minerals is necessary for further progress. Separation of the minerals has its difficulties and disadvantages. Difficulties are the extremely fine grain of the minerals in some rocks, the presence of small scale intergrowth structures, and, in sediments, the existence of iron oxide coatings on silicate grains. Disadvantages arise because the crucial magnetic properties of coercive force, remanence, and stability depend partly on the very features which are destroyed by separation namely the size and arrangement of the grains relative to each other and the texture of intergrowths.

Microscopic study in transmitted and reflected light can identify the different series of solid solutions in the oxide minerals but not the individual members of one series. It is valuable in the study of intergrowths though as the Japanese workers (Uyeda 1955) have shown some of these may be so fine as to demand the use of the electron microscope.

For the best results contributions are needed from each of the several methods of study, but among these purely magnetic measurements should be included. The ferromagnetic minerals have other magnetic properties as well as those of natural remanent magnetization and these could be used to get information about them. Néel (1954) has pointed out the value of magnetic measurements in crystallography, and many of his arguments apply to rocks. Chevallier *et al.* (1954) have, by measurements of Curie Point and saturation magnetization, obtained the chemical compositions of magnetic phases in certain rocks and these agree excellently with those obtained by chemical analysis of carefully separated samples ; the rocks were coarse-grained gabbros, where separation is easier than in basalts, though still laborious. The magnetic properties of initial susceptibility, saturation magnetization, remanence, coercive force and anhysteretic magnetization and their decay with temperature have standard definitions and do not depend on the particular procedure or type of apparatus used to obtain them, an advantage in view of the multiplicity and confusing nomenclature of the experimental methods of rock magnetism. Chevallier (1932) showed that because of the demagnetizing field of each grain, the *initial susceptibility* depends on the shape, arrangement and concentration of the grains rather than on their composition. The *saturation magnetization*, provided a sufficiently high field of the order of 10 000 gauss is used, depends only on the specific saturation intensity of the material of the grains and the amount of this material present regardless of its shape, grain size or distribution. The *Curie Point*, provided again that it is measured in a high field, depends only on the composition of the magnetic material (in such cases as Fe_2O_3—α and γ—the crystal structure is also involved). Considerable information, from the work of Chevallier and of the Japanese school, is now available on the Curie Points and specific saturation intensity of rock-forming ferromagnetic minerals. The factors governing remanence, coercive force and anhysteretic magnetization have been discussed in detail by Néel (1954, 1955) ; texture in the petrological sense of size, shape and arrangement of grains and of inclusions within them, is more important than chemical composition. Information about these factors can be obtained by measuring these magnetic properties.

By courtesy of Professor Chevallier a preliminary attempt has been made to use some of these methods.

Figure 1 shows some of the thermomagnetic curves obtained on Icelandic basalts collected by Hospers (1954). The apparatus used and the interpretation of these curves have been described elsewhere (Chevallier and Pierre, 1932, Nagata 1953, Chevallier *et al.* 1954). A field of about 1000 gauss is used but the scale of magnetization J is not linear owing to the movement of the specimen on the arm of a torsion balance in an inhomogenous field. The heating and cooling curves are shown by arrows. Both reversible and irreversible curves are found but they occur indiscriminately in Recent lavas, and in both normal and reversed Tertiary lavas, a point in favour of the reversal of the geomagnetic field. Most lavas have a Curie Point near 500°c although some have a lower one as well which usually disappears in the cooling curve.

Fig. 1

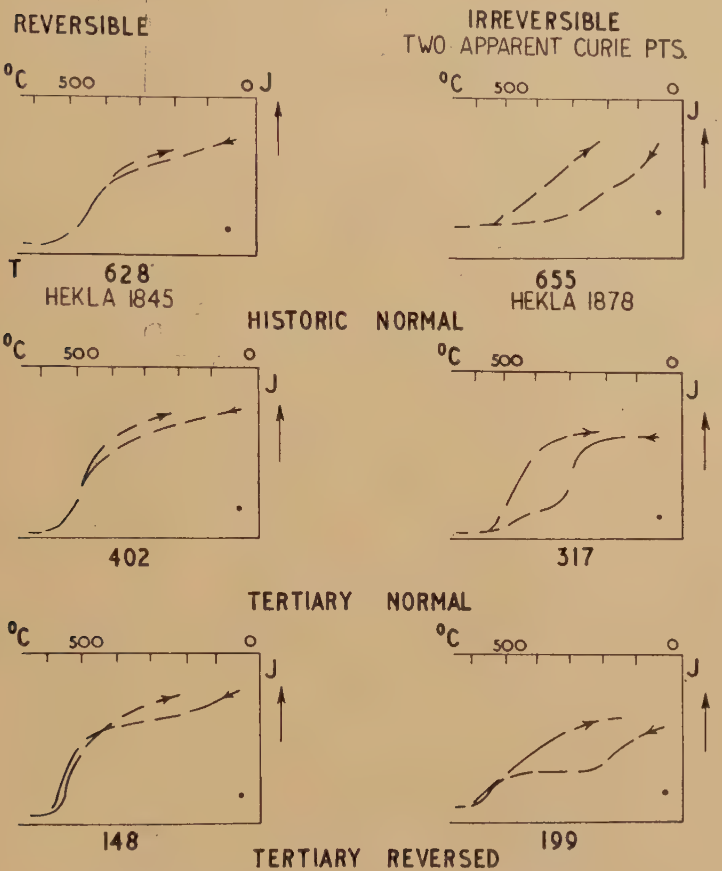

Thermo-Magnetic Curves for Icelandic Basalts.

Figure 2 shows some unusual curves obtained on specimens of a Deccan Trap measured by Irving in 1953. (Irving 1954). The decrease in magnetization at 300°c must represent a Curie Point as the effect is reversible with temperature. Above 350°c there is an increase in magnetization by an amount depending on the time. In all three cases the cooling curves after heating to 650°c and subsequent heating and cooling curves are similar, showing a single Curie Point at about 520°c. Interpreting the Curie Points as due to titano–magnetites, it appears that one of composition 62% Fe_3O_4 (by weight) has been replaced by one of

Fig. 2

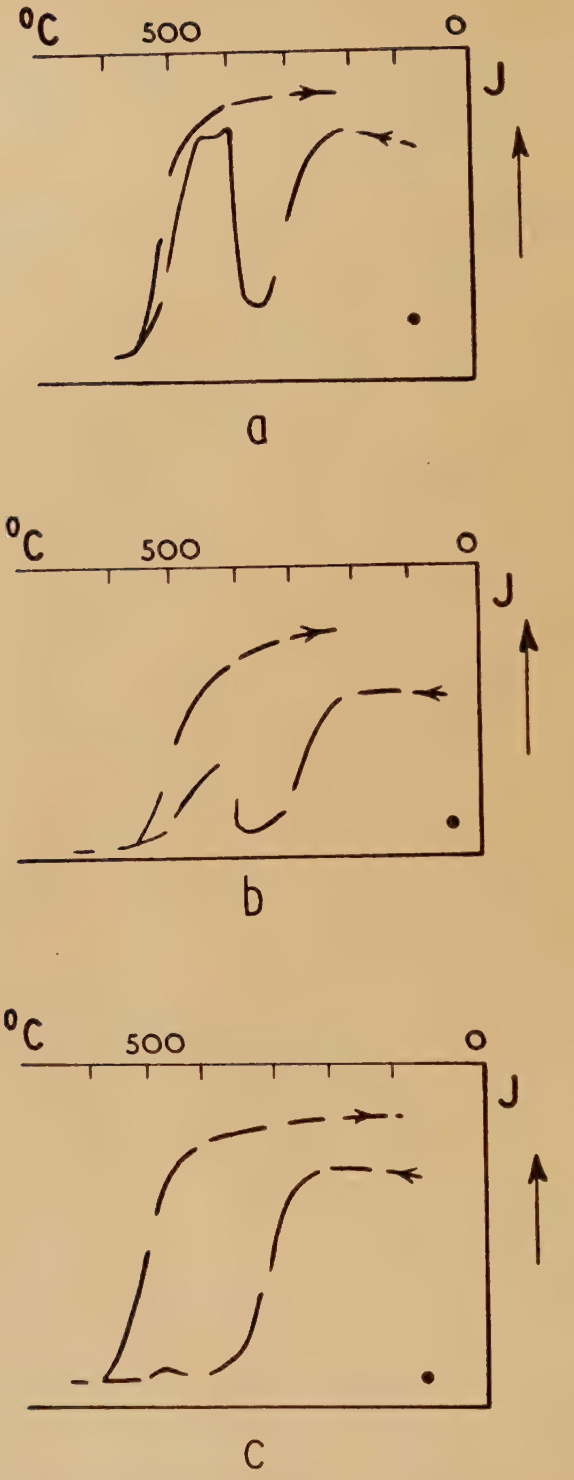

Thermomagnetic Curves for Deccan Trap I.D.I.
(*a*) Slow heating, 350°c to 450°c in 20 min.
(*b*) Normal rate of heating, 20°c to 650°c in 30 min.
(*c*) Fast heating, 300°c to 650°c in 7 min.

composition 90% Fe_3O_4, near that of magnetite (Chevallier *et al.* 1955, p. 364). Exsolution of a titano–magnetite of intermediate composition might produce magnetite and a titano–magnetite of composition near ulvöspinel (Fe_2TiO_4). The saturation magnetization of the separated ferromagnetic mineral fraction (which showed exactly the same phenomena) was measured both before and after heating to 650°c giving 14 e.m.u./gm and 35 e.m.u./gm respectively. The specific saturation intensities of the suggested titano–magnetites are 41 e.m.u./gm and 79 e.m.u./gm. It immediately appears that the separated fraction is not pure, possibly due to magnetite–ilmenite intergrowths. The separate contains $14/41 = 0{\cdot}34$ gm of 300°c material per gm of separate before heating and $35/79 = 0{\cdot}44$ gm of 520°c material after heating. From the compositions of the former the proportion of magnetic Fe_3O_4 molecule in the unheated separate is $14/41 \times 0{\cdot}62 = 0{\cdot}21$ gm/gm and in the heated separate is $35/79 \times 0{\cdot}9 = 0{\cdot}4$ gm/gm. It therefore appears on this interpretation that the amount of Fe_3O_4 molecule in the rock has increased on heating. This can also be the result of an exsolution effect for titano–magnetites containing less than about 35% Fe_3O_4 (by weight) have Curie Points below 0°c and cannot be detected by magnetic measurements at room temperature. It therefore seems possible that two members of the titano–magnetite solid solution series have, on heating, re-exsolved into two new phases close to the end members of the series. This is only a very tentative hypothesis and further work, particularly at low temperature, is necessary.

This rock has reversed magnetization which might have been produced by exsolution. In a single phase possessing remanent magnetization the first crystallites of a new magnetic phase growing by exsolution might be subjected to the reversed demagnetization field of the host and thus become reversely magnetized. Once the crystallites are magnetized further layers added to them will be magnetized in the same direction provided they do not become so large that closure domains can form. The process might continue until the original single phase has been entirely replaced by two phases, one magnetic and reversed and the other non-magnetic at ordinary temperatures. Such a mechanism and the speed of reaction observed in the experiments would need a very fine grained intergrowth. Any intergrowths present are certainly on too fine a scale to be observed in ordinary polished sections either before or after heating (J. Bolfa, private communication).

It is possible that exsolution phenomena of this sort are responsible for the irreversibility of the thermo–magnetic curves for some Iceland basalts but these cases are complicated by the presence of two separate Curie Points (or groups of Curie Points). Perhaps the exsolution has not been completed.

Two other examples of the value of Curie Point determinations in very different types of rocks are illustrated in fig. 3. X-ray powder photographs of the ferromagnetic fraction of Torridonian sandstones indicated haematite only, within the limits of the method. The thermo–magnetic curve shows a sharp drop in magnetization at 575°c, the Curie Point of magnetite, as well as one at 675°c, the Curie Point of haematite. Although the magnetization scale is not linear it is obvious that magnetite is present, in an amount which magnetically is probably more important than the amount of haematite. Which mineral is responsible for the natural remanent magnetization remains to be discovered perhaps by thermal destruction of the natural magnetization.

Fig. 3.

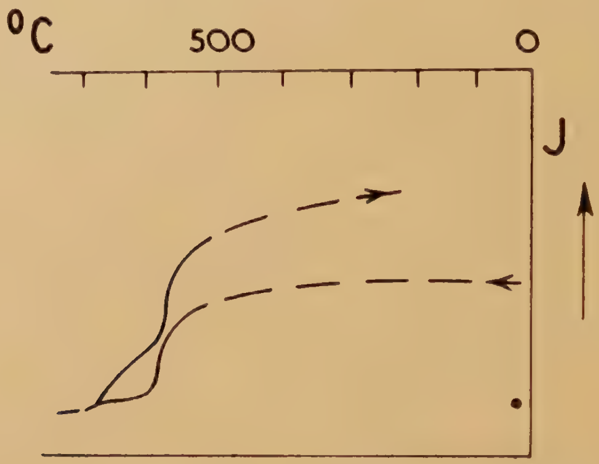

Torridonian Sandstone M.C. 17, 2 Haematite-rich Band.

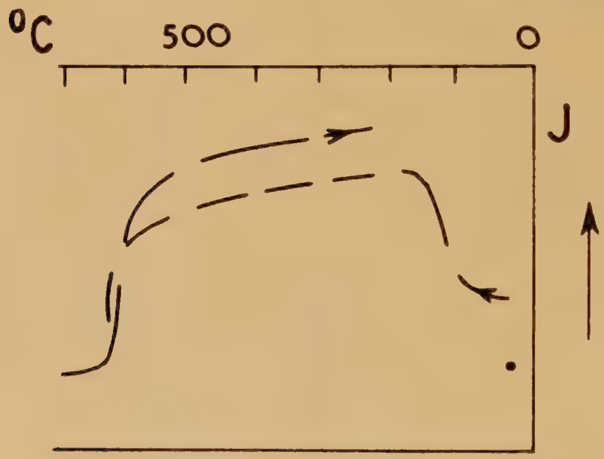

Adirondack Gneiss 105.

The specimen of Adirondack gneiss, No. 105, was kindly supplied by Dr. J. R. Balsley of the U.S. Geological Survey. A single magnetic lemente of Curie Point approximately 610°c is indicated. The mineral responsible is probably a member of the haematite–ilmenite solid solution series near the haematite end, that is a titano–haematite. The increase of magnetization at 100°c is a phenomenon often associated with haematites and has been explained by Néel (1949) as being due to the fact that at room temperature the coercive force of these materials is greater than the applied field, but that it falls quickly with temperature.

The few data available for the titano–haematites would suggest a composition for this phase of 610°c Curie Point of 7% $FeTiO_3$ 93% Fe_2O_3—α (by weight).

Such an estimate is, as in other cases, independent of intergrowth structures, etc. in the rock, and can be made on the crude rock. A ferromagnetic phase of the observed Curie Point must be present, the rest of the estimate is of course deduction from observations made on the magnetic properties of pure separated minerals. Possibly the minerals forming fine scale intergrowths in actual rocks may have other properties, but the differences are likely to be very small. Certainly such methods of attacking the problems of magnetic minerals have their advantages, and perhaps a certain elegance, but having their own individual drawbacks they should be combined with microscopic, radiographic, and chemical study wherever possible.

REFERENCES

CHEVALLIER, R., 1932, *C.R. Acad. Sci. Paris*, **194,** 1327, 1468.

CHEVALLIER, R., BOLFA, J., MATHIEU, S., 1955, *Bull. Soc. franç. Minér. Crist.*, **78,** 307, 365.

CHEVALLIER, R., MATHIEU, S., VINCENT, E. A., 1954, *Geochim. Cosmochim. Acta*, **6,** 27.

CHEVALLIER, R., PIERRE, J., 1932, *Ann. Phys.* (10th Sér.), **18,** 383.

HOSPERS, J., 1953, *Proc. Kon. Nederl. Akad. van Wetenschappen*, ser. B, **56,** No. 5, 467, 477 ; 1954, *Ibid.*, **57,** No. 1, 112.

IRVING, E., 1954, *Thesis*, Cambridge.

NAGATA, T., 1953, *Rock Magnetism* (Tokyo : Maruzen Co. Ltd.), p. 70.

NÉEL, L., 1949, *Ann. Phys.*, **4,** 249 ; 1954, *Bull. Soc. franç. Minér. Crist.*, **77,** 257 ; 1955, *Advanc. Physics*, **4,** 191.

RUNCORN, S. K., 1956, *Bull. Geol. Soc. Amer.*, **67,** 301.

UYEDA, S., 1955, *J. Geomag. Geoelec.*, **7,** 9.

Some Field and Laboratory Studies of the Depositional Remanence of Recent Sediments

By D. H. Griffiths, R. F. King and A. E. Wright
Department of Geology, University of Birmingham

§ 1. Introduction

The remanent magnetism of recent sediments is not typical, for it is almost certainly entirely depositional; that is, its direction is determined by orientation of magnetic particles during sedimentation and compaction, and not by any secondary chemical or thermal processes. Results of depositional experiments made on glacial varved clays are therefore of limited applicability, even though certain older sediments may be magnetized in the same way; but are of interest because in principle they can give accurately dated information about changes in the geomagnetic field over the past few thousand years. If they are to give useful information concerning the secular variation in the past, the 'scatter' which is accepted in ordinary palaeomagnetic measurements cannot be tolerated, and the effect of any aligning influences other than the earth's field must be understood well enough for some correction to be made to the direction of the remanence.

Our measurements on varves from five different Swedish sites and on historically dated varves from Iceland suggest to us that disturbing factors, such as water-currents, are often of overriding importance. For example, the results from two sites separated by a hundred yards from each other in a recently drained glacial lake (Hagavatn) in Iceland, shown in fig. 1, agreed remarkably well with each other, but showed wide variations in declination which departed markedly from the known secular variation pattern in the 18th century, and which must surely be due to water-currents varying in direction.

The results for varves from New England published by Johnson *et al.* (1948) also show a marked periodic variation in declination, but in view of our Icelandic results, we doubt whether this can be assumed to reproduce the secular variation over 5000 years, as they suggest.

Ising (1942) has also published results on Swedish varves of about the same age as these: over a 350-year section they show a steady alteration in both declination and inclination which he interprets as an instability effect. Our own experience of Swedish varves suggests that they are, on the whole, magnetically stable, and we would prefer to interpret Ising's results, too, in terms of disturbing factors, or as a genuine field change.

§ 2. THE 'INCLINATION' AND 'BEDDING' ERRORS

We have been trying to investigate these disturbing factors by means of laboratory sedimentation experiments, with the ultimate aim of making some correction for them. The first results have already been published (King 1955) and need be summarized only briefly here.

Fig. 1

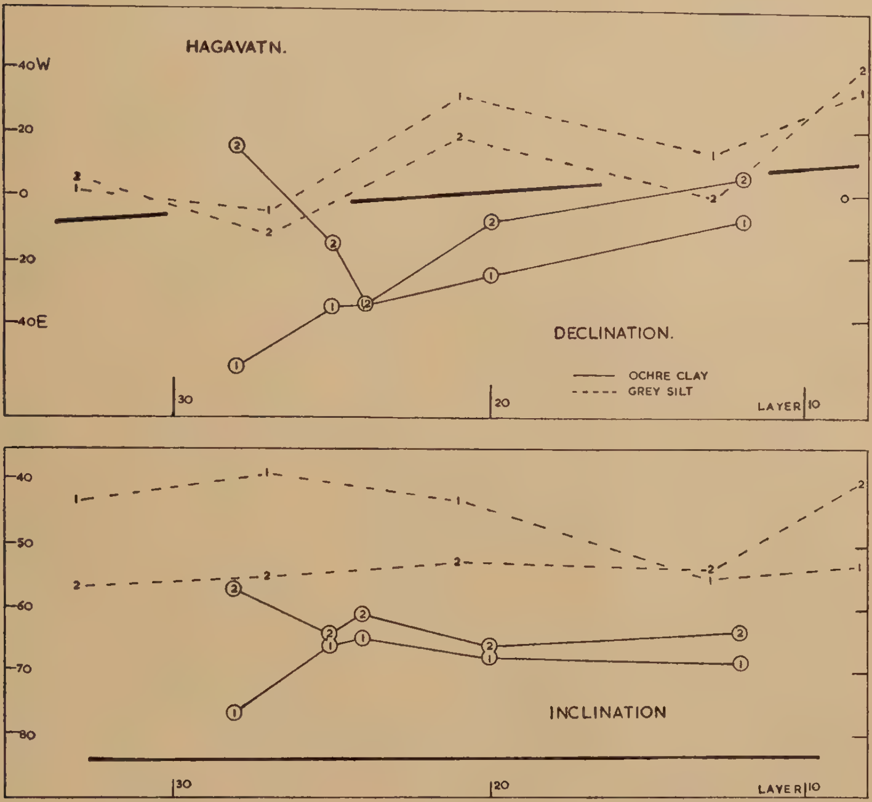

Declination and inclination measurements on varves from Hagavatn, Central Iceland. The period covered is about A.D. 1700–1800, and the heavy lines show the known secular variation over this period. Site 1 and site 2 were about 100 yards apart.

Using varved 'clay' material with grain sizes covering the range 1–20 μ, we found that sediments deposited in still water on a horizontal surface had a remanence in the magnetic meridian but at a shallower inclination than that of the ambient field. The amount of this 'inclination error' is about 10–30° for a field inclination of 65°. Johnson and his colleagues found a similar effect of up to 20° in their deposition experiments, and also found that the inclination error decreased with increasing field strength. Our experience is that the effect of field strength is only very small.

It is obviously important to know whether the inclination of naturally deposited sediments is also less than that of the geomagnetic field, but the evidence is conflicting on this point. The American results show no periodicity in the inclination corresponding with that in the declination, but merely a steady increase from 40° to 60°. These inclinations may well be less than that of the field, but the 5000-year varve sequence was not taken from one exposure, and it is difficult to account for an inclination error which increases with age as such, rather than with depth of burial or with grain size.

Ising's measurements also give inclinations less than that of the *present* field but over his 350-year sequence the inclination *decreases* from 50° for the older (coarser) varves to 30° for the younger (finer) ones. It is conceivable that this may represent a genuine change in field direction, with large and constant inclination error.

Our own results from Sweden give inclinations not far from the present value—some greater, some less. We are therefore doubtful whether any correction should be made to the inclination, though Brynjolfsson (1956) suggests that the magnetic pole at the time of deposition of these varves may have been less than 10° away.

The Icelandic varves were laid down at a time for which the field inclination can be deduced approximately, and are interesting in that the coarse material, which was sampled separately, gives a larger inclination error (fig. 1) than does the fine winter layer : this is to be expected from our later sedimentation experiments.

The other main effect we have investigated in the laboratory has been that of deposition on a sloping surface. This is found to result in a rotation of the remanence vector in the sense which would be expected if the magnetic particles were rolling slightly down the slope. This ' bedding error ' can of course affect the declination of the remanence as well as the inclination, in fact it implies that results from dipping beds must be corrected whether the inclined bedding planes indicate post-depositional tilting or deposition on a pre-existing slope. Our field results from Prästmon and Undrom (Griffiths 1955) are brought into agreement only if correction is made for a geological dip which is almost certainly depositional, and it seems that this is an example of the ' bedding error ' in natural conditions of deposition. The amount of correction required here happened to be equal to the geological dip, but we have found in the laboratory that the bedding error may be either larger or smaller than this.

§ 3. The Effect of Water-Currents

The effect of deposition in moving water has unfortunately proved very difficult to study experimentally. Our first experiments gave indications of very large deviations of the remanence in currents of only a few cm/sec. The direction of deviation was the same as that which would be produced by a slope of the bed downwards in the direction of the current.

§ 4. A Simple Model to Account for the 'Errors'

It was found that the variation of the inclination and bedding errors with intensity and direction of the magnetic field acting during deposition could be accounted for well by supposing the sediment to contain round and flattened particles in roughly equal numbers (King 1955). The flattened particles, settling horizontally, reduce the inclination of the remanence, whilst the rounder ones, in rolling into equilibrium positions on the bed, do so through greater angles in the down-hill direction, giving rise to a bedding error.

Fig. 2

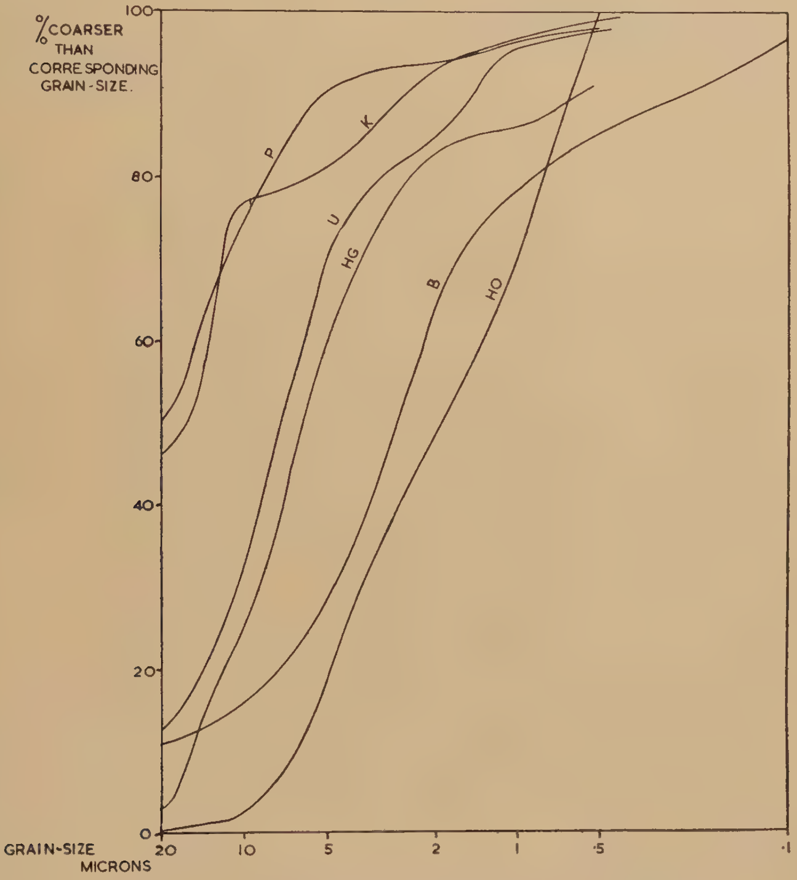

Particle size distributions for some varved sediments.

Key

Bispfors: glacial varves, age *c* 10 000 years.

Prästmon, Undrom: neighbouring sites on the Angerman river. Age *c* 2000 years.

Kramfors: recent (A.D. 1400–1900) varves from the delta of the Angerman river.

Hagavatn: varves from a lake on the ice-margin, *c* A.D. 1700–1800. Grey silt and ochre clay.

Fig. 3

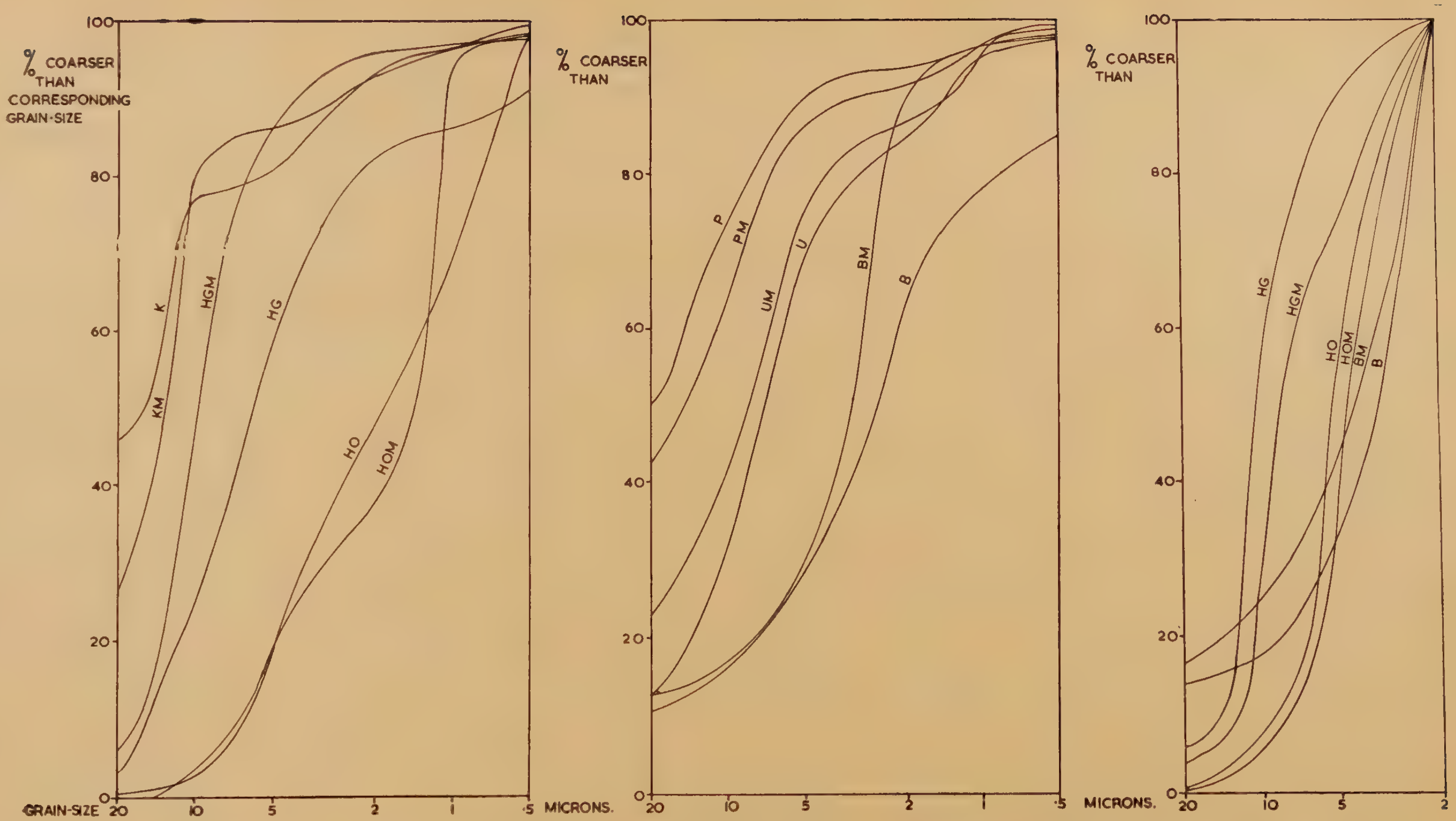

Comparison of particle size distributions of magnetic fractions with those of sediments as a whole.

The third diagram shows the distributions recalculated after omitting the weakly magnetic fraction below 2 microns.

Key: K—Kramfors; HG—Hagavatn Grey; HO—Hagavatn Ochre; P—Prästmon; U—Undrom; B—Bispfors; M—Magnetic Fraction.

This model is now thought to be inconsistent with the results of a detailed size and shape analysis of the particles which has been carried out by one of us (A.E.W.). These results will now be described and a new theory of the inclination error developed.

§ 5. Size and Shape Analyses of the Sediments

Size analyses were made by conventional sedimentation methods. By measuring the saturation magnetic intensities of samples of different grain sizes for each sediment (assuming saturation intensity to be a measure of weight of magnetic material present), it was possible to obtain the size distribution of its magnetic content. Figure 2 shows cumulative curves for the grain sizes of a number of the varved sediments. These fall into three groups. The sediments from Prästmon and Kramfors are the coarsest, those from Bispfors and from the ochre varves at Hagavatn the finest, whilst the Undrom and grey Hagavatn varves lie in between. Figure 3 shows a comparison of the cumulative curves compared with those for the respective magnetic fractions. Generally speaking the two follow closely. This means that the size distribution of the non-magnetic and the magnetic grains of a particular sediment are very similar, and that one might expect that the behaviour of the two types of grains, mechanically speaking, will be similar.

Magnetic separations were also carried out with a simple separator. It was possible to reduce the percentage of magnetic material present to about 30% of its original value, the remainder being almost certainly due to inclusions in paramagnetic grains.

Analyses were made of the distribution of sphericity in the sediments (Wright 1956). As an index of sphericity the ratio

$$\left(\frac{\text{volume of particle}}{\text{volume of circumscribing sphere}}\right)^{1/3}$$

was used, assuming the particles to be ellipsoids. Measurements were made from micro-photographs of grains dispersed on a glass slide. These were shadowed at an angle in a vacuum chamber so that the height could be obtained from the shadow length. Figure 4 shows histograms of the sphericity distributions for various sediments and their magnetic fractions. There is little obvious difference in the distributions for the different sediments. The maxima all lie in the 0·7–0·9 region, and as a particular sphericity range includes particles of different shapes it is probable that small differences in the sphericity distributions between sediments have no significance.

Note that the sphericity distributions for the magnetic fractions are almost identical with those of their associated sediments.

Similar shape analyses were also made on a number of sized fractions. There appears to be a slight increase of sphericity with decrease of grain size.

Fig. 4

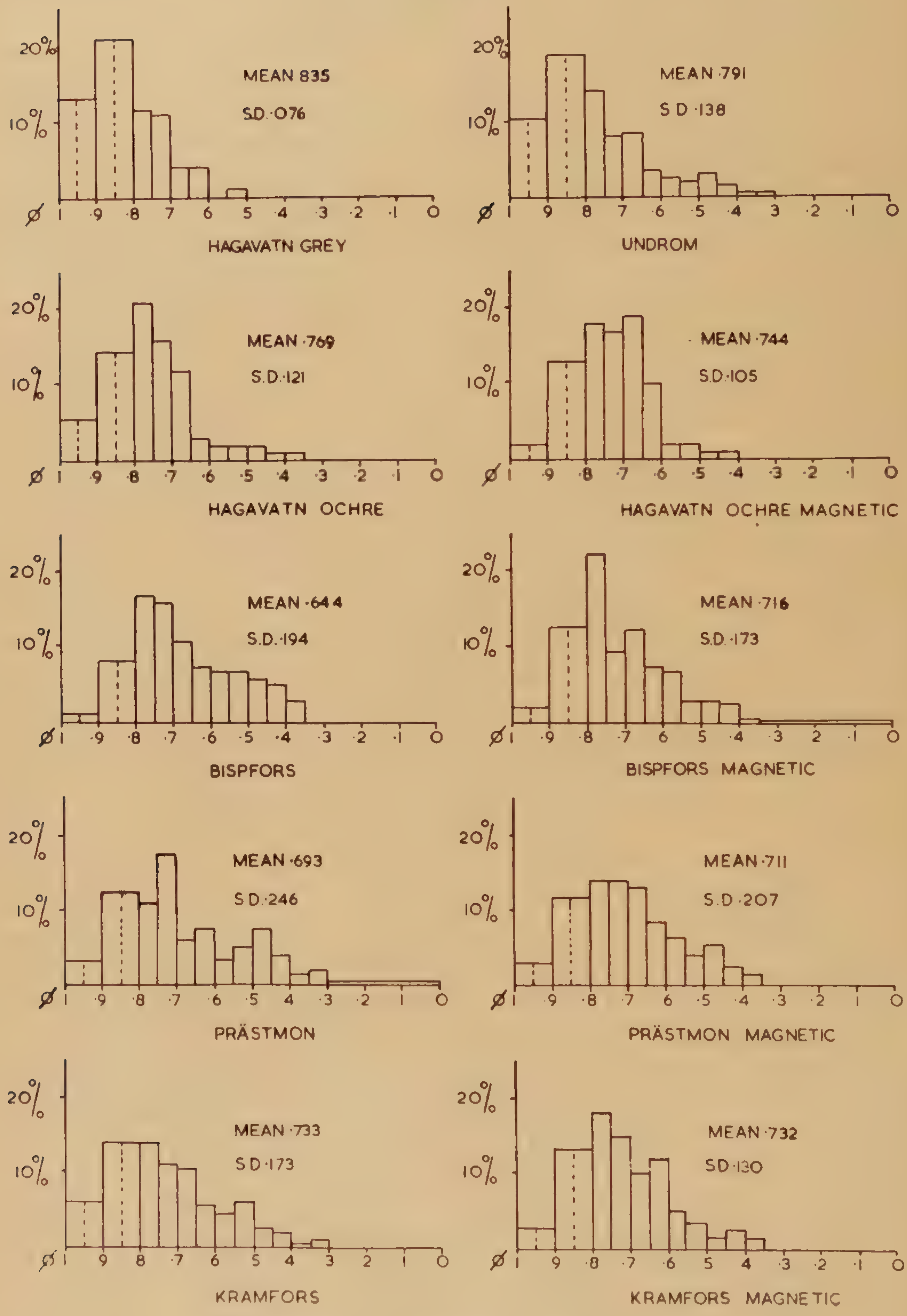

Histograms of sphericity distributions.

§ 6. SEDIMENTATION OF SIZED FRACTIONS

Sets of sedimentation experiments were made on sized fractions of the various sediments to find out the effect of grain size on the inclination and bedding errors. There was found to be a close dependence of inclination error on grain size which was independent of the source of the sediment. The inclinations decreased with increasing grain size. The bedding error on the contrary increased with decreasing grain size. Figure 5 shows the inclination and bedding errors plotted against grain size. Qualitatively speaking this result is to be expected from the original theory and from the fact that sphericity does increase with decreasing grain size. With increasing sphericity more particles may be expected to behave as spheres rather than as flats, thus decreasing the inclination error. Since there are more spheres to roll a consequent increase in bedding errors is to be expected. Unfortunately even a very marked increase in sphericity does not account quantitatively for the very large bedding errors found in the fine grained specimens, and some modification of the theory of deposition as originally postulated is necessary.

Fig. 5

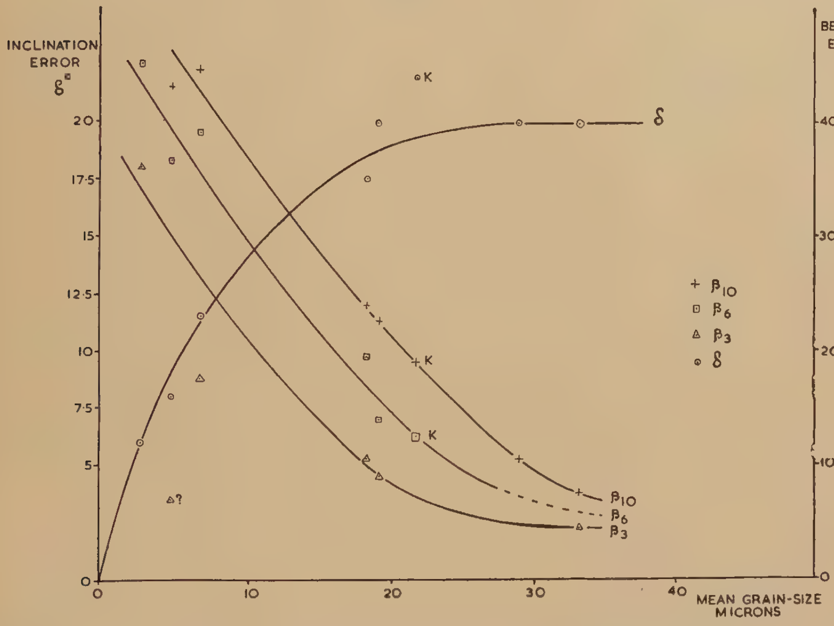

Variation of inclination error and bedding error with particle size. Bedding errors for slopes of 3°, 6° and 10°.

Before going on to consider possible modifications of the theory, some relevant details of the data should be recorded. Although there is a qualitative agreement between the results of sedimentation experiments and field measurements there are in some instances considerable discrepancies in magnitude between the inclination and bedding errors obtained during sedimentation and in nature. For example, although the inclination errors of the Hagavatn–Icelandic field results (fig. 1) are qualitatively correct the inclination error in the grey layers is much larger than one would expect from tank experiments for an average grain size of 8 μ. It is over 30° instead of 12°. The discrepancy is less in the finer ochre layers. In the Swedish varves from Prästmon, Undrom, and Kramfors the inclination error in the finer layers appears to be less than the expected value, though the inclination errors for the coarser layers do appear to be roughly correct. Recent results on some varves from the Indal River also show a measure of agreement with tank experiments. A number of layers covering a fairly wide range of grain sizes was collected from a varve sequence covering a very short time interval. A preliminary plot of grain size against inclination error agrees with that obtained from sedimentation experiments, but even here there are some discrepancies.

Similar discrepancies are found for the bedding error. Correlation between the sequences at Undrom and Prästmon (Griffiths 1955) was achieved by applying a bedding correction equal to the geological tilt of the beds. According to the laboratory results, this would be correct for a grain size of about 30 μ. In fact the grain size is certainly no more than 20 μ, so that the bedding error should be at least twice as great. Moreover, an ‘ effective ’ grain size of 30 μ would imply an inclination error of 20°, leading to a vertical field during deposition.

At Bispfors, the bedding correction which must be applied to achieve correlation between beds of different geological dip is considerably larger than at Prästmon, but is still smaller than the experimental bedding error by a factor of two.

To summarize, inclination errors in nature may be greater than, equal to, or less than the experimentally derived values. Bedding errors in nature usually appear to be less than the values experimentally determined.

§ 7. A Modified Theory of the Inclination and Bedding Errors

We have not found it possible to construct a satisfactory theory to cover all the facts, though we feel the rolling theory is essentially correct. It seems likely that the rolling takes place not only on deposition, but perhaps also as a result of changes from an open to a more close packing in the sediment. These changes in packing probably take place in a thin surface layer, a stable condition being reached very quickly. Subsequent compaction probably has little effect. The inclination error probably results merely from a rolling of spherical particles about horizontal axes, there being no necessity for invoking flat particles. For example, if after hitting the bottom previously perfectly aligned spherical particles roll through varying but unspecified angles about a horizontal axis lying in the meridian, then the resultant of their magnetizations will have an inclination less than that of the aligning magnetic field. Statistically speaking if the rolling takes place equally to the east and the west, then the declination will be unaffected. Similar modes of rotation about horizontal axes in other azimuths merely contribute to this effect. The greater the rolling the greater the inclination error. In fact the complete ‘ randomization ’ of a bed of magnetized and perfectly aligned spheres by rotations about horizontal axes distributed evenly through 360°, provided each sphere is only rotated about a single axis, produces a horizontal resultant magnetization in the plane of the aligning field. It is reasonable to believe that rolling at the moment of deposition, and in the subsequent short period of compaction, does take place mainly about horizontal axes. Notice that the theory does not demand, as did the original theory, any particular angle through which the particles must roll. The greater the rolling, the shallower the inclination.

Bedding errors are caused, as in the original form of the theory, merely by the fact that rolling on a slope will have a preferred direction.

Differences in inclination and bedding error for different grain sizes, and for natural and artificial sediments may be due to differences in the initial packing structure and to the degree of collapse, both of which affect the degree of rolling. Some work in the porosity of sands may be relevant. Kolbuszewski (1950) has shown that the porosity of sands increases with the intensity of deposition (i.e. the weight per unit area falling in unit time) and that the porosity decreases with velocity of fall. He has also shown that the porosity is affected by the grading of the sediment. If the initial structure of the sediment is responsible for the magnitude of the inclination and bedding errors it is obvious that discrepancies between sedimentation experiments and natural conditions are likely to occur. For example the intensity of deposition in the tank is about 100 times that in nature. Sedimentation experiments with a much reduced intensity of deposition are being undertaken to test this.

It is not really clear just how the initial structure affects the errors. It is perhaps reasonable to assume a greater rolling in the coarse material, since it forms a more closely-packed structure on first deposition : this is the explanation given for the greater inclination error in the coarse material. If this explanation is correct there should of course also be a greater bedding error in the coarse material. The contrary is in fact true, and we have not been able to devise a simple satisfying explanation. It may be that the fine sediments have a relatively stable open structure on a horizontal surface which becomes unstable on even a small slope, and thus the rolling of the small particles exceeds that of the coarse under such conditions.

§ 8. CONCLUSIONS

The ultimate aims of this investigation are

(*a*) To obtain secular variation data from varve series.

(*b*) Possibly to use the remanence of varves to help in their geological correlation.

(*c*) To determine what relevance the work has to solid rock magnetism.

So far we have determined how, under laboratory conditions, the direction of remanence for a particular sediment depends on its grain size and on the slope of the surface on which it is deposited. We have shown qualitatively the effect of currents, and it should be possible to work out quantitative relationships. We have also shown that the effects found in the laboratory occur under natural conditions of deposition, though probably to a different extent. Although we can as yet only guess at the reason for this, it may well be possible to determine directly the effect of particle size and bedding slope in nature. The effect of water-currents, both in nature and in the laboratory, is much more difficult to determine, but we hope that this may be done for any particular sediment by a combination of measurements of remanence and susceptibility anisotropy with sedimentation experiments.

ACKNOWLEDGMENTS

We are most grateful for the cooperation of a number of people in Sweden, namely Dr. Carl Caldenius of the Geological Survey, Professor Gustav Ising, Mr. Lars Granar, Dr. R. Liden and Dr. B. Kullenberg. Our thanks are also due to Professor Shotton for his support and interest, and to the Royal Society for a generous grant.

REFERENCES

BRYNJÓLFSSON, A., 1956, **6,** 247.
GRIFFITHS, D. H., 1955, *Mon. Not. Roy. Astro. Soc., Geophys. Suppl.*, **7,** 103.
ISING, G., 1942, *Ark. f. Mat., Astron. o. Fysik.*, **29a,** No. 5, 42.
JOHNSON, E. A., MURPHY, T., and TORRESON, O. W., 1948, *Terr. Mag.*, **53,** 349.
KING, R. F., 1955, *Mon. Not. Roy. Astro. Soc., Geophys. Suppl.*, **7,** 115.
KOLBUSZEWSKI, J., 1950, *Research*, **3,** 478.
WRIGHT, A. E., 1956, *J. Sed. Petrology* (in the press).

Remanent Magnetism of the Russell Belt of Gneisses, Northwest Adirondack Mountains, New York†

By J. R. Balsley and A. F. Buddington
U.S. Geological Survey, Washington 25, D.C.

A study (Balsley and Buddington 1954) of the magnetic properties and the chemical and mineralogical composition of the iron–titanium oxides of several hundred specimens of metamorphic rocks from the Adirondack Mountains, New York indicates that rocks in which the predominant ' magnetic ' mineral is magnetite have essentially ' normal ' magnetization, that is, that their north-seeking pole is down, usually not exactly parallel to the present magnetic field of the earth. The rocks in which the predominant magnetic mineral is in the ilmenite–hematite series have remanent magnetization that is essentially ' reversed ', that is, the north-seeking pole is up. The magnetic properties of rocks containing mixtures of the two minerals are transitional between those of the first two groups of rocks as if the remanent magnetization of the rocks were the vector sum of the differing remanent magnetizations of the two types of mineral grains.

The coercivity of the magnetite is characteristically a few hundred gauss ; the coercivities of the ilmenite and hematite are more than 4000 gauss. Runcorn (1955) has proposed that the relationship between direction of magnetization and mineral content can be better explained by assuming that both the magnetite and the ilmenite–hematite were originally magnetized in the same direction at a time when the earth's field was reversed, and that because of its higher coercivity, the ilmenite–hematite has maintained this magnetism while the magnetite with lower coercivity has lost it and now shows only an isothermal remanent magnetization that has been produced in the last few thousand years.

Because the rocks examined have been widely distributed throughout the Adirondack Mountains and represent a complete suite of rock types and range of chemical and mineralogical composition, it is not possible to treat these data statistically. A statistical study was made of the origin of the remanent magnetization in a belt of gneisses referred to as the Border Belt, an area of about 50 miles long and about 5 miles wide.

The ' Border Belt ' (fig. 1) is a elongate mass of interlayered gneisses trending essentially northeast–southwest, but with the strike of the foliation varying from about north to about east Although the layers are rather complexly folded the lineation remains essentially constant throughout most of the area studied, the average strike of lineation is about 320° and the dip of foliation averages 45° to the northwest. At the

---

† Publication authorized by the Director, U.S. Geological Survey.

Fig. 1

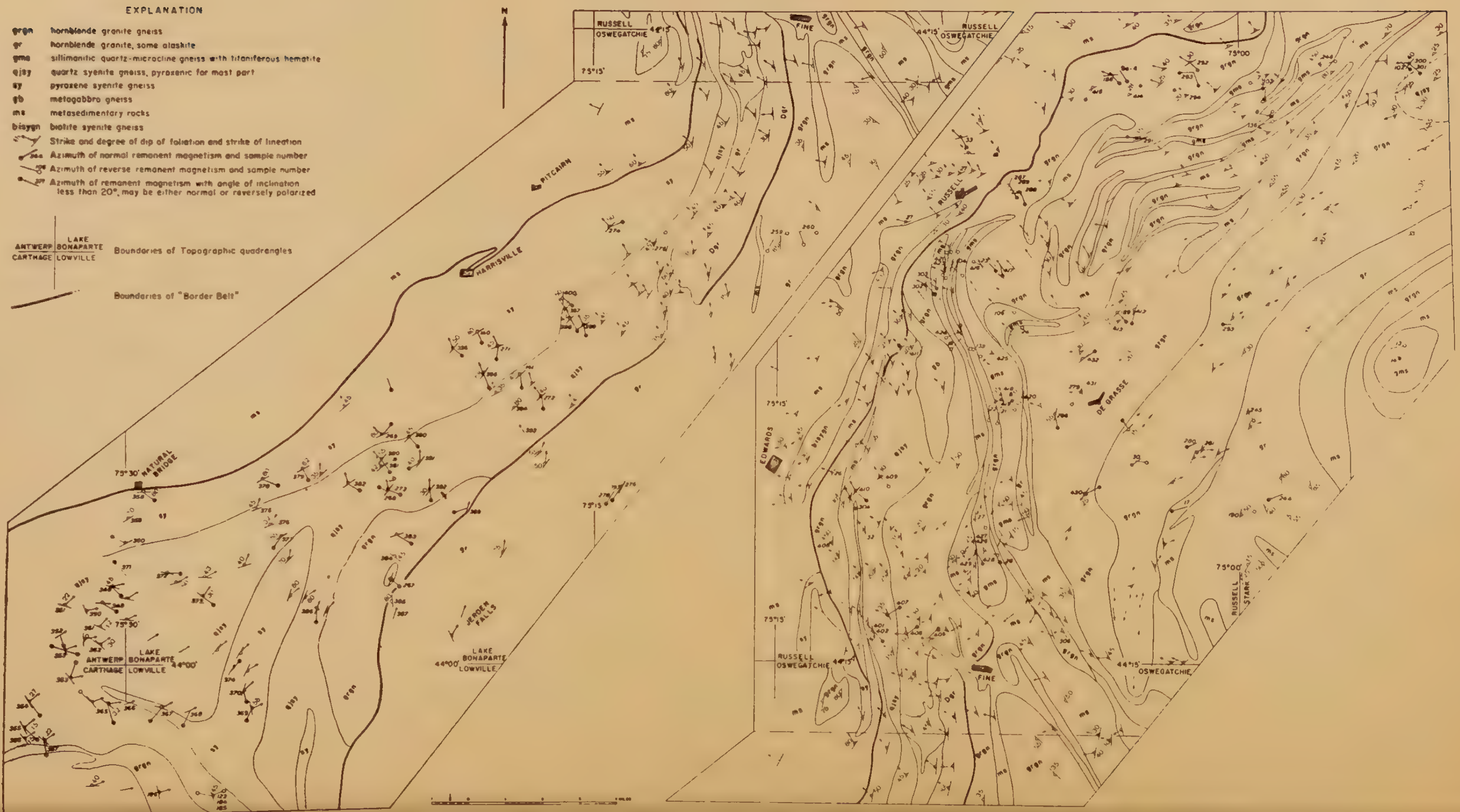

GEOLOGY AND PALEOMAGNETIC DATA OF "BORDER BELT", NW ADIRONDACK AREA

EXPLANATION
grgn hornblende granite gneiss
gr hornblende granite, some alaskite
gms sillimanitic quartz-microcline gneiss with titaniferous hematite
qjsy quartz syenite gneiss, pyroxenic for most part
sy pyroxene syenite gneiss
gb metagabbro gneiss
ms metasedimentary rocks
bisygn biotite syenite gneiss
Strike and degree of dip of foliation and strike of lineation
Azimuth of normal remanent magnetism and sample number
Azimuth of reverse remanent magnetism and sample number
Azimuth of remanent magnetism with angle of inclination less than 20°, may be either normal or reversely polarized
ANTWERP
LAKE BONAPARTE
CARTHAGE
LOWVILLE
Boundaries of Topographic quadrangles
Boundaries of "Border Belt"
N
RUSSELL
OSWEGATCHIE
44°15'
75°15'
FINE
75°00'
PITCAIRN
HARRISVILLE
NATURAL BRIDGE
75°30'
44°00'
EDWARDS
DE GRASSE
JERDEN FALLS
STARK

extreme southern tip of the area shown in fig. 1 the lineation changes abruptly to about northeast and the average dip to about 30°.

The rocks of the Border Belt include a varied suite of gneisses—pyroxene syenite gneiss, pyroxene quartz syenite gneiss, hornblende granite gneiss, and sillimanite quartz-microcline gneiss—but the geologic evidence indicates that the entire mass of interlayered rock has reacted as a unit and

Fig. 2

REMANENT MAGNETISM OF PLUTONIC GNEISSES IN "BORDER BELT"
(50 Miles long and ± 5 miles wide)

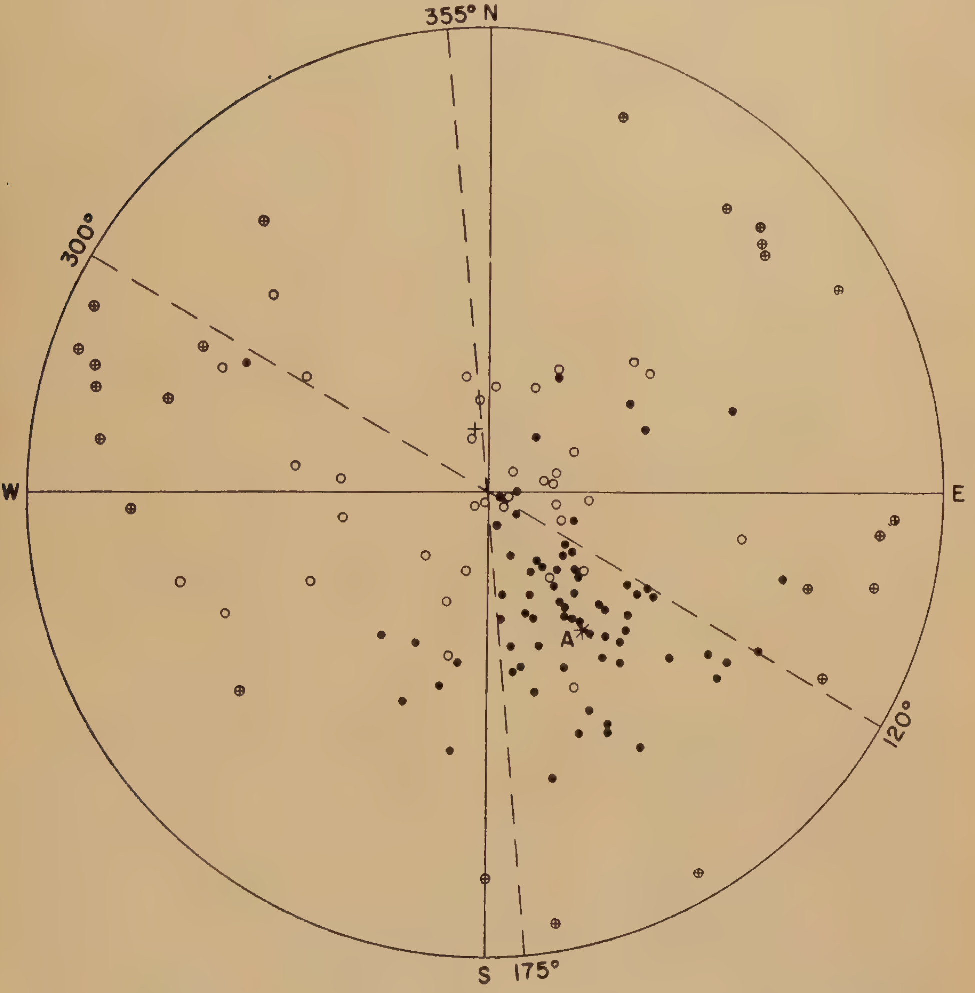

● N-seeking pole down, inclination > 20°, magnetite the major or predominant magnetic mineral.

○ S-seeking pole down, inclination > 20°, titaniferous hematite the predominant magnetic mineral.

⊕ Magnetism Normal or Reverse but with inclination < 20° and ferric-ilmenite (including 4 with titaniferous hematite) major or predominant magnetic mineral.

✳ Average of data for N-seeking pole down with azimuths between 120° and 175° and inclination > 20°, includes 82% of total azimuths for such rocks.

+ N-seeking pole of earth's present magnetic field.

has undergone a more or less homogeneous metamorphism, probably within the temperature range of 400° to 550°c.

One hundred and twenty-eight samples of the rocks in this belt were collected and their magnetic properties and mineralogical composition measured. About a quarter of the samples were analysed chemically to provide a check on the mineragraphic determinations. The directions of the remanent magnetization of the samples have been plotted on a polar diagram (fig. 2), and the relation between the mineralogy and remanent magnetizations of the rocks are tabulated in the table.

Summary of mineralogy and data on remanent magnetism

Number of sample	‘ Magnetic ’ oxide minerals[†]	Azimuths of declination of R.M.	Average angle of inclination of R.M.	Direction of R.M.
67	Magnetite predominant to major; ‘ Ferricilmenite ’[‡] minor.	Range 120°–175° for 82% of samples; average 144°.	50°	Normal
37	Titaniferous hematite predominant to exclusive. Magnetite quite minor or absent.	Effectively absent from sector 300°–350° and rare in sector of rocks with magnetite major to predominant.	63°	Reverse
24	Ferricilmenite major to predominant; ‘ Ilmenomagnetite ’[§] minor. Four samples have titaniferous hematite in place of ferricilmenite.	Effectively absent from sector of rocks with magnetite major to predominant and from sector opposite to this.	20°	75% reverse 25% normal

[†] In this column and text to follow, the term ‘ major ’ will be used for the mineral which forms 35 to 75% of the metal oxide mineral assemblage, ‘ predominant ’ where it forms 75 to 96%, and ‘ exclusive ’ where it constitutes 97 to 100% of the oxide minerals.

[‡] Ilmenite with 6 to 13% Fe_2O_3 in solid solution.

[§] Magnetite with microintergrowths of ilmenite.

The remanent magnetization of the rocks with magnetite as the major or predominant magnetic mineral is normal and shows a strong concentration at approximately 56° from the present field. The pronounced concentration of the direction of remanent magnetization at such a large angle to the present magnetic field indicates that magnetization is stable, that is, it is not easily affected by the present direction of the earth's field. Because all the paleomagnetic evidence indicates that the magnetic pole has been in essentially its present position during recent time, this magnetization of the magnetite cannot be isothermal remanent magnetization assumed during the last few thousand years.

Why the magnetization shows such a concentration and at such an angle to the present field is not yet understood. It is possible that the direction may represent a previous direction of the earth's magnetic field at the time these rocks cooled through the Curie point. It is worth noting, however, that the direction of the remanent magnetization of the rocks containing magnetite is almost exactly perpendicular to the lineation of the rocks in the vertical plane containing the lineation. This relationship may be explained in two ways. The shape of the magnetite grains may have been affected by the metamorphic forces that produced the foliation and distorted and reoriented the silicate grains. If the magnetite grains have been elongated by this means, this shape may have established an easiest direction of magnetization which would affect the remanent magnetization. However, an elongation of the magnetite grains would more likely be either in the direction of the lineation or at right angles to it, but in the horizontal rather than in the vertical plane. Because magnetite is an isotropic mineral it is not likely that the magnetization could be related only to a crystallographic orientation of essentially spherical grains of magnetite. Petrofabric analyses of the oriented thin sections of these rocks will be made to determine the shape and alignment of the magnetite grains and if this alignment is related to the direction of magnetization. Because the directional susceptibility of these rocks would be similarly affected by an alignment of elongated grains of magnetite, it will also be measured to investigate the shape factor.

The direction of the remanent magnetization of the magnetite may also be related to a magnetostrictive effect similar to that observed by Graham (1956). Under these conditions the direction of magnetization should be related to the stress conditions existing within the area during the last stages of metamorphism and therefore related to the lineation. A few specimens (nos. 348, 349, 353–355, 357, 365, 370) in the southwestern end of the Border Belt (fig. 1) seem to indicate that the direction of magnetization does not follow the major change in the lineation, but is consistent throughout the entire belt as if it were related to a broad stress pattern, perhaps post-lineation. Additional specimens will be collected to verify this hypothesis.

In rocks of reverse remanent magnetization, that is, with a north-seeking pole up, the major, predominant, or exclusive portion of the oxide mineral assemblage is almost without exception a member of the Fe_2O_3–$FeO.TiO_2$–(TiO_2) system. It is obvious from the diagram (fig. 2) that the direction of magnetization of these rocks though consistently reversed is almost random but significantly absent from the sector containing the plot of 82% of the magnetization directions of rocks containing magnetite and from the sector opposite it. The reverse magnetization of these grains and the wide scatter in its direction indicates that the mechanism of magnetization is considerably different from that of the magnetite. Because hematite is magnetically anisotropic, the remanent magnetization of these rocks is probably strongly affected by the crystallographic orientation of the hematite. Whether the magnetization of these grains is produced by exsolution structures as previously suggested by Balsley and Buddington (1954) and others (Uyeda 1955, Neel 1955), or by disorder structures as proposed by Verhoogen (1956), any preferred orientation of the hematite grains within the rock would materially affect the direction of magnetization. Petrofabric analyses of the oxide minerals in oriented thin sections of these rocks will be made by x-ray to investigate any possible relationship between the direction of magnetization and the crystallographic orientation of these minerals.

Thus, the magnetic data indicate that in the rocks of the Border Belt containing magnetite minerals there is a stable normal magnetization at 56° from the present field, and that in the rocks containing members of the ilmenite–hematite series a magnetization is reversed but of widely scattered directions. Because both mineral groups must have acquired their magnetization at essentially the same time, it is not likely that both represent previous directions of the magnetic field. It seems probable that at least the ilmenite–hematite minerals have an inherent property that permits them to be magnetized at some direction other than that of the ambient field and in a general way opposite to it. Because these minerals are common in igneous rocks in which paleomagnetic measurements are made, care must be taken in using the remanent magnetization of these rocks to hypothesize a previous orientation of the magnetic field.

REFERENCES

BALSLEY, J. R., and BUDDINGTON, A. F., 1954, *J. Geomag. Geoelect.*, **6,** 176.
GRAHAM, J. W., 1956, *J. Geophy. Res.* (in press).
NEEL, LOUIS, 1955, *Advanc. Physics*, **4,** 217.
RUNCORN, S. K., 1955, *Advanc. Physics*, **4,** 276.
UYEDA, SEIYA, 1955, *J. Geomag. Geoelect.*, **7,** 9.
VERHOOGEN, J., 1956, *J. Geophy. Res.*, **61,** 201.

Reflection Microscopy of Ferromagnetic Minerals

By A. P. Millman
Department of Mining Geology, Imperial College, London

§ 1. Introduction

The last decade has seen rapid progress in the development of reflection microscopy of the opaque ore minerals. The recently devised technique (Barringer 1953, Rehwald 1954, Hallimond 1956) of preparing polished section surfaces by means of graded diamond dust has contributed a great deal to this progress, in that mineral aggregates of dissimilar hardness may now be polished to a uniform surface enabling paragenesis and textural examinations to be carried out at high magnifications. The superior quality of the polished surface also enables the microscopist to observe delicate anisotropic phenomena more clearly, and has been found to give more reproducible reflectivity determinations. Advances have also been made in the design of microscopic equipment, such as improved metal-coated reflectors in the vertical illuminator assembly and production of new types of bloomed low-power oil immersion objectives. Other developments have included devices for the accurate determination of rotation angles of opaque minerals in polarized light and for the measurement of reflectivity in monochromatic light employing a new type of microphotometer (Hallimond 1953). Research has also been carried out on the significance of bireflection interference figures for some groups of ore minerals (Hutchinson 1953). The application of replica electron microscopy to the study of mineral intergrowths at very high power has also been established in recent years (Kenyon 1953). These advances in technique have elevated the status of reflection ore microscopy from a rather ambiguous position to one of very great importance in the examination of opaque mineralogical material, for both the diagnostic recognition of the mineral components and for the interpretation of textural relationships and paragenesis of minerals in intimate intergrowth.

§ 2. Examples of Ferromagnetic Mineral Occurrences in Igneous Rocks

The general purpose of this review is to draw the attention of those engaged on research in rock magnetism to some aspects of their problems which the author considers may be more readily investigated by reflection microscopy than by the more conventional electron and x-ray diffraction techniques which cannot yield adequate data on mineral intergrowths and textures. It is indeed the very complexity of these intergrowths which may account for some of the apparently anomalous magnetic observations which have been detected. The examples chosen have been selected from some of the typical occurrences of ferromagnetic minerals in igneous rocks in different parts of the world. For details of the optical and physical properties of the individual minerals under the reflecting polarizing microscope, the reader is referred to Ramdohr (1955), Uytenbogaardt (1951) and Nicholls (1955).

§ 3. MAGNETITE, $FeO.Fe_2O_3$, ILMENITE, $FeO.TiO_2$, AND ULVOSPINEL, Fe_2TiO_4

The extensive solid solution of titanium in magnetite has been established, and where the solid solution has been preserved by rapid cooling, up to 14% TiO_2 has been found in homogeneous magnetite in a dyke-rock in West Australia (Edwards 1954). Such titaniferous magnetite shows anomalous optical anisotropism and other properties grading towards those of ilmenite. With slower cooling of titanium-bearing magnetite, the titanium exsolves from the solid solution as ilmenite, and this may occur in two forms. The first is as discrete crystals or aggregates of ilmenite grains at the margins of the magnetite. In the second form, where cooling has been more rapid, the ilmenite appears as laths in the octahedral (111) planes of the magnetite forming a highly characteristic intergrowth, as shown in fig. 1 (Plate). Both of these forms have been found in the Indian basalts whose magnetic properties are now being investigated by Professor Blackett. It has been reported that the content of exsolved ilmenite in the lattice intergrowth may be as high as 50% (Ramdohr, personal communication). In rare cases, titaniferous hematite (αFe_2O_3) may also exsolve into the octahedral planes of magnetite (fig. 1, Plate). In some rocks where ilmenite is the dominant ferromagnetic mineral, with minor titaniferous magnetite, exsolved magnetite may form in the (0001) basal plane direction of the host ilmenite. The importance of ulvospinel in solid solution/exsolution relationship with magnetite has been noted recently by Ramdohr (1953) and Vincent and Phillips (1954). This mineral, which is rather difficult to recognize, is found in magnetite as exsolved minute sub-lamellae and spikes in the (100) planes, that is at an angle with the planes containing the ilmenite lamellae. The ulvospinel is considerably darker than magnetite, and is similar to ilmenite but is isotropic. The minute size of the ulvospinel sub-lamellae may cause it to be overlooked, but at a magnification of × 1000 in oil a highly characteristic cloth-like or ‘ petit-point ’ texture is clearly seen. An example of this texture in ulvospinel-rich magnetite from Lac de la Blache, Quebec, is shown in fig. 2 (Plate).

§ 4. HEMATITE, αFe_2O_3, ILMENITE, $FeO.TiO_2$, AND RUTILE, TiO_2

Hematite and ilmenite have been shown to form a continuous solid solution at temperatures above 600°c (Ramdohr 1926). If the rocks in which these two minerals occur have been cooled rapidly, the solid solution is preserved, and the mineral formed shows properties intermediate between those of hematite and ilmenite. With slower cooling, unmixing takes place to form both ferriferous ilmenite and titaniferous hematite, and these may continue to exsolve forming ultimately ilmenite with 6% Fe_2O_3 in solid solution, and hematite with 10% TiO_2 (Edwards 1954). The exsolution textures produced are quite characteristic, the exsolved mineral appearing as elongated bodies or spindles in the (0001) plane which both hematite and ilmenite share. Within these spindles a further generation of exsolution product is often visible. The general seriate distribution of the exsolved mineral is characteristic, as shown in fig. 3 (Plate). The solid solution is so continuous that the identical textures are seen for hematite exsolved from host ilmenite, and for ilmenite exsolved from hematite. Rutile may occur as a third though more restricted component in the solid solution relationship. It may be found as early granular segregations and also as exsolved needles and blades in the rhombohedral directions in both hematite and ilmenite (Edwards 1954). Some specimens from Scotland examined recently by the author show that rutile exsolution spindles may also be formed in the basal plane directions of hematite. The rutile spindles extinguish obliquely to their length, whereas the ilmenite shows straight extinction.

§ 5. ALTERATION OF PRIMARY FERROMAGNETIC MINERALS

Many of the rocks in which the iron-bearing minerals are found have been exposed to the oxidizing action of circulating groundwaters above the water-table. Under these conditions, the iron-rich minerals will be attacked selectively and a new generation of ferriferous minerals may be formed, and this alteration may be accompanied by a progressive decrease in magnetic susceptibility. For example, in the case of magnetite, the important constituents which may be derived by oxidation include hematite (α–Fe_2O_3), maghemite (γ–Fe_2O_3), and the hydrated oxide geothite 4 (FeO.OH). The process of replacement of magnetite by hematite has been termed ‘ martitization ’.

The replacement usually begins at the margins of the magnetite grains, and then follows the octahedral partings. In the case of intergrown ilmenite lamellae and titaniferous magnetite, the hematite will replace the magnetite along the boundaries with the ilmenite, and may subsequently replace all the magnetite leaving unreplaced ilmenite lamellae in a pseudomorph after magnetite. This is shown in fig. 4 (Plate), a photomicrograph of a metamorphosed peridotite from Co. Donegal, Ireland. Occasionally the ilmenite lamellae are replaced by pseudobrookite (Ramdohr 1955). An unusual occurrence was noted recently by the author in the gabbro of Carrock Fell, Cumberland, where lamellar ilmenite in octahedral directions has been perfectly preserved in rutile pseudomorphs after titaniferous magnetite.

It is to be hoped that these few examples will serve to show the usefulness of reflection microscopy in the examination of opaque constituents of rocks. The subject of rock magnetism is of very great interest to geologists but they will be hesitant in their acceptance of geophysicists' conclusions unless they are based on adequate mineralogical and petrological data.

References

Barringer, A. R., 1953, *Bull. Instn. Min. Metall. Lond.*, **563,** 21.
Edwards, A. B., 1954, *Textures of the ore minerals* (Melbourne).
Hutchinson, R. W., 1953, *Econ. Geol.*, **48,** 492.
Hallimond, A. F., 1953, *Manual of the polarising microscope* (York: Cooke, Troughton and Simms); 1956, *Mining Mag.*, **95,** 271.
Kenyon, J., 1953, *Nature, Lond.*, **172,** 114.
Nicholls, G. D., 1955, *Advanc. Physics*, **4,** 113.
Ramdohr, P., 1926, *Neues Jb. Miner. Geol. Paläont*, **54,** Beil. Bd., Abt. A., 320; 1953, *Econ. Geol.*, **48,** 677; 1955, *Die Erzmineralien und ihre Verwachsungen* (Berlin: Akademie-verlag).
Rehwald, G., 1954, *Ind. Diamond Rev.*, **14,** 111.
Uytenbogaardt, W., 1951, *Tables for microscopic identification of ore minerals* (Princeton University Press).
Vincent, E. A., and Phillips, R., 1954, *Geochim. et Cosmoch. Acta*, **6,** 1.

Crystallization Magnetization †

By Richard R. Doell
Department of Geology and Geophysics, Massachusetts Institute of Technology,
Cambridge, Mass.

This note describes experiments made on some sediments from California. From these experiments it is concluded that the natural remanent magnetization measured in these rocks is not of the usual types, but was acquired by the low temperature formation of magnetic minerals at some time after the deposition of the sediments.

The sediments used for these studies are the ' blue ' sandstones, uppermost-Miocene in age, of the Neroly, Etchegoin, and Jacolitas formations of California. Samples were taken from three areas near the San Francisco Bay region. These are the : Corral Hollow samples taken from a folded region some 50 miles east of San Francisco (geological dips varying from 70°N to 70°S) ; Bailey Canyon samples from an area 30 miles NW of Corral Hollow, where the structure consists of a homocline dipping uniformly to the North at 30° ; and the Santa Cruz samples, taken near the town of Santa Cruz, where the blue sandstones are extremely flat lying.

The lithology of the blue sandstones has been studied by many workers, including McAndrews (1948), Patten (1947), and most recently, Lerbeckmo (personal communication). The most characteristic feature of these sandstones is a distinctive blue colour observed in the hand specimen. The colour is caused by a thin coating, of about 0·007 mm thickness, of a translucent material that covers all grains, but does not fill interstices. In thin section, this coating is colourless, but when coating the relatively large number of dark grains in the rocks, it gives rise to the distinctive colour. X-ray and chemical studies made by Lerbeckmo have identified this coating as an iron rich clay mineral having a Montmorillonite-type structure.

Detrital grains in all the rocks studied are very similar, the most common grain being a subangular rock fragment of andesitic origin. The heavy mineral assemblage is characterized by abundant hypersthene, with augite and hornblend in somewhat lesser amounts. It is generally assumed that these sediments are almost entirely derived from andesites, most likely those of the Sierra Nevada to the east.

Whereas the Corral Hollow and Bailey Canyon samples are moderately to well cemented with carbonates, the Santa Cruz rocks are almost devoid of cement of any type and are extremely friable. Otherwise, the Santa Cruz rocks appear, both in hand specimen and under the microscope, identical to the others.

---

† Published in detail in *Trans. A.G.U.*, **37**, 156, 1956.

Figure 1 shows the directions of magnetization, plotted on the Schmidt projection, of the samples collected at Corral Hollow. These are *in situ* directions, i.e. they are not corrected for the geologic dip of the beds. Plots of the directions of magnetization of samples from the other two areas have not been included in this brief note, but they show similar groupings about the same direction, the data from the Santa Cruz area exhibiting somewhat more scatter.

Fig. 1

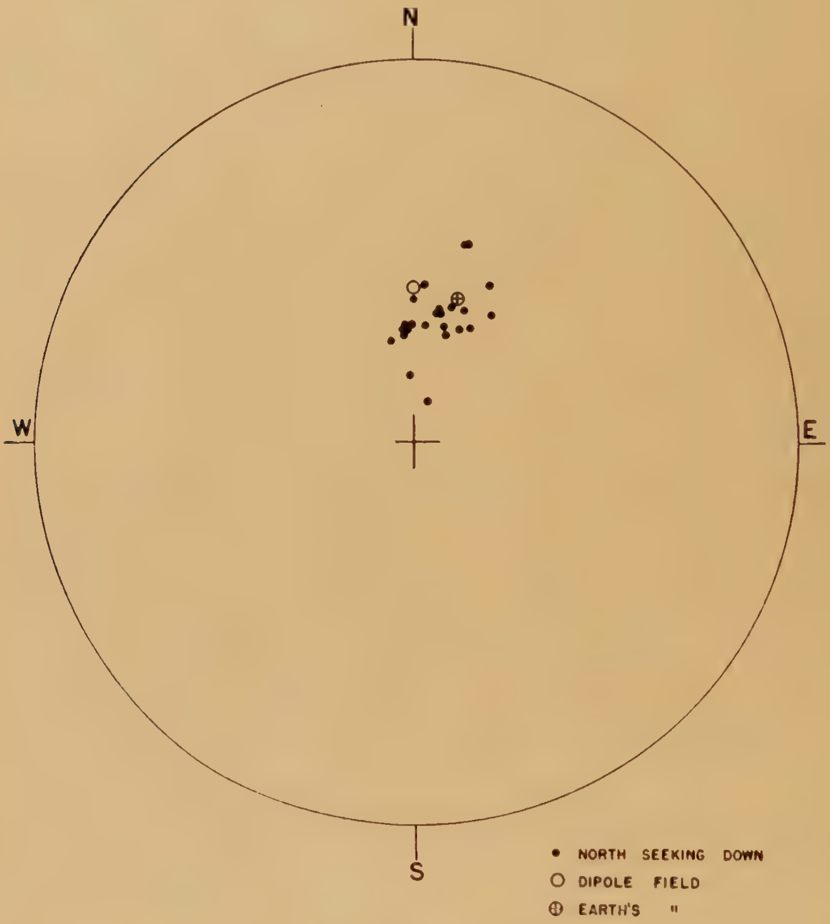

Corral Hollow.

In all three areas the mean directions of magnetization lay close to that of the present Earth's field. In view of the large geological tilts at Corral Hollow and Bailey Canyon, this suggests that the rocks from these sites did not acquire their present magnetic polarization during deposition. On the other hand the flat-lying Santa Cruz rocks may have been magnetized at the time of formation, but if this were so there should be some correlation between grain size and intensity of magnetization, the finer grained sediments possessing higher moments, as pointed out by Graham (1949). However the correlation between grain size and intensity is reverse to this, the finer less permeable samples showing the weaker magnetizations. From these rather crude considerations, and others, based on the type of magnetic grain present in these rocks, which will be discussed later, it appears that the magnetization of the Santa Cruz rocks as well as the others is not due to alignment of grains during deposition. The same reverse correlation is also observed in the Corral Hollow and Bailey Canyon Samples.

Averages of the intensities of magnetization for each of the three localities were computed. These are as follows : Corral Hollow, $2{\cdot}75 \pm 0{\cdot}50 \times 10^{-5}$ cgsu/cm^3 ; Bailey Canyon $1{\cdot}40 \pm 0{\cdot}60 \times 10^{-5}$ cgsu/cm^3 ; and Santa Cruz $0{\cdot}75 \pm 0{\cdot}15 \times 10^{-5}$ cgsu/cm^3. Since the magnetic detrital grains from the different areas are very similar, the differences in magnetization from the separate areas were thought to be correlated with other parameters. The most obvious correlation is the amount and degree of cementing. The Corral Hollow rocks are in general, the best cemented and least porous, although the Baily Canyon samples also show some well indurated types. As mentioned above, cement is almost entirely lacking from the Santa Cruz rocks.

Because of this general apparent correlation of magnetization with grain size, and with degree of cementation, which may be thought of as a general indication of post depositional chemical activity, the origin of the magnetization of these rocks was associated with the later authigenic processes.

The most compelling evidence for this conclusion comes, however, from the effects of heat on the total natural remanent magnetization. First though, it is of interest to consider fig. 2, which gives the results of experiment in which an isothermal remanent magnetization was induced in a few of the samples. The figure (which is typical of all of such experiments) shows the total (natural + isothermal remanent) magnetization as the I.R.M. increases and decays with time. In all cases, the 6 oe field was sufficient to induce such an isothermal component which did not decay completely after several hours, and which appeared to possess some relative stability. For example the application of a 10 oe a.c. field would only slightly remove the induced magnetization. However, by heating the sample to 100°c and cooling in a field free region, one could return to the original magnetization in all cases.

Subsequently, all samples were given this heat treatment to remove any I.R.M. that was present, and the average percentage loss in intensity during heating and its probable error were computed. These were $9{\cdot}5\% \pm 13{\cdot}5\%$. Thus the average loss is not significant. Further, the radius of Fisher's circles of confidence, corresponding to 95% probability, decreased from 5·5° to 4·5° during the treatment.

Some of the samples were heated to 200°c and cooled in a field free region. This time the average loss was $62 \pm 9\%$. These samples, heated to 200°c, were materially changed at this temperature. In particular, the thin clay coating was destroyed, and instead of the distinctive blue colour, the rocks were now a grey colour, resembling a typical graywacke, although not so well indurated.

Although it is possible that there is no connection between the magnetization and the coating, they are both essentially destroyed at temperatures between 100 and 200°c.

Fig. 2

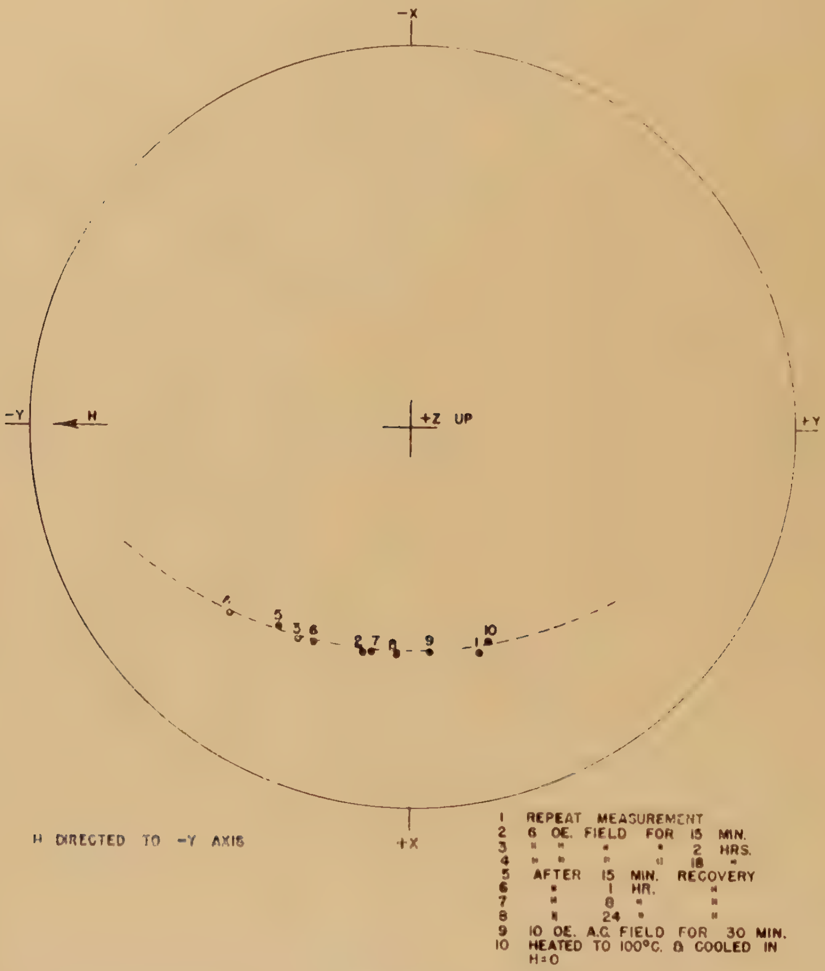

Specimen B–6–2.

Petrographic examinations made on these sandstones are also of interest. The samples were disaggregated and the detrital grains were cleaned in acidic and basic solutions ; the acidic to remove the carbonate cement, and the basic to remove the clay coating. The grains were then separated into magnetic and non-magnetic fractions, although a clean separation was impossible because of the character of the magnetic grains. The magnetic grains are principally composed of a glassy material containing inclusions of an opaque mineral. The amount of opaque inclusions varied up to about 50% of the grain, but was usually very much less. The glassy material is, of course, the ground mass material of the original andesites. After examination of these grains it became clear that they would probably never have acquired a magnetization due to alignment during deposition.

By further crushing and separation some of the opaque material was isolated and used for making x-ray powder diffraction patterns and for spectrochemical analyses. The material was identified as magnetite having a cell dimension of 8·40 Å. The results of the spectrochemical analyses, indicated less than 1% TiO_2, in keeping with the cell constant of 8·40 Å following Povillard's (1956) studies. No other anions besides Fe were present in amounts exceeding about 1%.

Some thin sections of the Neroly formation show an opaque material filling or partially filling some of the interstices. This filling is relatively rare in most sections. However, in all of the sections available one can detect a thin dark rim on the side of the coating away from the grain. Lerbeckmo states that this rim has a very high refractive index, and is most likely magnetite or hematite.

The following considerations are important in these studies :

(1) The detrital magnetic grains from the three different areas show no differences either in character or relative amounts present. This is, of course, to be expected since the sandstones presumably have a common source rock.

(2) The three-fold difference of the average magnetization of the samples collected from the different localities can be correlated with original permeability.

(3) Magnetization by alignment of detrital grains during deposition is excluded by the field relationships and the character of the magnetic grains.

(4) Thermo-remanent magnetization is also not possible, since there is no evidence of metamorphism. Moreover, the relatively large decrease in magnetization at temperatures below 200°C does not allow for a T.R.M. of the detrital grains since magnetites low in titanium have Curie Points above 500°C.

(5) The magnetization is not thought to be of the usual isothermal type because (*a*) such magnetization can be induced in the rocks, and subsequently easily removed, without affecting the natural remanent magnetization measured in the rocks, and (*b*) the behaviour with temperature is not that assigned to isothermal remanent magnetization, i.e. a linear decrease (such a decrease is also expected for viscous magnetization).

The natural remanent magnetization observed in these rocks is thought to be due to the dark rim on the clay coating, which, as stated previously, probably has a high iron content, and is most likely an iron oxide mineral.

This magnetization is therefore the result of a low temperature deposition of magnetic minerals at a time after the formation of the sediments, and is clearly unrelated to the magnetization, if any, of the detrital grains. To distinguish magnetization by this process from I.R.M. and T.R.M., it is termed ‘ Crystallization Magnetization ’.

It also seems reasonable to expect such a magnetization to possess stability, at least in some cases. For example, if the grains are small enough to consist of only one domain, one might expect the direction of magnetization to be in the direction of the applied field. Moreover, one might conclude that the grain would develop with its direction of easy magnetization also parallel to the applied field, since this would be the lowest energy configuration. Magnetization of such grains should therefore possess a high degree of stability.

References

Graham, J. W., 1949, *J. Geophys. Res.*, **54,** 131.
McAndrews, M. G., 1948, *Thesis,* University of California.
Patten, P. R., 1947, *Thesis,* University of California.
Povillard, E., 1950, *Ann. de Chim.,* **5,** 164.

Remarks relative to Maxwell's Formula for the Magnetic Susceptibility of Disseminated Materials

By L. B. Slichter
Institute of Geophysics, University of California, Los Angeles, California.

One of the formulae (Puzicha 1941, Nagata 1953) occurring in the subject of rock magnetism expresses the effective magnetic susceptibility of the rock aggregate in terms of (*a*) the susceptibility of the component magnetic particles, (*b*) their volume–concentration, and (*c*) their mean demagnetization factor. This formula has been attributed to various sources, but references to the very early work of Clerk Maxwell seem to be missing in the literature. In his treatise *Electricity and Magnetism* Maxwell (1873, 1881) discussed the effective electrical conductivity of a medium containing a dispersion of small conducting spheres. With change of notation, his results are, of course, equally valid for the corresponding magnetic case. Since his solution is very direct, it may be of interest to reproduce it here.

Let the magnetic permeability of the medium be μ_0, and that of the small spheres, μ_i. The distance between the particles is taken to be so great that interaction effects are negligible. Let the magnetic field intensity in the medium (except near a small sphere) be uniform, and of value H_0. The magnetic moment of one of the spheres, of radius a, is, then

$$m = H_0\,(\mu_i - \mu_0)(\mu_i + 2\mu_0)^{-1}\,a^3. \qquad \text{(1)}$$

Let the total number of these spheres be n, and let them be confined to a spherical volume of radius A, throughout which their average volume–density is v. Then the total moment of the aggregate is

$$M = H_0\,(\mu_i - \mu_0)(\mu_i + 2\mu_0)^{-1} n\,a^3. \qquad \text{(2)}$$

In terms of the effective permeability, $\bar{\mu}$, of the aggregate, this moment may also be written

$$M = H_0\,(\bar{\mu} - \mu_0)(\bar{\mu} + 2\mu_0)^{-1}\,A^3. \qquad \text{(3)}$$

Noting that the average volume density, v, is $na^3\,A^{-3}$, one obtains from eqns. (2) and (3) the following expression for $\bar{\mu}$

$$\frac{\bar{\mu} - \mu_0}{\bar{\mu} + 2\mu_0} = v\,\frac{(\mu_i - \mu_0)}{(\mu_i + 2\mu_0)}. \qquad \text{(4)}$$

It is clear that this result is *not* affected if the small spheres are distributed as to size. Explicitly, the equivalent permeability is

$$\bar{\mu} = \mu_0\,[1 + 2vR]\,[1 - vR]^{-1} \qquad \text{(4a)}$$

where $R = (\mu_i - \mu_0)\,(\mu_i + 2\mu_0)^{-1}$, and $-\frac{1}{2} < R < 1$. Thus when v is small

$$\bar{\mu} = \mu_0\,(1 + 3vR). \qquad \text{(4b)}$$

Since the absolute value of R is less than unity, the effective permeability is, as is well known, determined primarily by the concentration.

Alternatively, the magnetic moment in eqn. (1) is often written in terms of the susceptibility and internal field strength, H_i, as follows

$$m=\frac{4}{3}\pi a^3 k_i H_i=4\pi\, a^3 k_i \mu_0\,(\mu_i+2\mu_0)^{-1}\,H_0 \quad . \quad . \quad . \quad . \quad (5)$$

from which, on comparing with eqn. (1), the usual definitive relation between k_i and μ_i is obtained

$$4\pi\, k_{i0}=\mu_i\,\mu_0^{-1}-1. \quad . \quad . \quad . \quad . \quad . \quad . \quad . \quad . \quad (6)$$

(It is to be noted that this formula is often specialized for the case $\mu_0=1$, which disguises the fact that the susceptibility is a relative quantity, jointly determined by μ_i and μ_0, and *not* a true constant of material.) From (6) and (4) it follows that

$$\frac{\bar{k}}{1+(4\pi/3)\,\bar{k}}=v\frac{k_i}{1+(4\pi/3)\,k_i} \quad . \quad . \quad . \quad . \quad . \quad . \quad . \quad (7)$$

where the factor $4\pi/3$ is the demagnetization factor for the sphere. More generally, if the particles are similar ellipsoids with corresponding axes aligned in the direction of H_0 with demagnetization factor N_i, and if the enclosing volume is also of ellipsoidal shape with a principal axis along H_0, and with associated demagnetization factor $\bar{N}$, then eqn. (7) takes the form

$$\bar{k}\,(1+\bar{N}\bar{k})^{-1}=v\,k_i\,(1+N_i k_i)^{-1} \quad . \quad . \quad . \quad . \quad . \quad . \quad . \quad (8)$$

or

$$\bar{k}=v\,k_i\,[1+N_i k_i-v\,\bar{N}\,k_i]^{-1}. \quad . \quad . \quad . \quad . \quad . \quad . \quad . \quad (9)$$

This familiar result (3) is conveniently used in the form

$$v\,\bar{k}^{-1}=k_i^{-1}+N_i-\bar{N}\,v. \quad . \quad . \quad . \quad . \quad . \quad . \quad . \quad . \quad (10)$$

Thus $v\,\bar{k}^{-1}$ is a linear function of the concentration. Since the intercept at $v=0$ is the *sum* of the demagnetization factor *and* the reciprocal susceptibility of the particles, the separate determination of these quantities, under the assumed conditions of small concentrations and negligible interaction effects, is impossible. This essential ambiguity is a noteworthy feature of such disseminations. The determination of k_i is further handicapped by the rather large value of N_i relative to k_i^{-1}. Thus N_i is generally between 3 and 4 (Nagata 1953) whereas the value of k_i is in the neighbourhood of unity, but highly variable dependent on the source of the magnetite. Puzicha (1941) finds values for k_i between 0·25 and 2·5. It seems likely that an important part of the spread in the determinations of the susceptibility of disseminated magnetite particles arises from uncertainties in the effective values of the demagnetization factors.

For example, measurements by the author (Slichter 1928) relative to the effective susceptibility of pulverized magnetite in an inert matrix gave a value for the intercept, $k^{-1}+N_i$, in eqn. (11) of about 3·8. Thus if $N_i=3$, then $k_i=1{\cdot}25$; but if $N_i=3{\cdot}5$, then $k_i=3{\cdot}33$. Since the magnetization is primarily along the long dimension of the magnetic particles, subsequent deformation of a rock containing elongated magnetic particles may be expected to alter its direction of magnetization. Shearing deformations obviously should be especially effective in producing such direction changes.

REFERENCES

MAXWELL, CLERK, 1873, *Electricity and Magnetism* (Oxford : Clarendon Press), 1st Edn.; 1881, *Ibid.*, **1**, 403, 2nd Edn.

NAGATA, TAKESI, 1953, *Rock Magnetism* (Maruzin Co. Ltd.), p. 94, eqns. (3–6).

PUZICHA, KURT, 1941, *Beits. Angew. Geophysik*, **9**, 177, eqn. (3).

SLICHTER, L. B., 1928, *A.I.M.E.E. Technical Publication*, 120. (Reproduced in A.I.M.M.E. “ Geophysical Prospecting ”, 1929.)

Chemistry and Magnetic Properties of some Ferrimagnetic Oxides like those occurring in Nature

By E. W. Gorter

Philips Research Laboratories, N.V. Philips' Gloeilampenfabrieken,
Eindhoven-Netherlands

§ 1. Introduction

Ferrimagnetic oxides are found useful in the electronics industry by virtue of their high resistivity, which makes them applicable at high frequencies. At these frequencies metallic ferromagnetics are unusable because of eddy currents. All technically important ferrimagnetic oxides contain ferric ions. Since the simultaneous occurrence of ferrous and ferric ions in one type of lattice site leads to electronic conductivity, the oxides investigated by workers in industry usually do not contain ferrous ions. The ferrimagnetic oxides occurring in nature, on the other hand, almost all contain ferrous ions. Nevertheless, the knowledge obtained on materials not containing ferrous ions may help towards a better understanding of those that do.

The author will assume the reader to have some knowledge of the chemistry and magnetism of oxides, since these subjects have been treated in this journal in the extensive review articles by Nicholls (1956) and Néel (1956).

The figure that has been shown most often during this conference is the composition diagram $FeO–TiO_2–Fe_2O_3$ given again in fig. 1 (*a*), with the two (now three (Akimoto 1957, Akimoto *et al.* 1957)) lines for the solid solution series :

$Fe^{II}Fe_2^{III}O_4–Fe_2^{II}Ti^{IV}O_4$,
or $Fe^{III}_{2-2a}Fe^{II}_{1+a}Ti^{IV}_{a}O_4$, with spinel structure.

$Fe_2^{III}O_3–Fe^{II}Ti^{IV}O_3$,
or $Fe^{III}_{2-2a}Fe^{II}_{a}Ti^{IV}_{a}O_3$, with hematite (ilmenite) structure.

$Fe_2^{III}Ti^{IV}O_5–Fe^{II}Ti_2^{IV}O_5$,
or $Fe^{III}_{2-2a}Fe^{II}_{a}Ti^{IV}_{1+a}O_5$, with pseudobrookite structure.

The use of formulae like $(1+a)FeO.Fe_2O_3.a2FeO.TiO_2$, $Fe_2O_3.TiO_2$, etc. is very impractical when it is desired to denote cation distribution (by brackets), or magnetic structure (by arrows) in the formula. Using the ordinary type of formula, it is much more practical to use a diagram which refers to one ion of each metal, i.e. in the present case put $\frac{1}{2}Fe_2O_3$

Fig. 1 (*a*)

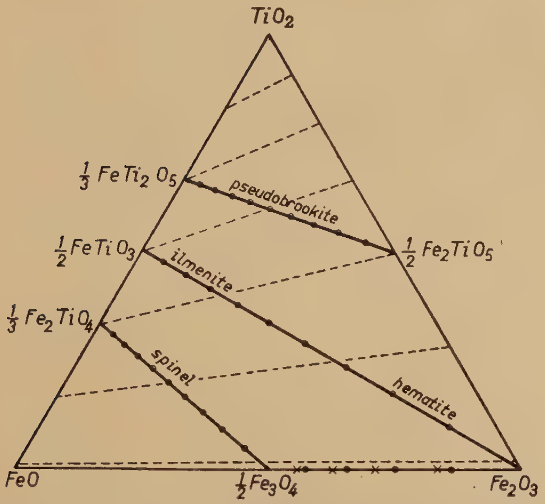

Usual representation of the composition diagram FeO–TiO_2–Fe_2O_3. The oxidation lines (broken lines) are not parallel. In the three solid-solution series $Fe_{2-a}Ti_{1+a}O_5$, $Fe_{2-a}Ti_aO_3$ and $Fe_{3-a}Ti_aO_4$ (thick drawn lines) the points $a=0{\cdot}1$, $0{\cdot}2$ . . . $1{\cdot}0$ (circles) do not lie at equal distances. Between Fe_3O_4 and Fe_2O_3 the points $a=0{\cdot}2$, $0{\cdot}4$, etc. are represented by crosses for a formula $(1-a)Fe_3O_4 . aFe_2O_3$ and by circles for a formula $(1-a)Fe_3O_4 . aFe_{8/3}O_4$.

Fig. 1 (*b*)

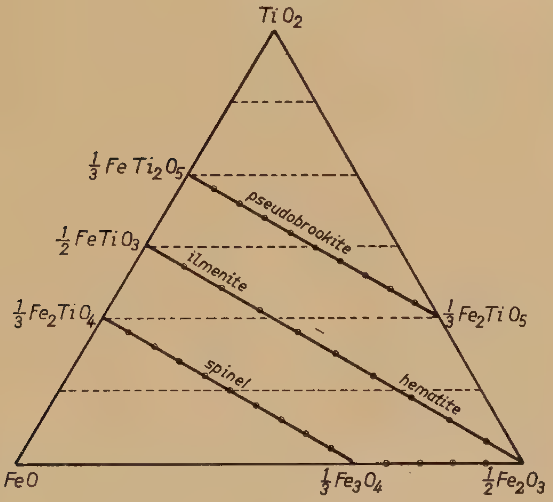

Representation of the same diagram with $\frac{1}{2}Fe_2O_3$ instead of Fe_2O_3. Note that now the oxidation lines are horizontal and that the points $a=0{\cdot}1$, $0{\cdot}2$, etc. on the three solid-solution lines lie at equal distances, and also the points in the series Fe_3O_4–$Fe_{8/3}O_4$.

instead of Fe_2O_3 (fig. 1 (*b*)). When this is done, one sees that, in contrast with fig. 1 (*a*),

(*a*) the position of a compound on the edge of the diagram corresponds to its chemical formula ;

(*b*) the position on the line of a solid solution in each of the three series varies linearly with *a* ;

(*c*) the oxidation lines, e.g. from Fe_2TiO_4 to Fe_2TiO_5, are horizontal.

The advantage given under (*b*) applies also for solid solutions Fe_3O_4–Fe_2O_3 in as far as such solid solutions exist (see § 2.3).

The three lines do not represent phase regions, but only the lines on which stoiochiometric compositions Me_3O_4, Me_2O_3 and Me_3O_5 are found. For the pseudobrookite and hematite–ilmenite structures no materials with non-stoiochiometric compositions are known to the author. For the spinel structure it is known for several cases that there is slight, if any, solubility at high temperature of MeO in $Me^{II}Me_2^{III}O_4$. There is very appreciable, but not complete, solubility of Fe_2O_3 in $MeFe_2O_4$: on quenching such a solid solution is maintained, but on slow cooling αFe_2O_3 separates. In the diagram the extension of the spinel phase region, above the stoiochiometric spinel line, depends on temperature.

The occurrence of a miscibility gap at lower temperatures in the Fe_3O_4–Fe_2TiO_4 system does not seem to be in great doubt. In the Fe_2O_3–$FeTiO_3$ system a miscibility gap occurs which at higher temperature closes : Akimoto (1957) for the first time gives properties of a continuous series of solid solutions prepared by quenching from a high temperature. The pseudobrookite series was prepared by Akimoto *et al.* (1957) by quenching from 1150°C : it is quite possible that at lower temperature separation into two pseudobrookite phases will occur. We shall discuss the factors that influence the separation of a solid solution into two phases below.

§ 2. CRYSTAL CHEMISTRY OF THE SPINEL STRUCTURE

The spinel structure is characterized by a cubic, almost close-packed, oxygen lattice in which metal ions lie on tetrahedral sites surrounded by a regular tetrahedron of oxygen ions and on octahedral sites, surrounded by six oxygen ions whose centres form a slightly distorted octahedron. We have for a change in figs. 2 (*a*), 2 (*b*) and fig. 3 represented this cubic structure, an ordinary cubic description of which is given by Gorter (1954 a), in a hexagonal unit cell containing six formula units Me_3O_4, i.e. six tetrahedral (A) ions, twelve octahedral (B) and twenty-four oxygen ions.

All ions in the cell lie in the set of {110} planes around the triad axes indicated by $[0\,0\,z]$, $[\frac{1}{3}\,\bar{\frac{1}{3}}\,z]$, etc. in fig. 3, which shows such a (110) plane. Figures 2 (*a*) and 2 (*b*) give views of basal planes of the hexagonal cell at the indicated heights.

Fig. 2 (*a*)

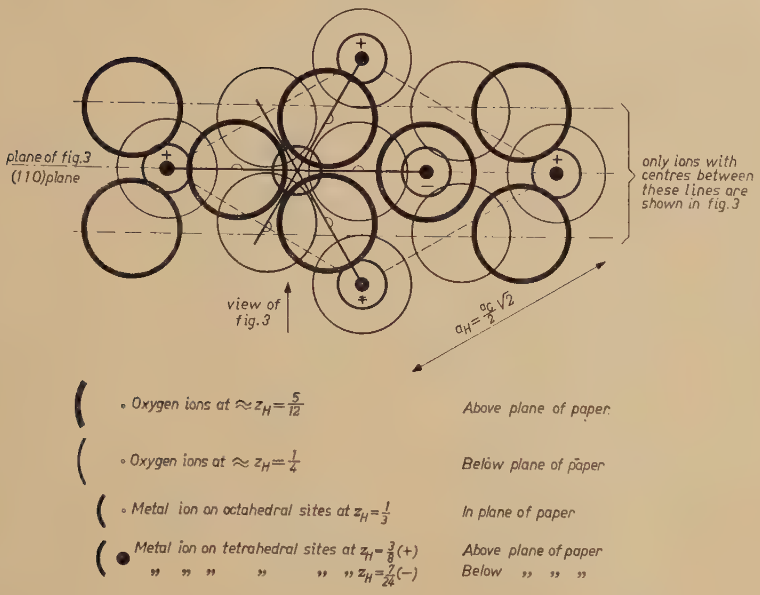
+
+
+
−
+
plane of fig.3
(110)plane
only ions with centres between these lines are shown in fig.3
view of fig.3
$a_H = \frac{a_C}{2}\sqrt{2}$
∘ Oxygen ions at $\approx z_H = \frac{5}{12}$
Above plane of paper
∘ Oxygen ions at $\approx z_H = \frac{1}{4}$
Below plane of paper
∘ Metal ion on octahedral sites at $z_H = \frac{1}{3}$
In plane of paper
● Metal ion on tetrahedral sites at $z_H = \frac{3}{8}$(+)
Above plane of paper
" " " " " " $z_H = \frac{7}{24}$(−)
Below " " "

Fig. 2 (*b*)

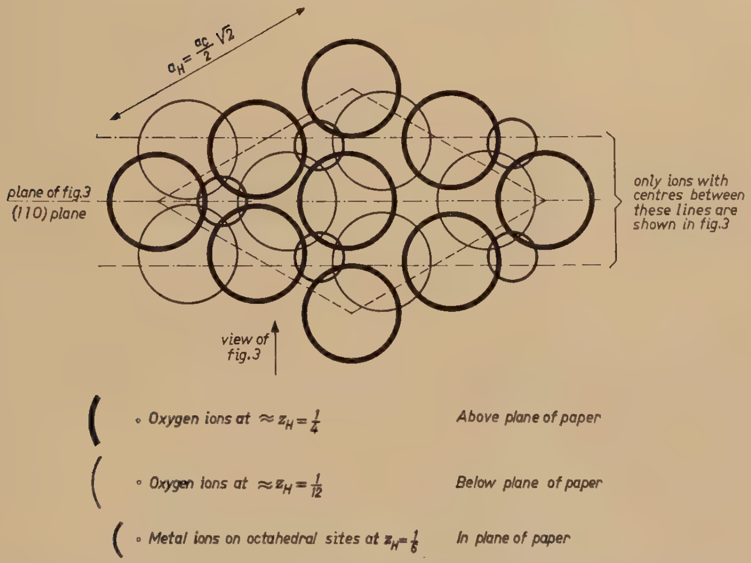
$a_H = \frac{a_C}{2}\sqrt{2}$
plane of fig.3
(110) plane
only ions with centres between these lines are shown in fig.3
view of fig.3
∘ Oxygen ions at $\approx z_H = \frac{1}{4}$
Above plane of paper
∘ Oxygen ions at $\approx z_H = \frac{1}{12}$
Below plane of paper
∘ Metal ions on octahedral sites at $z_H = \frac{1}{6}$
In plane of paper

In these figures the spinel structure is represented in a hexagonal unit cell, with cell edges $a_H = \frac{1}{2}a_C\sqrt{2}$ along cubic [110] axes and $c_H = a_C\sqrt{3}$ along a cubic [111] axis. The broken lines show the edges of the hexagonal unit cell.

Figures 2 (*a*) and 2 (*b*) show the hexagonal planes ($z=\frac{1}{3}$) and ($z=\frac{1}{6}$) respectively (|| a cubic (111) plane).

Fig. 3.

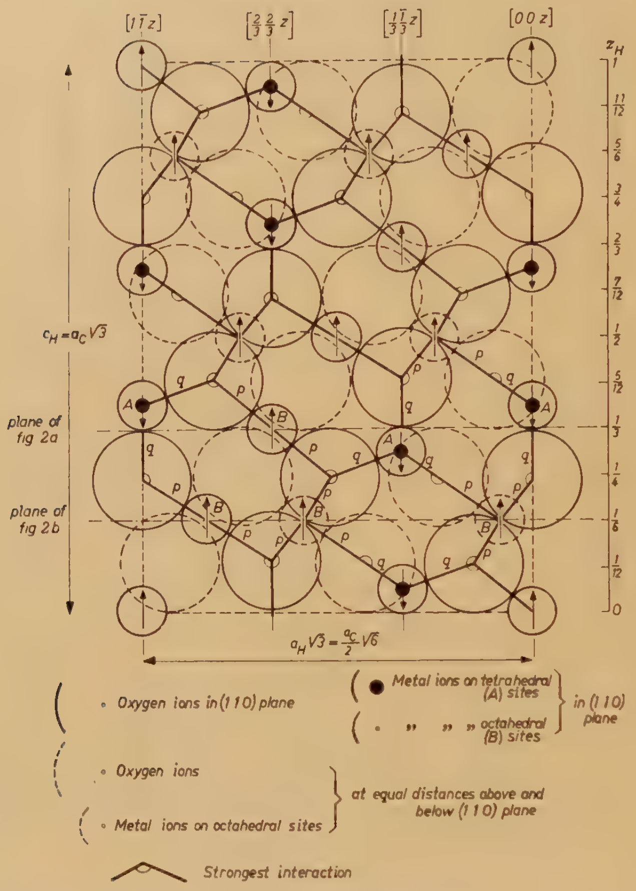
[1 1̄ z]
[2/3 2/3 z]
[1/3 1̄/3 z]
[0 0 z]
z_H
1
11/12
5/6
3/4
2/3
7/12
1/2
5/12
1/3
1/4
1/6
1/12
0
$c_H = a_C\sqrt{3}$
plane of fig 2a
plane of fig 2b
A
B
p
q
$a_H\sqrt{3} = \frac{a_C}{2}\sqrt{6}$
Oxygen ions in (1 1 0) plane
Metal ions on tetrahedral (A) sites
" " " octahedral (B) sites
in (1 1 0) plane
Oxygen ions
Metal ions on octahedral sites
at equal distances above and below (1 1 0) plane
Strongest interaction

In this figure the spinel structure is represented in a hexagonal unit cell, with cell edges $a_H = \frac{1}{2}a_C\sqrt{2}$ along cubic [110] axes and $c_H = a_C\sqrt{3}$ along a cubic [111] axis. The broken lines show the edges of the hexagonal unit cell.

Figure 3 shows a section of a hexagonal (110) plane through the hexagonal unit cell perpendicular to the plane of figs. 2 (*a*) and 2 (*b*). Figures 2 and 3 have been drawn for an oxygen parameter $u = 0{\cdot}383$, i.e. the oxygen ions are slightly displaced with respect to ideal close packing, away from the tetrahedral ions, as occurs in most ferrimagnetic spinels. The ions indicated by broken lines lie in front of and behind the plane of the paper. Relative directions of ionic magnetic moments are indicated by arrows.

In order that an oxide with spinel structure is formed, the metal ions must have ionic radii between ~0·5 and ~1·0 Å, but no restriction applies as regards valency: 29 different ions with valencies ranging from 1 to 6 are known to occur in oxidic spinels, viz.:

(*a*) the noble gas ions Li^+, Mg^{2+}, Al^{3+}, Ti^{4+} (Na^+, Ca^{2+}, Sc^{3+}†);

(*b*) the ions with 18 electron-shell configuration (Ag^+‡) Zn^{2+}, Ga^{3+}, Ge^{4+}, Cd^{2+}, In^{3+}, Sn^{4+};

(*c*) the divalent ions of the first transition series Mn^{2+}, Fe^{2+}, Co^{2+}, Ni^{2+}, Cu^{2+};

(*d*) the trivalent ions of the first transition series V^{3+}, Cr^{3+}, Mn^{3+}, Fe^{3+}, Co^{3+};

(*e*) the tetravalent ions of the first transition series V^{4+}, Mn^{4+};

(*f*) ions of the other transition series: Rh^{3+} (Mo^{6+}, W^{6+}‡).

2.1. *Binary Spinels*

Verwey and Heilmann (1947) noted that in a number of binary spinels a certain order of preference for the tetrahedral sites exists. This depends in the first place on charge and size of the ions (Verwey *et al.* 1948, de Boer *et al.* 1950). Verwey *et al.* (1948) have calculated the lattice energy of a purely ionic crystal as a function of the charge distribution and for different values of the oxygen parameter u, i.e. as a function of the size of the ions in the different sites.§ The calculation shows that larger ions with a low valency will have a preference for tetrahedral sites, e.g. Ag^+, Mn^{2+}, like small ions with high valency, e.g. Ge^{4+}. Small ions with low valency (like empty lattice sites, hydrogen, see below) and large ions with high valency, e.g. Ti^{4+}, Sn^{4+}, will have a preference for octahedral sites.

Apart from this, a specific preference is shown by certain ions for either fourfold or sixfold coordination. Fourfold coordination may be favoured by the tendency for sp^3 covalent bonding: this is active in the ions under (*b*). Sixfold coordination may be favoured either by the tendency for d^2sp^3 covalent bonding, or by crystalline-field effects (Romeijn 1953): Ni^{2+} and Cr^{3+} have a strong preference for sixfold coordination for this reason. A tendency for the formation of covalent bonds, of the square dsp^2 type, of Cu^{2+} and Mn^{3+} ions on octahedral sites is thought by Goodenough and Loeb (1955) to be responsible for the tetragonal deformation of the spinel $CuFe_2O_4$ ($c/a=1·06$) and most manganites, e.g. $Mn^{II}(Mn_2^{III})O_4$ ($c/a=1·16$).

---

† Only in small quantities up to 0·2–0·5 ion per formula unit Me_3O_4.

‡ Only in Ag_2MoO_4 and Ag_2WO_4.

§ For a convenient representation of their results see Gorter, 1954 a, fig. 7.

The size-and-charge effect may outbalance the specific preference: this is for example the case for Sn^{4+} which is found on octahedral sites. The noble-gas ions mentioned under (*a*) and the ions with half-filled 3d shell Mn^{2+} and Fe^{3+} have no specific preference for either coordination; the remaining ions probably only have weak preferences.

Originally a division was made for binary spinels $MeMe'_2O_4$ in normal spinels $Me[Me'_2]O_4$, like $Zn[Al_2]O_4$, $Zn[Fe_2]O_4$ (the octahedral ions are enclosed in brackets), in which each of the sites is occupied by a different type of ion (similar to the situation in many other crystal structures), and inversed spinels like $Co^{II}[Ti^{IV}Co^{II}]O_4$ and $Fe^{III}[Me^{II}Fe^{III}]O_4$, where the two ions Me′ are found on both sites, on the octahedral sites together with Me. Binary spinels with different valency combinations like $Fe^{III}[Li^{I}_{0\cdot5}Fe^{III}_{1.5}]O_4$ and $Li^{I}[Li^{I}_{1/3}Ti^{IV}_{5/3}]O_4$ (Jonker 1957) might be called inverse, but could not be called normal for other (hypothetical) distributions.

2.2. *Methods of Investigating Cation Distribution*

More recent investigations have taught that purely normal or purely inverse spinels are an exception rather than the rule. This has been made possible by more accurate methods of investigation. The methods used have been the following:

(*a*) Measurement of the saturation magnetization at low temperatures. Néel's theory of ferrimagnetism (1948) postulated a strong dominant negative exchange interaction between ions on tetrahedral (A) and those on octahedral (B) sites, and weaker negative AA and BB interactions. In simple cases, i.e. for which the AB interaction is really dominant, it is possible to find the saturation magnetization at 0°K, expressed in Bohr magnetons per formula unit Me_3O_4 ('the saturation moment') by simply subtracting the sum of the ionic magnetic moments occurring on the A sites from those on the B sites, or vice versa.

In contrast with the atoms in metals, the magnetic first transition metal ions in oxides have magnetic moments that are simple whole numbers, equal to the number of 3d electrons n_d if less than 5, and equal to $10-n_d$ for $n_d>5$, i.e. $3\,\mu_B$ for Cr^{3+}, $5\,\mu_B$ for Mn^{2+} and Fe^{3+}, $4\,\mu_B$ for Fe^{2+}, $3\,\mu_B$ for Co^{2+} and $2\,\mu_B$ for Ni^{2+}. Small orbital contributions raise the moment of Ni^{2+} from 2 to about 2·3 and of Co^{2+} from 3 to about 3·7; the moment of Fe^{2+} is only very slightly higher than $4{\cdot}0\,\mu_B$ (Guillaud 1951, Gorter 1954 a). In binary spinels the cation distribution can be obtained from the saturation moment.

In many cases for ferrimagnetic spinels with Curie temperature below roughly 600°K, the saturation magnetization at 0°K is lower than can be explained in the above way. This is due to a weakening of the AB interaction, e.g. by dilution of the A sites by diamagnetic ions like Zn^{2+} ions. The BB interaction, which would tend to place the B spins antiparallel to each other, can then make itself felt and, therefore, spoils the parallel alignment of the B spins. Yafet and Kittel (1952) have calculated that the lowest energy is obtained when the B sub-lattice is split up into two (or rather four) sub-lattices, each with different spin orientation, but with a resultant orientation still antiparallel to that of the A lattice. Direct proof of such a superstructure formation of spins has not so far been published.† The Curie temperature limit of about 600°K above which no such triangular arrangements are known to occur may be understood from the fact that the Curie temperature is mainly determined by the strongest, i.e. AB interaction. A BB interaction which is strong enough to lead to triangular configurations would lower the Curie temperature roughly by a third, and the highest known Curie temperature for a spinel is 675°C. Although below 600°K we must be watchful for triangular configurations at 0°K, it is not impossible that antiparallel arrangements occur for much lower Curie temperatures. It must be emphasized that saturation magnetization (σ) measurements at room temperature are without value for finding the cation distribution, since the shape of the saturation magnetization *vs.* temperature curve for ferrimagnetics may vary greatly. Measurements at hydrogen or even helium temperature are preferable to those at liquid–air temperature: the latter can be used only when the Curie temperature is very high and the σ *vs* T curve is very concave towards the T-axis, such as for Fe_3O_4.

(*b*) X-ray diffraction is of course in principle the best method for studying cation distributions. Unfortunately one is often interested in spinels containing different ions of the first transition series, which have scattering powers very near to one another. Therefore, the intensity difference for different cation distributions is not very large, and, moreover, the intensities are also altered by a change in oxygen parameter. At the best a combination of distribution parameter x and oxygen parameter u is obtained. Nevertheless, by comparing ratios of intensities of pairs of reflections that are more sensitive to a change in distribution parameter than to a change in oxygen parameter u, it is often possible to obtain much more accurate information than was previously obtained (Bertaut 1951, Romeijn 1953).

(*c*) Neutron diffraction, apart from giving information on the direction of magnetic spins, barely otherwise obtainable, is a magnificent tool for the investigation of cation distribution, because the effective scattering cross sections for neutrons of the transition metal ions are often widely different. Titanium, which occurs in practically all oxides in which workers in rock magnetism are interested, is specially favourable in this respect, since the scattering cross section is very much smaller than for the other ions.

The study of electronic conductivity (Romeijn 1953), of light absorption or reflectivity spectra (Romeijn 1953, Schmitz-DuMont 1957), of ferromagnetic resonance (Gorter 1954 a, b, Smart 1954) and the possibility of using other physical methods all with a view of obtaining information on the cation distribution, will not be discussed here.

---

† See, however, E. Prince, for $CuCr_2O_4$, to be published.

2.3. *The Simple Case of* $MgFe_2O_4$

Magnesium ferrite, $MgFe_2O_4$, was one of those spinels for which the inversed arrangement $Fe[MgFe]O_4$ was first discovered by x-ray investigation (Barth and Posnjak 1932). For this formula the magnetic moments of the ferric ions, each 5 μ_B, would cancel each other so that the saturation moment would be 0 μ_B. The value found for a slowly cooled sample is 1·1 μ_B, which can be explained by a formula $Fe_{1-x}Mg_x[Mg_{1-x}Fe_x]O_4$ (Gorter 1950, 1954 a) with $x=0{\cdot}11$.

Pauthenet and Bochirol (1951) quenched samples of $MgFe_2O_4$ from different temperatures and from the saturation moments found the cation distribution. The distribution parameter x varied with temperature according to a Boltzmann distribution law given by Néel (1950) :

$$x(1+x)/(1-x)^2=\exp(-E/kT)$$

in which E is the energy involved in the interchange of a Mg ion on a B site and a Fe ion on an A site.

For the case of $MgFe_2O_4$, from measurements above ∼400°c, they found $E/k \sim 1220°$K, so that at room temperature one calculates $x=0{\cdot}015$. When one finds a value $x=0{\cdot}11$ this must mean that the cooling rate has not been sufficiently slow in order to maintain thermal equilibrium below a ‘ freezing-in ’ temperature, which for a saturation moment of 1·1 μ_B is found from the above formula to be 650°K. The cation distribution for any spinel must be regarded as that corresponding to such a freezing-in temperature, which varies with the cooling rate, with the type of ions present, and generally with all factors that determine the diffusion rate of the ions at a certain temperature.

An example of such a factor recently found is given here. Magnesium ferrite was sintered at 1450°c and slowly cooled. A saturation moment of 2·2 μ_B† (and a Curie temperature of 330°c) was found (Gorter, unpublished results), corresponding to a freezing-in temperature of 1230°c, which is very much higher than for the sample slowly cooled from 1250°c (1·1 μ_B), and even higher than for our sample quenched from 1250°c (1·4 μ_B) (Gorter 1950). The probable cause of this paradox is the disappearance, at the highest sintering temperature, of lattice defects, which aid diffusion.

The ionic distribution found after slow cooling is always the distribution corresponding to such a freezing-in temperature, which must be regarded as an average temperature. Since oxides have a very low thermal conductivity ($\sim 1{\cdot}0\times 10^{-2}$ cal/cm/sec/°c) it is very difficult to cool a piece of oxide material at the uniform rate. It is therefore very likely that the parts nearer to the surface are cooled more rapidly and have a more statistical distribution. Indications of such a non-uniform cation distribution have been found in the solid–solution series $NiFe_{2-a}Al_aO_4$, for samples cooled at a rate of ¼°c/min (Gorter 1954 a).

---

† The slight reduction of the material, corresponding to the analysis (0·7 wt % Fe^{2+}) would cause an increase of ∼0·02 μ_B.

It is seen that for $MgFe_2O_4$ the Curie temperature is also decreased by inversion, which is understood from the Néel theory.

Also the cell edge of $MgFe_2O_4$ varies with x at an approximate rate of $\Delta a/\Delta x = 0{\cdot}06$ for Fe^{2+}-free samples (Gorter, unpublished results), corresponding to regularities in cell edges observed by Verwey and Heilmann (1947). It is for very few spinels possible to give one defined value of the saturation moment, the Curie temperature and the cell edge, except for a few cases, like probably Fe_3O_4.

The metastable form of ferric oxide, 'γFe_2O_3', which occurs in nature as maghemite, has been found often to contain some water, i.e. it may be a solid solution $(1-a)Fe[Fe_{5/3}\square_{1/3}]O_4 . aFe[H_{0\cdot5}Fe_{1\cdot5}]O_4$† (Braun 1952, Verwey 1954). This need not to be true when some other impurity, e.g. Na, Ca or Mn ions, is present.

Complete miscibility occurs between 'γFe_2O_3' and precipitated 'Fe_3O_4' that also contains water (Starke 1939, David and Welch 1956), but not between Fe_2O_3 and Fe_3O_4.

2.4. *Valency of Transition Ions*

Another problem occurs in spinels that contain one element or two or more of those that can occur in more than one valency state, viz. Ti, V, Cr, Mn, Fe, Co, Ni and Cu. Chemical analysis cannot answer the question which pair of valencies is present in such materials, e.g. in Fe_3O_4, Co_3O_4, Mn_3O_4 on the one hand, and Fe_2TiO_4, $MnFe_2O_4$ and $Cu_{0\cdot5}Fe_{2\cdot5}O_4$ on the other hand. Low-temperature magnetic saturation measurements may decide in some cases, but in the case of Fe_3O_4 a value of $4\mu_B$ is obtained both for a formula $Fe^{III}[Fe^{II}Fe^{III}]O_4$ and for a formula $Fe^{II}[Fe^{II}Fe^{IV}]O_4$.

A decision is usually made on grounds of the existence or non-existence of related compounds. For instance, failure to obtain a spinel Zn_2CoO_4 Robin (1952) makes us believe that Co^{4+} ions do not occur in spinels in more than trace amounts. Similar arguments can be adduced for Fe^{4+} and for Ni^{3+} and Ni^{4+} (Gorter, unpublished results). For the case of Fe_2TiO_4, the existence of titanates Mn_2TiO_4, Co_2TiO_4 and Zn_2TiO_4, and our failure to synthesize spinels $MnTi_2O_4$, $CoTi_2O_4$ and $NiTi_2O_4$ from the metal Mn, Co or Ni and TiO_2 in sealed silica tubes at 1050°C, for Ni also for 48 hours at 1100°C (Gorter, unpublished results) make us believe that the formula of Fe_2TiO_4 should be $Fe_2^{II}Ti^{IV}O_4$. It must be realized, however, that materials we fail to prepare today, may be prepared tomorrow by somebody else.

For manganese ferrite, a formula $Mn^{II}Fe_2^{III}O_4$ would give $5\mu_B$ for any cation distribution. Nevertheless, a stoichiometric preparation with $4{\cdot}6\,\mu_B$ has been reported (Guillaud 1951).

Although it has recently been suggested that mixed valencies like $Mn^{2+}+Mn^{3+}+Fe^{3+}+Fe^{2+}$ can occur together, perhaps even in one lattice site† (Harrison *et al.* 1957), the experimental data including the recent neutron diffraction investigations (Corliss and Hastings 1956, Nathans *et al.* 1957) cannot at present be explained in this way.

---

† Discussion remark, 1951, *J. Phys. Radium*, **12**, 199.

Another interesting case is the spinel $Cu_{0\cdot5}Fe_{2\cdot5}O_4$. Kordes and Röttig (1951) consider this to be $Cu^{I}_{0\cdot5}Fe^{III}_{2\cdot5}O_4$, and not a solid solution between $Cu^{II}Fe_2O_4$ and $Fe^{II}Fe_2O_4$, because the Curie point (390°c) lies below those of cupric ferrite and ferrous ferrite (490°c and 570°c respectively). Bertaut and Delorme (1953) prepared the same compound and found that it decomposes at lower temperatures into $\frac{1}{2}CuFeO_2$ and Fe_2O_3. They rightly consider this a proof that the spinel solid solution is only stable because of the contribution of the entropy term to the free energy, but wrongly that the gain in entropy is due to a completely statistical distribution of the cupric, ferrous and ferric ions over the A and B sites, i.e. corresponding to a formula

$$Cu^{II}_{1/6}Fe^{II}_{1/6}Fe^{III}_{2/3}[Cu^{II}_{1/3}Fe^{II}_{1/3}Fe^{III}_{4/3}]O_4.$$

They found the saturation moment to be $4{\cdot}10\,\mu_B$, very near to the value $4\frac{1}{6}\mu_B$ calculated for the above distribution. Another sample, which had a correct oxygen content, had a saturation moment of $4{\cdot}50\,\mu_B$ (Gorter, unpublished results). The explanation of the French workers implies that the entropy term is solely responsible for the cation distribution. In that case any other preparation with the correct composition could only have a saturation moment between 4·17 and $2{\cdot}5\,\mu_B$, the latter value being that for a hypothetical inverse cupric-ferrous ferrite $Fe[Cu^{II}_{0\cdot5}Fe^{II}_{0\cdot5}Fe]O_4$. We should like to suggest that in this material all ferrous ions present occur on octahedral sites. This leaves the following possibilities :

(*a*) the copper ions present in the A sites are monovalent :

$$Cu^{I}_{x}Fe^{III}_{1-x}[Fe^{III}_{x}(Cu_{0\cdot5-x}Fe_{0\cdot5-x})Fe^{III}_{1+x}]O_4\,;$$

(*b*) the copper ions in tetrahedral sites are divalent :

$$Cu^{II}_{y}Fe^{III}_{1-y}[Fe^{II}_{y}(Cu_{0\cdot5-y}Fe_{0\cdot5-y})Fe^{III}_{1+y}]O_4.$$

A value of $4{\cdot}5\,\mu_B$ gives $x=0{\cdot}2$ or $y=0{\cdot}25$. There is no difference in saturation moment whether on the B sites the ions that are enclosed between parentheses are $Cu^{I}+Fe^{III}$ or $Cu^{II}+Fe^{II}$ ions. The reason that more copper ions than correspond to a statistical distribution can occur in tetrahedral sites may be either that they are univalent, and Cu^{I} is known to occur preferably in low coordination (e.g. in twofold coordination in Cu_2O), or that the distribution of the copper ions is altered because of the presence of ferrous ions on octahedral sites.

Despite its simple formula, $Cu_{0\cdot5}Fe_{2\cdot5}O_4$ may well contain three or four different ions. Our reasons for thinking that the ferrous ions, if present, occur on the octahedral sites only will be discussed under 'ternary spinels'. Examples of cases where an ion with a strong preference for B sites changes the usual distribution of the other ions will also be given.

---

† Discussion remark 1957, *Proc. Instn elect. Engrs* B, **104**, Suppl. 5, 228.

2.5. *Ternary Spinels*

Spinels containing three different metal ions may often conveniently be considered to be solid solutions between two binary spinels. This does not mean, however, that these binary spinels exist in the pure state. For instance, the spinel Ni_2TiO_4 does not exist, but solid solutions with nickel ferrite, $a\,Ni_2TiO_4.(1-a)NiFe_2O_4$, or $Ni^{II}_{1+a}Fe^{III}_{2-2a}Ti^{IV}_{a}O_4$, may be prepared up to $a=0{\cdot}5$ (Gorter 1954 a). Similarly $Li_{0\cdot5}Cr_{2\cdot5}O_4$ does not exist, but lithium ferrite–chromite solid solutions, viz. $Li_{0\cdot5}Fe^{III}_{2\cdot5-a}Cr^{III}_{a}O_4$, have been prepared up to $a=2{\cdot}0$ (Gorter 1954 a). For ternary spinels we shall see that it is not permissible to assume that a solid solution will have a cation distribution that is an average of those of the end-members. In one of the first series to be investigated by X-rays, i.e. between (normal) Zn ferrite $Zn[Fe_2]O_4$ and (roughly inverse) copper ferrite $Fe[CuFe]O_4$ (Verwey and Heilmann 1947) it happened to be that Zn remains in A sites and Cu (almost completely) in B sites throughout the series.

We saw that the cell edge of a spinel generally depends on the cation distribution. Thus, in ferrites, e.g. a complete (hypothetical) inversion from normal to inverse would involve an increase in cell edge of roughly 0·06 Å. Therefore, a deviation from the average cation distribution is detected, not only by a deviation of the intensity ratio, e.g. I_{331}/I_{311} *vs.* composition, but also by a deviation from Vegard's law. The former method of detection is much more sensitive than the latter.

Guillaud and Sage (1950), for a series of nickel zinc ferrites $Ni_{1-a}Zn_aFe_2O_4$, find a linear Vegard behaviour for the cell edge, but a fairly strong deviation from the calculated values for the ratio I_{220}/I_{400}. This probably means that a small proportion of the zinc ions occupied octahedral sites. Romeijn (1953), in the series nickel–zinc aluminates $Ni_{1-a}Zn_aAl_2O_4$, finds a small positive deviation from Vegard's law, but a curve with a minimum of about zero for the intensity ratio I_{331}/I_{311}. In the system $Co_{1-a}Zn_aAl_2O_4$, however, both quantities vary linearly with composition. An intensity analysis showed that $CoAl_2O_4$ is normal like $ZnAl_2O_4$, but that $NiAl_2O_4$ has a distribution $Ni_{0\cdot25}Al_{0\cdot75}[Ni_{0\cdot75}Al_{1\cdot25}]O_4$. Apparently the amount of aluminium in A sites does not change linearly with a for the Ni compounds. For the system nickel–ferrite–chromite $NiFe_{2-a}Cr_aO_4$ the cell edges only are given by Romeijn. For $a=0, \frac{1}{4}, \frac{1}{2}, \frac{3}{4}$ and 1 they are 8·337, 8·320, 8·305, 8·310 and 8·328 Å respectively. The fairly deep minimum in the middle is explained by the fact that between inverse nickel–ferrite $Fe[NiFe]O_4$ and normal nickel–chromite $Ni[Cr_2]O_4$ the nickel ions do not move from B to A sites linearly with a, i.e. via a distribution $Fe_{0\cdot5}Ni_{0\cdot5}[Ni_{0\cdot5}Fe_{0\cdot5}Cr]O_4$ for $a=\frac{1}{2}$, but via a distribution $Fe[NiCr]O_4$ for this composition. This is in accordance with the rules given by Verwey and Heilmann on the cation distribution and is due to the specific preferences of Ni^{2+} and Cr^{3+} ions for B sites. The saturation moment for Romeijn's sample $FeNiCrO_4$ was measured (Gorter, unpublished results) and a value of

$0{\cdot}6\,\mu_B$ was found, whereas for the arrangement $Fe[NiCr]O_4$ a value $0{\cdot}3\,\mu_B$ is calculated: this indicates that the distribution is only slightly different from that given.

One generally has to be very careful, however, in deducing the cation distribution from the saturation moment for one single composition, as the following example will show.

In the course of an investigation (Gorter 1954 a) with the object of obtaining spinels showing the anomalous saturation magnetization *vs* temperature curves predicted by Néel (1948), we prepared a series of solid solutions $NiFe_2O_4$–$Ni_{1{\cdot}5}FeTi_{0{\cdot}5}O_4$, mentioned above. It was expected that Ni^{2+} and Ti^{4+} ions would occupy octahedral sites, i.e. that $Ni_{1{\cdot}5}FeTi_{0{\cdot}5}O_4$ would have the distribution $Fe[Ni_{1{\cdot}5}Ti_{0{\cdot}5}]O_4$, thus giving an excess moment on the A sites of $1{\cdot}55\,\mu_B$. The experimental value was $1{\cdot}45\,\mu_B$, which seems an excellent agreement. The values for the intermediate compositions, however, which for this assumption should pass through zero, had a minimum at $1{\cdot}24\,\mu_B$. Evidence that the 'excellent agreement' was only pure coincidence was obtained by three different methods: a theoretical calculation of Curie temperatures by Niessen, a measurement of the effective g factor by microwave resonance† and neutron diffraction patterns kindly made by C. G. Shull for $a=0$, $0{\cdot}3$ and $0{\cdot}5$. There cannot be any doubt that the distribution for $a=0{\cdot}5$ is $Fe_{0{\cdot}7}Ti_{0{\cdot}3}[Ni_{1{\cdot}5}Fe_{0{\cdot}3}Ti_{0{\cdot}2}]O_4$, for which a moment of $1{\cdot}45\,\mu_B$ with excess moment on the B sites is calculated.

For ternary spinels Smart has extended Néel's treatment by introducing two Boltzmann expressions each with a different interchange energy (Smart 1954). The behaviour of the spinel $FeNi_{1{\cdot}5}Ti_{0{\cdot}5}O_4$ can be understood by assuming that the nickel ions do not take part in the equilibrium and remain in the B sites, e.g. by assuming that the interchange energy $Ni_{(B)}$–$Fe_{(A)}$ is very large. The cation distribution, given above, obtained for a slowly cooled preparation, has almost statistical distribution of the Fe^{3+} and Ti^{4+} ions among those sites not occupied by Ni^{2+}. It was surprising, therefore, to find that quenching from 1200°c gave a distribution with less Ti^{4+} on A sites, i.e. farther away from the statistical distribution. This seems to indicate that the Fe–Ti distribution is not only determined by the entropy term, but also by the energy term, in this case an ordering energy in the tetrahedral position.

Gradual replacement in $FeNi_{1{\cdot}5}Ti_{0{\cdot}5}O_4$ of Ni^{2+} by Mn^{2+} or Zn^{2+} leads to a gradual migration of Ti to the B sites, as is deduced from saturation magnetization measurements (Gorter 1954 a).

The cation distribution in the series $Fe[Li_{0{\cdot}5}Fe_{1{\cdot}5}]O_4$–$Fe_{0{\cdot}5}Li_{0{\cdot}5}[Cr_2]O_4$ or $Li_{0{\cdot}5}Fe_{2{\cdot}5-a}Cr_aO_4$, also obtained from magnetic saturation measurements, could for the Li^+ ions be checked by accurate x-ray diffraction measurements (by P. B. Braun). A composition $a=1{\cdot}5$ does not have the distribution $Fe[Li_{0\cdot5}Cr_{1\cdot5}]O_4$, but $Fe_{0\cdot8}Li_{0\cdot2}[Li_{0\cdot3}Fe_{0\cdot2}Cr_{1\cdot5}]O_4$. This series differs from the NiFeTi spinel series in that here three-quarters of the lithium moves from B to A sites in the narrow composition range between $a=1\cdot25$ and $a=1\cdot7$. The explanation, suggested by Braun, is that here at both endpoints ordering energy can be gained in only one of the lattice sites ; this is clear from the LiFe distributions and the superstructures found by Braun in these compositions, i.e. a 1 : 3 order in the B sites in $Fe[Li_{0\cdot5}Fe_{1\cdot5}]O_4$ (Braun 1952) and a 1 : 1 order in the A sites in $Fe_{0\cdot5}Li_{0\cdot5}[Cr_2]O_4$ (Gorter 1954 a). The above-mentioned sudden migration of Li^+ ions leads to an anomaly in the lattice constant as a function of a, and also to an anomaly in the Curie temperature *vs.* a curve, which has a minimum at $a=1\cdot5$ and a maximum at $a=1\cdot7$ (Gorter 1954 a).

---

† The use of this method (Gorter 1954 a, b, Smart 1954) is restricted to ferrimagnetics containing Ni^{2+} ions, and perhaps Co^{2+} ions.

In the system $Fe[NiFe]O_4$–$Ni_{0\cdot25}Al_{0\cdot75}[Ni_{0\cdot75}Al_{1\cdot25}]O_4$, investigated both by Maxwell's group at the U.S. Naval Ordnance Laboratory and by ourselves (Maxwell and Pickart 1953, McGuire 1954, Smart 1954, Gorter 1954 a) the interchange energy $Ni_{(B)}$–$Fe_{(A)}$ is large, but not infinite, indicating that Ni^{2+} and Al^{3+} are fairly evenly matched partners in their fight for the B sites.

As regards cation distribution the ferrous ion will play a unique rôle in materials containing Fe^{3+} ions because the interchange of Fe^{3+} and Fe^{2+} between A and B sites involves only the transfer of an electron, so that the activation energy of the diffusion will be small. This means that the freezing-in effect at higher temperatures will not occur for Fe^{2+} ions, but that a room temperature equilibrium is obtained. Since there is no reason for assuming that the interchange energy $Fe^{2+}_{(B)}/Fe^{3+}_{(A)}$ is exceptionally small, it may well be that the ferrous ions during cooling from higher temperatures exert a certain influence on the distribution of the other ions, like that of Ni^{2+} on the distribution of Fe^{3+} and Ti^{4+} ions. For a discussion of the saturation moments in the system $Fe^{II}Fe^{III}_{2-a}Al_aO_4$, investigated by Guillaud and Michel (1951) for $a=0$–$0\cdot2$, see Gorter (1954 a).

2.5.1. *Saturation magnetization vs temperature curves*

It follows from Néel's theory (1948) that when in a solid-solution series the difference between the B and A sub-lattice magnetization at 0°K passes through zero, all Néel's anomalous saturation magnetization *vs.* temperature curves must be found for different compositions. Only one condition must be fulfilled, viz. that no triangular spin configuration occur. In the latter case no anomalous saturation magnetization *vs.* temperature curves must be expected at all ; such a behaviour has been found in the series $MnFe_2O_4$–$MnCr_2O_4$ (Gorter 1954 a). If the cation distribution in all systems investigated by the author, mentioned above, would have followed the Verwey–Heilmann rules, the difference of the sub-lattice magnetizations at 0°K would have passed through zero in all of them. In the systems $Ni_{1\cdot5-a}Mn_aFeTi_{0\cdot5}O_4$ and $Li_{0\cdot5}Fe_{2\cdot5-a}Cr_aO_4$ the difference of the sub-lattice magnetizations does approach zero but does not pass through this value. As a result only one anomalous type of curve occurs in each system, a P type in the former system and the N type, for which a reversal of the spontaneous magnetization with temperature takes place, in the latter system. In the system $NiFe_{2-a}Al_aO_4$ the difference of the sub-lattice magnetizations at 0°K does pass through zero and here all anomalous curves† are indeed found. The presence of some of the Al^{3+} ions in A sites moves the composition for which the saturation moment is zero from $a=0{\cdot}45$ to $a=0{\cdot}62$. For samples quenched from 1350°C, however, the magnetization of the B sub-lattice remains the larger one, also for $a>0{\cdot}62$. For such materials a long anneal below the Curie temperature may cause a reversal of the remanent magnetization. The implications of such a behaviour for rock magnetism are discussed by Néel (1956) and by Verhoogen (1956), and we shall not discuss them again.

The author wishes to draw attention to a very anomalous saturation magnetization *vs.* temperature curve found (Lotgering 1956) for ferrimagnetic $Fe_{0{\cdot}90}S$, i.e. for a composition slightly different from that of natural pyrrhotite ($Fe_{0{\cdot}875}S$). The saturation magnetization at 200°C drops to a very low value, increases sharply before it drops at the Curie point. The remanent magnetization does not reverse. The phenomenon is due to a mechanism completely different from those discussed above.

2.5.2. *Miscibility gaps*

A few words will be said on the difficulty of finding out whether a synthetic solid solution is stable at a certain temperature or not. When heating to a certain temperature yields two spinels, there is no proof that a solid solution between the two is not stable at that temperature. For instance, when the author first tried to prepare a series of solid solutions $Li_{0{\cdot}5}Fe_{2{\cdot}5-a}Al_aO_4$‡, at 1150°C two spinels were obtained. It may be that the single mixed-crystal phase is stable but is not obtained because of a great difference in reactivity of Fe_2O_3 and Al_2O_3 with Li_2CO_3. For the sake of illustration only, we give a purely speculative reaction mechanism which yields two spinels :

$$Li_2CO_3+(5-a')Fe_2O_3 \rightarrow (4-a')Li_{0{\cdot}5}Fe_{2{\cdot}5}O_4+a'/2LiFeO_2+CO_2 \quad (a'=a/2),$$
$$a'/2LiFeO_2+a'Al_2O_3 \rightarrow a'Li_{0{\cdot}5}Fe_{0{\cdot}5}Al_2O_4.$$

When it was later found that heating to a much higher temperature in this case is possible without fear for loss of lithium, a single spinel phase was obtained which did not separate into two spinels on prolonged heating at lower temperatures. This does not prove, however, that the one-phase spinel is stable, for example at 1100°c, since the annealing will effect a separation only at a sufficiently high temperature, so that diffusion is not too slow, but of course not at a temperature still in the one-phase region. For $a=1{\cdot}0$ a separation into two spinels was finally found after annealing at 1100°c for 48 hours and at 500°c for 72 hours (Gorter, unpublished results). In order to show that a solid solution is stable at a certain temperature, it is at least necessary to show that it can be formed at or below that temperature without having been heated to a higher temperature; the existence of a two-phase region is only demonstrated when it has been shown that at a higher temperature a one-phase region exists which separates into two phases at the given temperature. There is no need to tell mineralogists how much help a microscope can be to differentiate between exsolved and incompletely reacted products.

---

† The N-type curve is found only for the remanent magnetization but not for the saturation magnetization as a result of an inhomogeneity of the cation distribution (Gorter 1954 a), cf. p. 344.

‡ A magnetic investigation of this system has just been reported by A. E. Carter *et al.* (1957).

Let us try to recapitulate our findings by some speculations on the system Fe_3O_4–Fe_2TiO_4, on which very few data are known. The low-temperature miscibility gap seems to be well established by microscopic study of minerals (Nicholls 1956). The interpretation of the data obtained by Pouillard (1950) on impure preparations depends on the assumption that Vegard's law holds: we have seen that this will probably only occur if in both lattice sites the occupation is intermediate between those of the two end members of the series. Assuming ferrous titanate to be completely inverse, such a distribution is represented by a formula $\mathrm{Fe}^{\mathrm{III}}_{1-a}\mathrm{Fe}^{\mathrm{II}}_{a}[\mathrm{Fe}^{\mathrm{II}}\mathrm{Fe}^{\mathrm{III}}_{1-a}\mathrm{Ti}^{\mathrm{IV}}_{a}]\mathrm{O}_4\langle 1\rangle$. This distribution, for which a saturation moment of $4-4a$ is calculated, is suggested by Akimoto (1955). We have given reasons why we must expect that a distribution with ferrous ions in B sites is more likely, i.e. $\mathrm{Fe}^{\mathrm{III}}[\mathrm{Fe}^{\mathrm{II}}_{1+a}\mathrm{Fe}^{\mathrm{III}}_{1-2a}\mathrm{Ti}^{\mathrm{IV}}_{a}]\mathrm{O}_4\langle 2\rangle$ for which the saturation moment is $4-6a$. A distribution with some Ti^{4+} ions in A sites, $\mathrm{Fe}^{\mathrm{III}}_{1-x}\mathrm{Ti}^{\mathrm{IV}}_{x}[\mathrm{Fe}^{\mathrm{II}}_{1+a}\mathrm{Fe}^{\mathrm{III}}_{1-2a+x}\mathrm{Ti}^{\mathrm{IV}}_{a-x}]\mathrm{O}_4\langle 3\rangle$, with a saturation moment $4-6a+10x$, cannot be ruled out.

For $a>0{\cdot}5$ the second formula changes into $\mathrm{Fe}^{\mathrm{III}}_{2-2a}\mathrm{Fe}^{\mathrm{II}}_{2a-1}[\mathrm{Fe}^{\mathrm{II}}_{2\cdot 0-a}\mathrm{Ti}^{\mathrm{IV}}_{a}]\mathrm{O}_4$ and formula $\langle 3\rangle$ correspondingly. There is not much sense, however, in calculating saturation moments for higher a values, because then certainly triangular spin configurations will occur.

§ 3. Magnetic Structure and Crystal Structure

We shall now turn our attention to the origin of the negative exchange interactions, postulated by Néel.

Unlike in metals, the interaction in ionic compounds is not direct, but indirect via the adjoining anions. A theory of this so-called super-exchange, first proposed by Kramers in 1934, was given by Anderson (1950). The result of Anderson's calculation is that for Fe^{3+}, or other ions with five or more 3d electrons, the two metal ions will have anti-parallel spins; for Cr^{3+} ions, or other ions with less than five 3d electrons the two metal ions will have parallel spins. A second important result of Anderson's theory is that the super-exchange interaction is strongest

for a collinear configuration Me–O–Me, decreasing for an intermediate, and weakest for a right-angle configuration
$$\begin{array}{ll}\text{Me–O} \\ \quad\;\; | \\ \quad\; \text{Me}\end{array}$$

Since a certain overlap of electron densities of the 3d and 2p orbits is necessary, the super-exchange interaction must decrease with increasing distance Me–O.

When the crystal structure, i.e. all distances and angles, is known, it is often possible to predict for an ionic compound the *relative* orientation of the magnetic ions, using the above data on sign, angles Me–O–Me and distances Me–O. Since a quantitative theory of the dependence of the strength of the super-exchange interaction on angle and distance is lacking, it is only possible to make a comparison between two configurations Me–p–O–q–Me when either the angle or the distances p and q are approximately equal. Other things have to be taken into account: the number of times a certain configuration Me–O–Me occurs, the type of ion (Fe^{3+}, Ni^{2+}, Mn^{2+}, etc.) that takes part in the interaction etc. For a fuller discussion see Gorter (1957).

Such predictions can be checked by neutron diffraction: for antiferromagnetics by this means only, and for ferrimagnetics also by saturation magnetization measurements near 0°K.

3.1. *The Spinel Structure*

In the case of structures with an only slightly distorted close-packed oxygen lattice like that occurring in the spinel structure, the problem of assigning spin directions is fairly simple, because the distances Me–O fall into two distinct groups, those of nearest neighbours Me_A–$O=q$ and Me_B–$O=p$, and much larger ones, Me_A–$O=r$ and Me_B–$O=s$ and t (Gorter 1954 a, § 1.1). For Fe_3O_4, $p=2{\cdot}03$ Å, $q=1{\cdot}88$ Å, $r=3{\cdot}46$ Å, $s=4{\cdot}10$ Å, $t=4{\cdot}15$ Å.

In spinels the strongest interaction must therefore be the A–O–B interaction with distances p and q and an angle of about 125°. The strongest A–A interaction, with distances q and r and an angle of about 80°, should be very weak. The strongest BB interactions, with distances p and p and an angle of about 93·5° (or others, involving one larger distance but with a very large angle) will be weak, but stronger than the AA interaction. This result is that postulated by Néel before Anderson's theory was known. The magnetic structure, indicated by arrows in fig. 3, resulting from a dominant negative AB interaction, indicated by thick lines in fig. 3, has been confirmed by neutron diffraction for several ferrites (Shull *et al.* 1951 b, Hastings and Corliss 1953, Corliss *et al.* 1953).

For antiferromagnetic $KFe_{11}O_{17}$ (Went *et al.* 1952, Gorter 1954 a) the magnetic structure is equally easily found from the crystal structure. For some other compounds, e.g. the compound $BaFe_{12}O_{19}$, the main constituent of the permanent-magnet material Magnadur or Ferroxdure (Went *et al.* 1952), and for the recently described new ferrimagnetic oxides with applications for very high frequencies (Jonker *et al.* 1956) e.g. $Ba_2Zn_2Fe_{12}O_{22}$, with crystal structures (Braun 1957) related to that of $BaFe_{12}O_{19}$, there is a choice between two magnetic structures (Gorter 1957) between which a choice can be made, e.g. by saturation magnetization measurements.

3.2. *Magnetic Structures in the Corund (Hematite) Structure*

Hematite, αFe_2O_3, is antiferromagnetic (Néel 1949) with a very small parasitic saturation moment of about 0·01 μ_B per formula unit (Pauthenet 1957). Chromic oxide Cr_2O_3 is also antiferromagnetic (Foëx and Graff 1939, Volger 1952, McGuire *et al.* 1956), and exhibits no parasitic ferromagnetism. The parasitic ferrimagnetism of αFe_2O_3, which is nowadays thought to be due to the magnetization of domain walls (Néel 1954, Yin-Yuan Li 1956 a) will not be discussed. The magnetic structures, i.e. the spin orientations, below the Néel temperatures have been determined by Shull *et al.* (1951 a) for α-Fe_2O_3 and by Brockhouse (1953) for Cr_2O_3.

Fig. 4

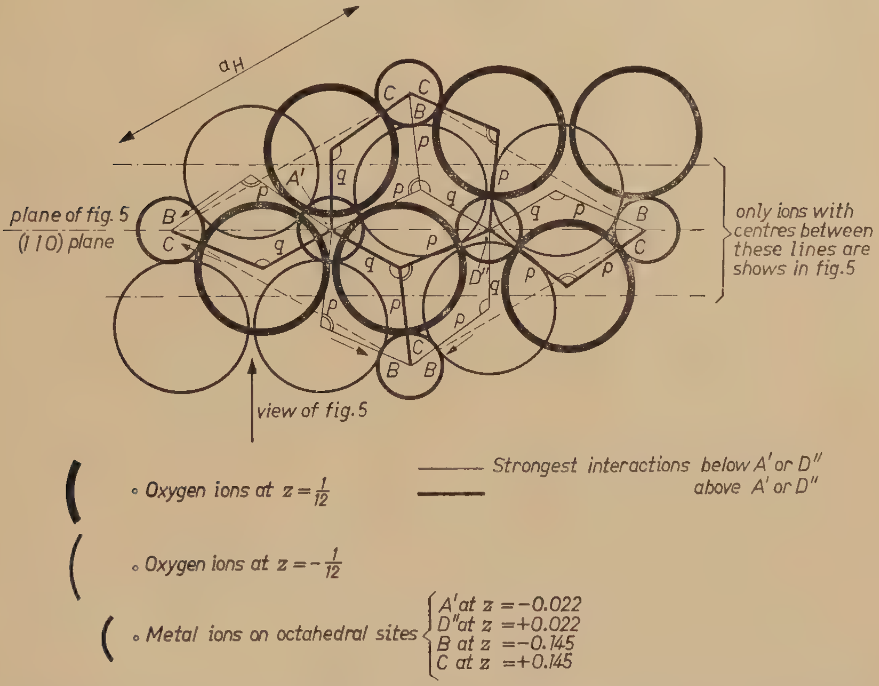

This figure shows the hematite structure in the hexagonal representation, in the plane $z=0$. The broken lines show the edges of the unit cell. Each metal ion has three neighbouring oxygen ions at a distance p in a plane below it and three at a distance q in a plane above it or vice versa, in a distorted octahedron.

The magnetic structure of hematite is easily explained from the distances and angles occurring in the structure (Pauling and Hendricks 1925), which is depicted in figs. 4 and 5. The two nearest-neighbour

Fig. 5

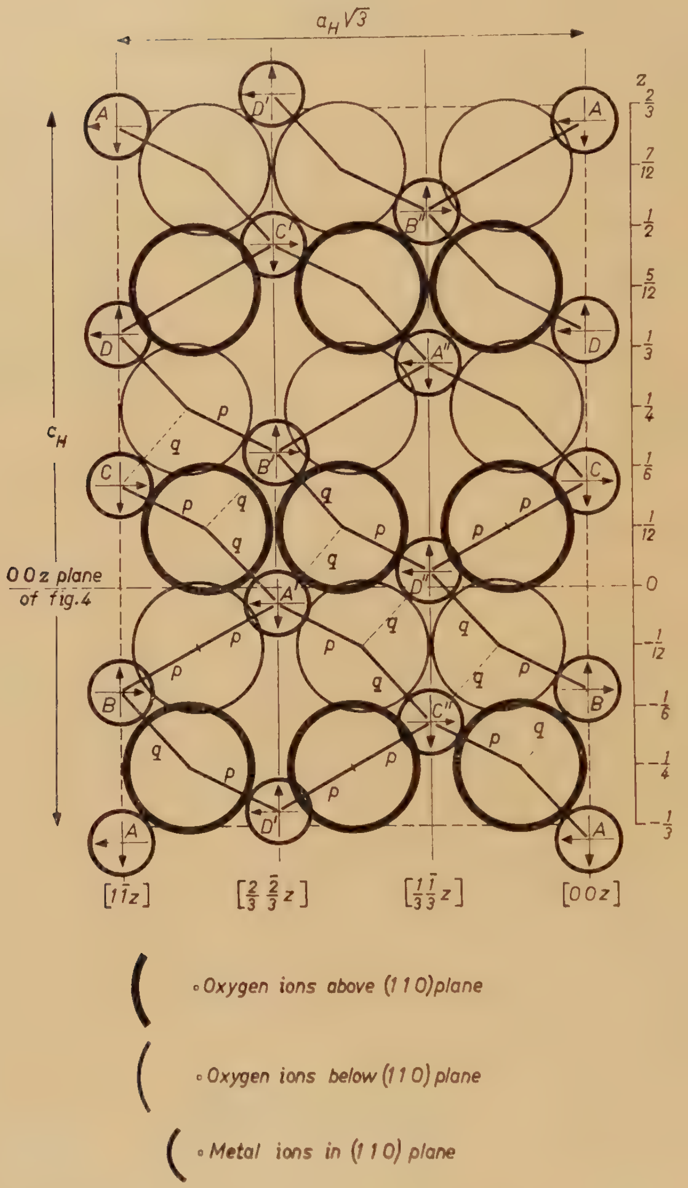

This figure shows the hematite structure in the hexagonal representation, in a (110) plane, perpendicular to that of fig. 4. Horizontal arrows indicate relative spin directions for αFe_2O_3, $(\overset{\uparrow}{A}\overset{\downarrow}{B}\overset{\downarrow}{C}\overset{\uparrow}{D})$; vertical arrows spin directions for Cr_2O_3 $(\overset{\downarrow}{A}\overset{\uparrow}{B}\overset{\downarrow}{C}\overset{\uparrow}{D})$.

distances Fe^{3+}–O^{2-} are indicated by p and q (in α-Fe_2O_3, $p=1{\cdot}97$, $q=2{\cdot}07$), the next-nearest distances, like in the spinel structure, are much larger. Disregarding all interactions involving these large distances, there remain for example for ferric ion A′, the following interactions, the projections of which in the (110) plane are indicated by thick lines in fig. 5.

Configuration	Angle
A′–p–O–p–B	∼117°
A′–q–O–p–C	∼133°
A′–p–O–q–C″	
A′–q–O–p–D″	∼94°
A′–q O -q–B′	∼88°

The strongest interaction will be the first two, which have the largest angles ; keeping in mind that the metal ions lie on crystallographic triad axes (see fig. 4), the magnetic structure of α-Fe_2O_3, indicated by horizontal arrows in fig. 5, can be completely understood from these two, negative, interactions only (Yin-Yuan Li 1956 b, Iida 1956).†

The magnetic structure of Cr_2O_3, indicated by vertical arrows in fig. 5, cannot be understood without assuming the A′–q–O–p–C (and A′–p–O–q–C″ etc.) interaction to be positive, as Yin-Yuan Li points out, and the A–p–O–p–B (etc.) interaction negative. According to Anderson's theory all interactions in Cr_2O_3 should be expected to be positive, making it a ferromagnetic, like for example the oxides with perovskite structure $La^{III}_{1-a}Me^{II}_{a}(Mn^{III}_{1-a}Mn^{IV}_{a})O_3$ for Me=Ba, Sr or Ca and for certain values of a (Jonker and van Santen 1950), and CrO_2 with rutile structure (Guillaud *et al.* 1944). In most other cases, however, ionic compounds of transition metals with less than five 3d electrons have been found to be antiferromagnetic, i.e. to contain negative interactions. The question why the A′–q–O–p- C interaction should be positive and the interaction A′–p–O–p–B negative is a very interesting one. It has been pointed out by Anderson and Hasegawa (1955) that the contribution of another term to the superexchange interaction, which was neglected in Anderson's original treatment, may make an important contribution. Both authors (see Iida 1956, Yin-Yuan Li 1956) mention that in the A′–q–O–p–C interaction the Anderson term may dominate over the Anderson–Hasegawa term. Iida (1956) states specifically that this should be attributed to the inequality of the distances in this case. If the positive sign of the A′–q–O–p–C interaction were due to the occurrence of a larger distance Me–O, (q), by analogy with the well-known Slater curve for direct interactions in metals, then an interaction with two equal distances q would give a positive interaction ; according to Iida, however, a negative interaction.

---

† Yin-Yuan Li (1956b) omitted the interaction A′–p–O–p–B and therefore had to take into account the interaction A′–q–O–p–D″ ; the error is corrected by Iida (1956).

In the Cr_2O_3 structure, the A′–q–O–q–B′ interaction is 'drowned' whatever its sign ; if a structure is available in which such an interaction Cr^{3+}–Cr^{3+} with two large distances like q, but with a larger angle, occurs, then the sign of such an interaction can be determined. (See under pseudobrookite structure.)

The case of ilmenite, $FeTiO_3$, is much more complicated. The crystal structure (Barth and Posnjak 1934) has been given as an ordered hematite structure, in which the AD′, A′D″ and A″D layers (fig. 5) are occupied Fe^{2+}, and the C″B, CB′ and C″B″ layers are Ti^{4+}.

We have seen in § 2.3 that for $MgFe_2O_4$ originally an ordered, i.e. inverse, structure was deduced from x-ray diffraction data, whereas more accurate methods showed it to be only about 90% inverse. We therefore have to reckon with the possibility that the order between the Fe^{2+} and Ti^{4+} ions is not complete, because x-ray diffraction cannot exactly determine the distribution of Fe and Ti ions among two lattice sites in a complicated structure.

If the ordering is assumed to be complete, a weak antiferromagnetic order inside the AD′ layers resulting from A–O–D″ (etc.) interactions could be present ; coupling between the Fe^{2+} layers could exist only if the interaction A′–O–A″ is not negligible (or A′–O–D, or both, in which latter case triangular spin configurations might result).

If the ordering is not complete, coupling between the Fe^{2+} layers might take place via Fe^{2+} ions in the Ti^{4+} layers. The experimental data are scanty : Chevallier (1953) measured the paramagnetic susceptibility of a synthetic $FeTiO_3$, prepared at 950°c, between 20° and -196°c, and found it obeys a Curie–Weiss law $1/\chi=C/T-\theta$ with $\theta=+23°$ and $C=0{\cdot}0260$ from which a correct calculation yields a paramagnetic moment per (gram) ion Fe^{2+} : $p_B=5{\cdot}61\,\mu_B$.† This is outside the range of values usually found ($5{\cdot}22$–$5{\cdot}53\,\mu_B$) for Fe^{2+}, and according to Yin-Yuan Li is proof that part of the Fe ions are Fe^{3+} and an equal part of the Ti ions are Ti^{3+}. Hamos and Stscherbina (1933) obtained a formula $Fe^{2+}Ti^{4+}O_3$ from the fine structure of x-ray absorption edges, but this method probably cannot give more than a qualitative answer. Although we saw in § 2.4 that in certain cases the presence of two metal ions both with two valencies must be assumed, the equilibrium has so far been assumed to be far on one side. Moreover, we see no reason for making assumptions for explaining an antiferromagnetic order which is quoted to exist (Nagata 1953 a, Néel 1956 a) but for which the author has found no evidence in literature so far. Ishikawa and Sawada (1956) prepared samples of $FeTiO_3$, quenched from 1350° and 1250°, and slowly cooled. For the sample quenched from 1350°c measurements between 20°c and 400°c give C and p_B values almost identical to those of Chevallier ; $\theta=+17$. The other samples gave lower C and p_B values ; the authors suggest that despite the use of a vacuum furnace this is due to slight reoxidation, and must not be interpreted therefore as indicating a different Fe^{2+}–Ti^{4+}

---

† Chevallier gives 5·49, Yin-Yuan Li (1956 b) corrects it to 5·65 μ_B.

distribution among the layers. Susceptibility measurements on a natural single crystal of ilmenite by Bizette and Tsaï (1956) from 20°C down to helium temperature show a very sharp peak at 68°K for the susceptibility parallel to the c-axis ($\chi_{\parallel}$) and a low peak for $\chi_{\perp}$. The authors explain this behaviour by assuming an antiferromagnetic Néel temperature at 68°K. In order to explain that $\chi_{\parallel}$ does not point to zero near 0°K and $\chi_{\perp}$ does not remain constant below 68° they assume that the composition is slightly non-stoiochiometric. The main objection against an assumption of ordinary antiferromagnetism, i.e. the fact that again θ is positive,† is left unexplained. This is certainly not a normal behaviour for an antiferromagnetic, nor is the great height of the $\chi_{\parallel}$ peak at 68°K. A satisfactory explanation for such a behaviour has not so far been given.

In the solid solution series $(1-a)\mathrm{Fe_2O_3}.a\mathrm{FeTiO_3}$ ferrimagnetic properties have been found on the ilmenite side of the miscibility gap, i.e. for $a > 0{\cdot}66$ by Chevallier *et al.* (1955) and for quenched samples for $a > 0{\cdot}55$ by Nagata *et al.* (1953 a, b), Akimoto (1954, 1955) and Nagata and Akimoto (1956). The explanation of these properties given by Nagata and Akimoto (1956), i.e. that the $\mathrm{Fe^{2+}}$–$\mathrm{Ti^{4+}}$-order is of the same type as in $\mathrm{FeTiO_3}$, and that this order begins to develop for $a > 0{\cdot}55$, seems very likely. The saturation magnetization for a nearing 1·0 will decrease also at 0°K, because the BC lattices are almost occupied by Ti ions, and AD′ type interactions, although weak, will then cause triangular spin arrangements to occur because they are larger in number than the D′–B–A′ interactions.

3.3. *The Pseudobrookite Structure*

We feel tempted to make some speculations about the magnetic structure of pseudobrookite $\mathrm{Fe_2^{III}Ti^{IV}O_5}$, not so far investigated experimentally. The pseudobrookite structure (Pauling 1930) is shown in fig. 6. The ions indicated by thick and by thin circles lie in alternate planes lying at a distance $c/2$, indicated on the right. The ferric ions lie in very distorted oxygen octahedra, the Ti ions in another type of distorted oxygen octahedra.

For the same reasons as given for $\mathrm{FeTiO_3}$ complete ordering of $\mathrm{Fe^{3+}}$ and $\mathrm{Ti^{4+}}$ ions must not be assumed to be finally proved. Assuming, however, that the $\mathrm{Fe^{3+}}$–$\mathrm{Ti^{4+}}$ order is complete then three different configurations with different angles and distances should be considered :

A′–p–O–p–A angle ~100°
A–p–O–q–B angle ~ 95°
B–q–O–q–C angle ~110°

with distances $p = 1{\cdot}95 = \pm 0{\cdot}03$ and $q = 2{\cdot}31$ Å. None of the interactions will be so strong as those that determined the magnetic structure in for example $\mathrm{Fe_3O_4}$ and α-$\mathrm{Fe_2O_3}$; also the number of magnetic ions per formula unit, as well as the density (4·4) are lower, so that the

---

† $\theta = +45 \pm 5°$ (from $\chi_{\parallel}$) and $+20 \pm 5°$ (from $\chi_{\perp}$), obtained by graphical extrapolation of $1/\chi$ *vs.* T by the author.

Néel temperature should be low on these counts only. All three interactions, also the weakest, are needed to form a three-dimensional magnetic lattice. The A′–p–O–p–A interaction will be the strongest; the A–p–O–q–B interaction involves one distance of 2·3 Å, and it is not known whether such interactions are negligible or not. Moreover, the angle is only 94°. The B–q–O–q–C interaction involves a more satisfactory angle but two distances of 2·3 Å. If it is assumed that in the absence of other interactions these three will lead to a (non-triangular) magnetic structure, it will be the antiferromagnetic one shown in fig. 6. The

Fig. 6

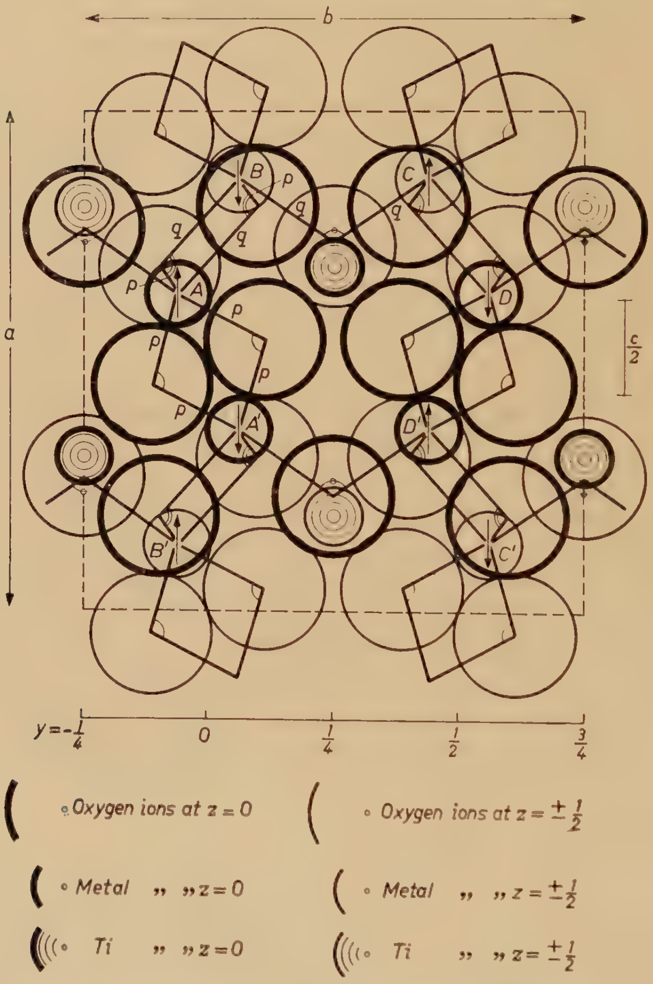

Orthorhombic crystal structure of pseudobrookite (Fe_2TiO_5). (a=9·79; b=9·93; c=3·725 Å). The thin circles lie at equal distances $c/2$ (indicated on the right) above and below the plane of the thick circles, or vice versa.

Néel temperature will be very low indeed for an oxide containing this concentration of Fe^{3+} ions.

It is interesting to note that if the distance of 2·3 Å is not too large for the formation of a magnetic structure, then a pseudobrookite with composition Cr_2TiO_5 would have another magnetic structure, and this will be different for either positive or negative B–q–O–q–C interaction, i.e.

spin interaction	A′	p–O–p	A	p–O–q	B	q–O–q	C	p–O–q	D
Fe_2TiO_5	↓	−	↑	−	↓	−	↑	−	↓
Cr_2TiO_5	↓	−	↑	+	↑	+	↑	+	↑
or	↓	−	↑	+	↑	−	↓	−	↑

Since the A′–p–O–p–A′ interactions are negative for all three cases, A′ is antiparallel to A, B′ to B, etc., and the ions A, B, C and D suffice for characterizing the antiferromagnetic structures. Thus, a low-temperature neutron diffraction investigation on such a substance might be useful for checking Iida's suggestion (see § 3.2).

§ 4. Exchange Coupling Between Two Phases

Reversal of remanent magnetization through the occurrence of type N spinels, or through the occurrence of spinels that have dominant B sub-lattice magnetization when quenched but dominant A sub-lattice magnetization after annealing, has not been encountered in nature so far (Néel 1956).

The well-known reverse thermo-remanent magnetization shown by materials consisting of two phases predicted by Néel (1951) and found by Nagata (1953 b) has in the case of the Haruna rock been shown to be due to ' echelons ' of sheets of spinel (cpt 460°c) exsolved in a matrix material of ferro-ilmenite (cpt 230°c). Similar sheets have been found on cooling spinel ferrites containing an excess of Fe_2O_3. Here the sheets of Fe_2O_3, in a matrix of spinel ferrite, are parallel not as a result of cooling in the earth's field as might have been suggested, but because the crystal orientations of the matrix spinel and exsolved α-Fe_2O_3 phases are related. It is seen from figs. 4 and 2 (a) that α-Fe_2O_3 and spinel have an oxygen layer in common, when one of the figures is turned over 30°.

a_{Hex} for hematite corresponds to $(\sqrt{3}/2)a_{\mathrm{Hex}} \equiv (\sqrt{6}/4)a_{\mathrm{cubic}}$ for magnetite.

In such a case super-exchange interaction may be active across the phase boundary. Meiklejohn and Bean (1956) have found a novel kind of magnetic anisotropy, which is not only uniaxial but also unidirectional, in hexagonal cobalt particles superficially oxidized to cubic antiferromagnetic CoO and cooled in a magnetic field from the Néel point of CoO (293°K) to 77°K; this anisotropy results in an asymmetrically displaced hysteresis loop. In the course of an investigation (Wijn *et al.* 1957) on rectangular hysteresis loops obtained in cobalt-ferrous ferrites after a magnetic annealing treatment Wijn observed similar although less drastically displaced hysteresis loops. This occurred in those field-cooled samples that showed a lower Fe^{2+} content than corresponds to the stoiochiometric formula $Co^{II}_{1-a}Fe^{II}_{a}Fe^{III}_{2}O_4$, and microscopic investigation showed an exsolution of α-Fe_2O_3 (unpublished results).

The explanation given by Meiklejohn and Bean, viz. that the magnetization of the Co phase is fixed by exchange coupling with the antiferromagnetic CoO which latter has a much larger anisotropy field, is, *mutatis mutandis*, also applicable in the case of the spinel–hematite material. In hematite the anisotropy field is known to be very large (Anderson *et al.* 1954). It may be important to take into account that such effects may occur in nature.

References

Akimoto, S., 1954, *J. Geomagn. Geoelect., Kyoto*, **6,** 1 ; 1955, *Jap. J. Geophys.*, **1,** 1 ; 1957, *Advanc. Phys.*, April.

Akimoto, S., Nagata, T., and Katsura, T., 1957, *Nature, Lond.*, **179,** 37.

Anderson, P. W., 1950, *Phys. Rev.*, **79,** 350.

Anderson, P. W., and Hasegawa, H., unpublished, quoted by Nagamiya, T., Yosida, K., and Kubo, R., 1955, *Advanc. Phys.*, **4,** 64.

Anderson, P. W., Merritt, F. R., Remeika, J. P., and Yager, W. A., 1954, *Phys. Rev.*, **93,** 717.

Barth, T. W. F., and Posnjak, E., 1932, *Z. Kristallogr.*, **82,** 325 ; 1934, *Ibid.*, **88,** 265.

Bertaut, F., 1951, *J. Phys. Radium*, **12,** 252.

Bertaut, F., and Delorme, C., 1953, *C.R. Acad. Sci., Paris*, **236,** 74.

Bizette, H., and Tsaï, B., 1956, *C.R. Acad. Sci., Paris*, **242,** 2124.

Braun, P. B., 1952, *Nature, Lond.*, **170,** 1123 ; 1957, *Philips Res. Rep.*, **12**.

Brockhouse, B. N., 1953, *J. chem. Phys.*, **21,** 961.

Carter, A. E., Miles, P. A., and Welch, A. J. E., 1957, *Proc. Instn Elect. Engrs*, **104B,** Suppl. 5, 141.

Chevallier, R., 1953, *Bull. Soc. chim. Fr.*, **20,** 973.

Chevallier, R., Bolfa, J., and Mathieu, S., 1955, *Bull. Soc. Franc. Minér.*, **78,** 365.

Corliss, L. M., and Hastings, J. M., 1956, *Phys. Rev.*, **104,** 328.

Corliss, L. M., Hastings, J. M., and Brockman, F. G., 1953, *Phys. Rev.*, **90,** 1013.

David, I., and Welch, A. J. E., 1956, *Trans. Faraday Soc.*, **52,** 1642.

de Boer, J. H., and Verwey, E. J. W., 1937, *Proc. phys. Soc.* A, **49,** 59.

de Boer, F., van Santen, J. H., and Verwey, E. J. W., 1950, *J. chem. Phys.*, **18,** 1032.

Foëx, J., and Graff, M., 1939, *C.R. Acad. Sci., Paris*, **209,** 160.

Goodenough, J. B., and Loeb, A. L., 1955, *Phys. Rev.*, **98,** 391.

Gorter, E. W., 1950, *Nature, Lond.*, **165,** 798 ; 1954 a, *Philips Res. Rep.*, **9,** 295, 321, 403 ; 1954 b, *Nature, Lond.*, **173,** 123 ; 1957, *Proc. Instn Elect. Engrs*, **104B,** Suppl. 5, 255.

Guillaud, C., 1951, *J. Phys. Radium*, **12,** 239.

Guillaud, C., and Michel, A., 1951, *J. Phys. Radium*, **12,** 65.

Guillaud, C., and Sage, M., 1950, *C.R. Acad. Sci. Paris*, **230,** 1749.

Guillaud, C., Michel, A., Bénard, J., and Fallot, M., 1944, *C.R. Acad. Sci., Paris*, **219,** 58.

HAMOS, L. v., and STSCHERBINA, X., 1933, *Nachr. Ges. Wiss. Gött., Math. physik. Kl.*, Fachgruppen 232.

HARRISON, F. W., OSMOND, W. P., TEALE, R. W., 1957, *Phys. Rev.* (in the press).

HASTINGS, J. M., and CORLISS, L. M., 1953, *Rev. mod. Phys.*, **25,** 114.

IIDA, S., 1956, *J. phys. Soc. Japan*, **12,** 1300.

ISHIKAWA, Y., and SAWADA, S., 1956, *J. phys. Soc. Japan*, **11,** 496.

JONKER, G. H., 1957, *Proceedings of the Third International Conference on the Reactivity of Solids*, Madrid.

JONKER, G. H., and VAN SANTEN, J. H., 1950, *Physica*, **16,** 337.

JONKER, G. H., WIJN, H. P. J., and BRAUN, P. B., 1956, *Philips tech. Rev.*, **18,** 145 ; 1957, *Proc. Instn Elect. Engrs*, **104B,** Suppl. 5, 249.

KORDES, E., and RÖTTIG, E., 1951, *Z. anorg. Chem.*, **264,** 34.

LI, YIN-YUAN, 1956 a, *Phys. Rev.*, **101,** 1450 ; 1956 b, *Ibid.*, **102,** 1015.

LOTGERING, F. K., 1956, *Philips Res. Rep.*, **11,** 190, fig. 7.

MCGUIRE, T. R., 1954, *Phys. Rev.*, **93,** 682.

MCGUIRE, T. R., SCOTT, E. J., and GRANNIS, F. H., 1956, *Phys. Rev.*, **102,** 1000.

MAXWELL, L. R., and PICKART, S. J., 1953, *Phys. Rev.*, **92,** 1120.

MEIKLEJOHN, W. H., and BEAN, C. P., 1956, *Phys. Rev.*, **102,** 1413,

NAGATA, T., 1953 a, *Rock Magnetism* (Tokyo : Maruzen Co., Ltd.) ; 1953 b, *Nature, Lond.*, **172,** 850.

NAGATA, T., and AKIMOTO, S., 1956, *Geofisica Pura e Applicata, Milano*, **34,** 36.

NAGATA, T., AKIMOTO, S., and UYEDA, S., 1953 a, *J. Geomagn. Geoelect., Kyoto*, **5,** 168 ; 1953 b, *Nature, Lond.*, **172,** 630.

NATHANS, R., PICKART, S. J., HARRISON, S. E., and KRIESMAN, C. J., 1957, *Proc. Instn Elect. Engrs*, **104B,** Suppl. 5, 217.

NÉEL, L., 1948, *Ann. Phys., Paris*, **3,** 137 ; 1949, *Ibid.*, **4,** 249 ; 1950, *C.R. Acad. Sci., Paris*, **230,** 190 ; 1951, *Ann. Geophys.*, **7,** 90 ; 1954, *Institut International de Physique Solvay*, 10*me Conseil de Physique*, p. 251 ; 1956, *Advanc. Phys.*, **4,** 191.

NICHOLLS, G. D., 1956, *Advanc. Phys.*, **4,** 113.

PAULING, L., 1930, *Z. Kristallogr.*, **73,** 97.

PAULING, L., and HENDRICKS, S. B., 1925, *J. Amer. chem. Soc.*, **47,** 781.

PAUTHENET, R., 1957, *Thèse*, Université de Grenoble.

PAUTHENET, R., and BOCHIROL, L., 1951, *J. Phys. Radium*, **12,** 249.

POUILLARD, E., 1950, *Ann. Chim.* (12), **5,** 190.

ROBIN, J., 1952, *C.R. Acad. Sci., Paris*, **235,** 1301.

ROMEIJN, F. C., 1953, *Philips Res. Rep.*, **8,** 304.

SCHMITZ-DUMONT, O., 1957, *Proceedings of the Third International Conference on the Reactivity of Solids*, Madrid.

SHULL, C. G., STRAUSER, W. A., and WOLLAN, E. O., 1951 a, *Phys. Rev.*, **83,** 333.

SHULL, C. G., WOLLAN, E. O., and KOEHLER, W. C., 1951 b, *Phys. Rev.*, **84,** 912.

SMART, J. S., 1954, *Phys. Rev.*, **94,** 847.

STARKE, K., 1939, *Z. phys. Chem.*, **42B,** 159.

VERHOOGEN, J., 1956, *J. geophys. Research*, **61,** 201.

VERWEY, E. J. W., 1954, *Proceedings of the Second International Symposium on the Reactivity of Solids*, Gothenborg, p. 242.

VERWEY, E. J. W., and HEILMANN, E. L., 1947, *J. chem. Phys.*, **15,** 174.

VERWEY, E. J. W., DE BOER, F., and VAN SANTEN, J. H., 1948, *J. chem. Phys.*, **16,** 1091.

VOLGER, J., 1952, *Nature, Lond.*, **170,** 1027.

WENT, J. J., RATHENAU, G. W., GORTER, E. W., and VAN OOSTERHOUT, G. W., 1952, *Philips tech. Rev.*, **13,** 194.

WIJN, H. P. J., VAN DER HEIDE, H., and FAST, J. F., 1957, *Proc. Instn Elect. Engrs*, **104B,** Suppl. 7.

YAFET, Y., and KITTEL, C., 1952, *Phys. Rev.*, **87,** 290.

The Role of Magnetostriction in Rock Magnetism

By John W. Graham
Carnegie Institution of Washington, Department of Terrestrial Magnetism
Washington 15, D.C.

In an earlier publication (Graham 1956) the facts and reasoning which prompted the author to emphasize at the London Conference (November, 1956) the importance of magnetostriction in rock magnetism were discussed. These include :

(*a*) 3000 lb axial compression on 1 in. cylindrical samples can cause a significant change in the natural remanent moment.

(*b*) Grossly scattered directions of magnetization of certain weathered rocks can be interpreted as being caused by residual stresses, resulting from weathering, acting on magnetostrictive material.

(*c*) The scatter of magnetization directions of cobbles in a particular conglomerate cannot be explained solely on the basis of partial stability ; it was necessary to postulate additional conditions as parts of the explanation of the scatter : i.e. non-hydrostatic stresses acting on magnetostrictive material.

(*d*) The regionally consistent magnetizations of some unmetamorphosed Paleozoic sediments cannot be explained satisfactorily by any of the currently popular methods of rock magnetism. It seems to the author that a satisfactory explanation may be found in the interaction of the stress history of the rocks and their magnetostrictive properties.

The interesting possibility that certain igneous rocks may acquire magnetization directions not parallel to the magnetic field applied during their formation also was discussed at the London Conference. Such a situation may occur readily in any type of rock when magnetization and stressing (or unstressing) take place at different times. As a brief example of the ideas discussed the argument may be applied to the problem of the magnetization mechanism of red beds. It is known that many were magnetized after deposition and that hematite is the mineral responsible for the magnetic moment. It is generally assumed (and the mechanism can be demonstrated in the laboratory) that the initial magnetization direction is parallel to the magnetic field applied during the deposition of the hematite, but it is not certain that this is the only step in the magnetization process. It is possible that the following may take place : the original sediments are deposited and subsequently buried by many thousands of feet of other sediments. Hematite is then deposited in the pore spaces and becomes 'permanently' magnetized in the direction of the prevailing earth's magnetic field. While at depth, the bulk sample is in static equilibrium, but owing to the strength of the sediments, it is not in hydrostatic equilibrium. Thus, on becoming exposed at the surface by erosion, the sample experiences an unloading and upward elongation. To the hematite which was deposited under hydrostatic equilibrium in the pore spaces at depth, this appears like a tension, and its magnetic moment is subject to change by magnetostriction at the time of unloading. Hence, the final measured direction of magnetization may have no simple relationship to the magnetic field applied during the deposition of the hematite. A regionally consistent bias of the magnetization directions could result from the fact that the unloading everywhere is primarily upwards. The magnitude of the effect should be subject to the mineralogic constitution of the sediments because elastic constants depend on composition.

It is obvious, if magnetostriction figures prominently in establishing magnetization directions, that serious error can result from using many rock magnetism data as the basis for conclusions about polar wandering, continental drift, and the extent of secular variation in the geologic past.

REFERENCE

GRAHAM, J. W., 1956, *J. Geophys. Res.*, **61**, 735.

Fig. 2

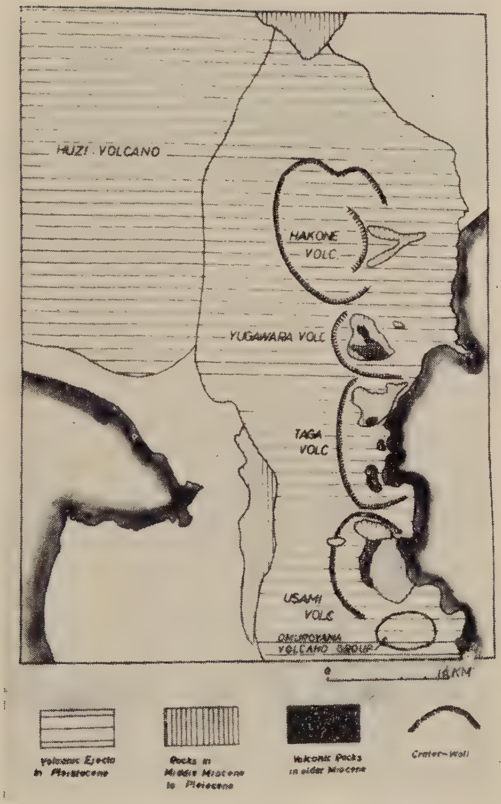
HUZI VOLCANO
HAKONE VOLC.
YUGAWARA VOLC
TAGA VOLC
USAMI VOLC
OMUROYAMA VOLCANO GROUP
0
10 KM
Volcanic Ejecta in Pleistocene
Rocks in Middle Miocene to Pleiocene
Volcanic Rocks in older Miocene
Crater-Wall

Geological map (simplified) of the *North-Izu and Hakone* volcanic region.

Plate 1

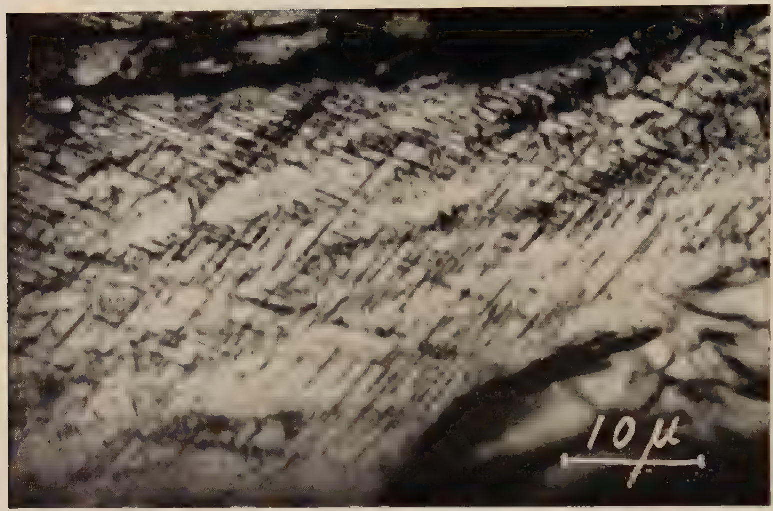

Haruna sample heat treated at 700°c for 10 minutes in an open air tube.

Plate 2

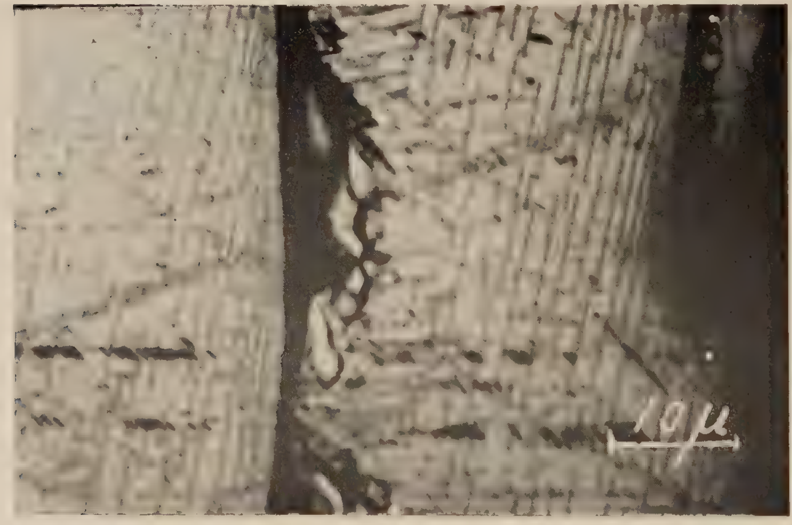

Sokota sample heat treated at 700°c for 10 minutes in an open-air tube.

Photomicrographs of the polished surfaces of the ferromagnetic samples concerned with the Haruna-type RTRM. The surfaces have been etched with HF for 1 minute.

Plate 3

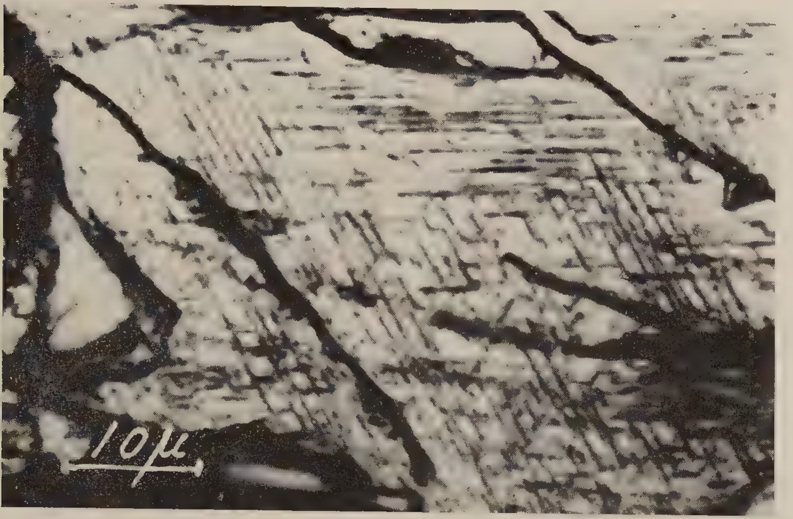

Himesima sample heat treated at 660°c for 10 minutes in an open-air tube.

Plate 4

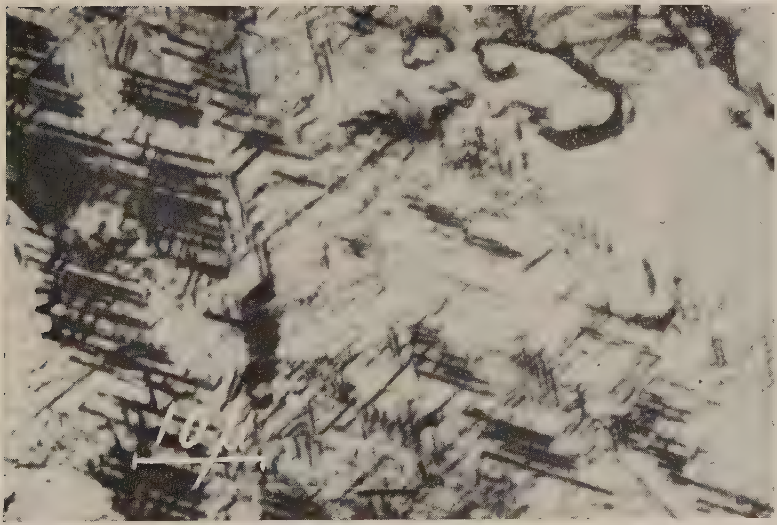

Gokurakuzi (1) sample heat treated at 650°c for 10 minutes in an open-air tube.

Photomicrographs of the polished surfaces of the ferromagnetic samples concerned with the Haruna-type RTRM. The surfaces have been etched with HF for 1 minute.

Plate 5

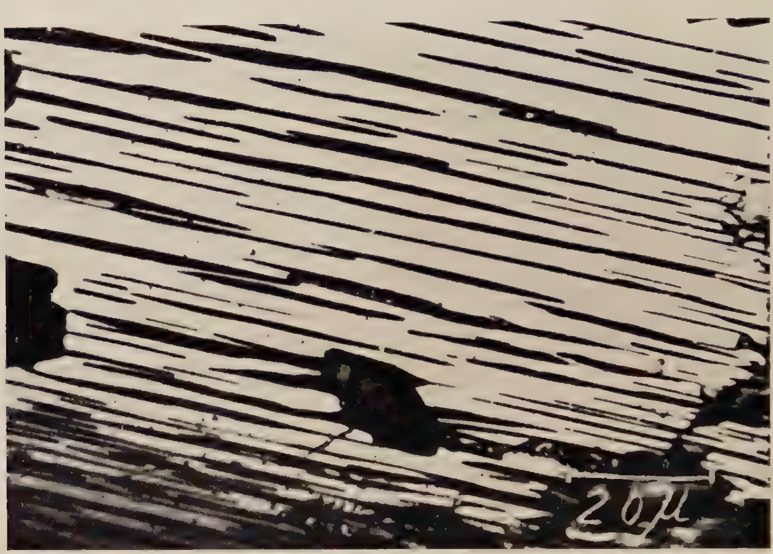

Photomicrograph of the polished surface of Gokurakuzi (1) heat treated in an evacuated sealed tube at 1200°c for 10 minutes. The surface has been etched with HF for 5 seconds and the black stripes are the Ti–Mt phase. This sample shows RTRM (see fig. 2 (d_1).

Plate 6

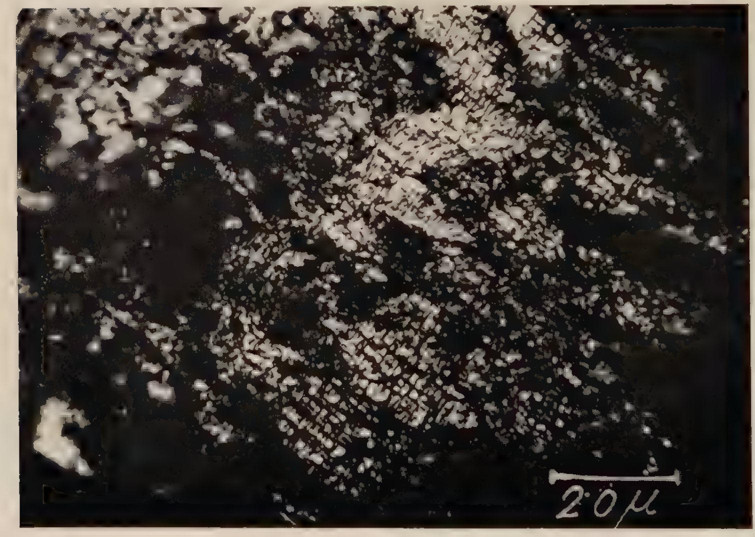

Minakami sample heat treated in an open-air tube at 620°c for 10 minutes. The black etched stripes are the titan–hematite.

Photomicrographs of the polished surfaces of the samples concerned with the intensification of the normal TRM due to heat treatment. The surfaces have been etched with HF for 5 seconds.

Plate 7

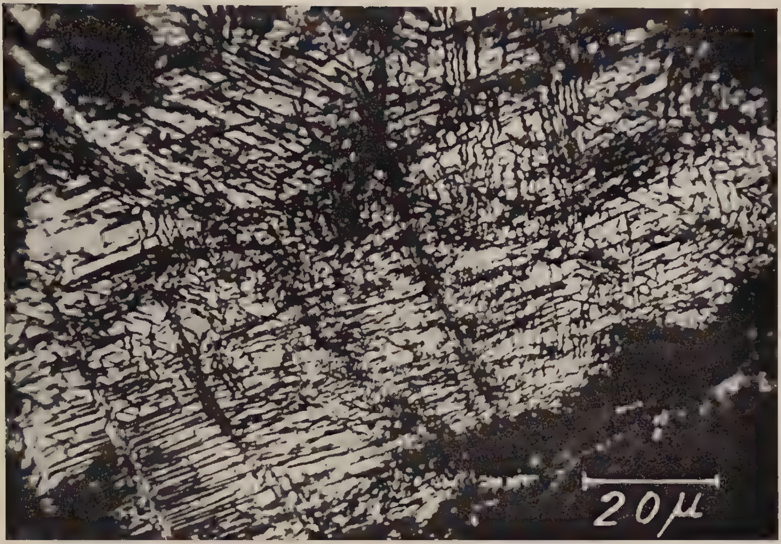

The ore-ilmenite sample heat treated in an open-air tube at 850°c for 10 minutes. The black etched stripes are the titan–hematite.

Plate 8

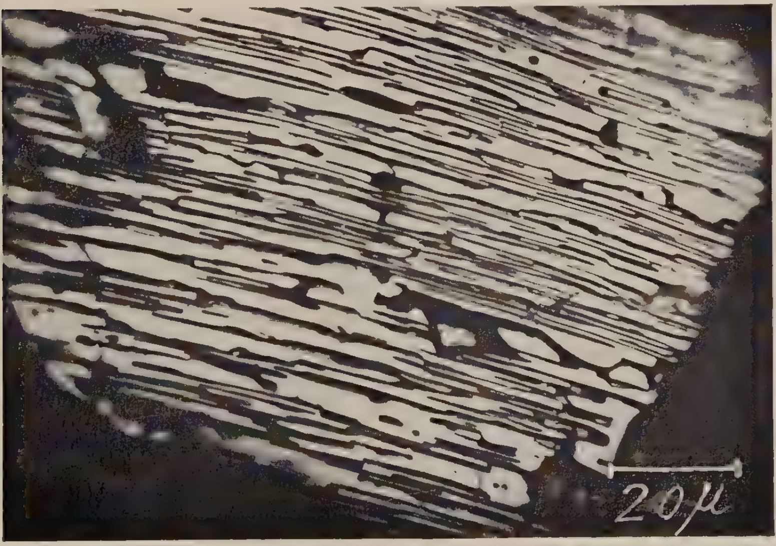

Minakami sample heat treated in an evacuated sealed tube at 1200°c for 10 minutes. The black etched stripes are the Ti–Mt.

Photomicrographs of the polished surfaces of the samples concerned with the intensification of the normal TRM due to heat treatment. The surfaces have been etched with HF for 5 seconds.

Plate 9

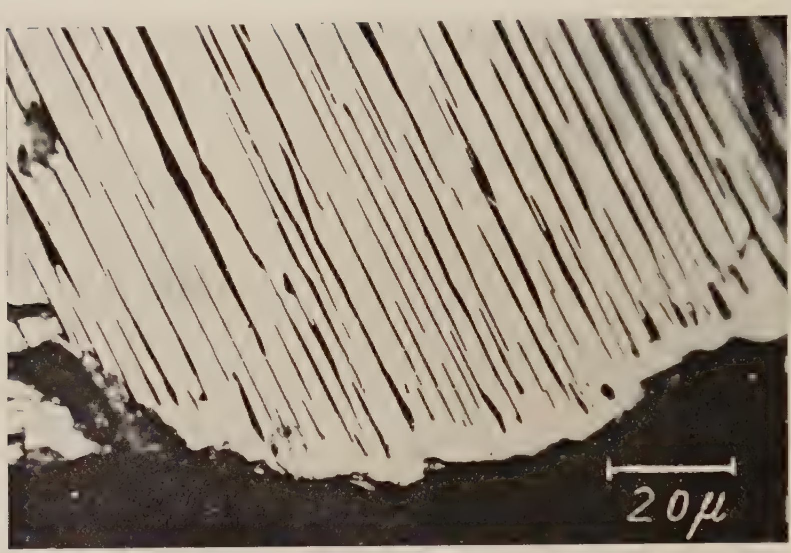

The ore-ilmenite sample heat treated in an evacuated sealed tube at 1200°c for 10 minutes. The black etched stripes are the Ti–Mt.

Photomicrographs of the polished surfaces of the samples concerned with the intensification of the normal TRM due to heat treatment. The surfaces have been etched with HF for 5 seconds.

Plate 10

Original sample.

Photomicrographs of the polished surfaces of the Niisima Ti–Mt sample. The surfaces have been etched with HF for 6 seconds.

Plate 11

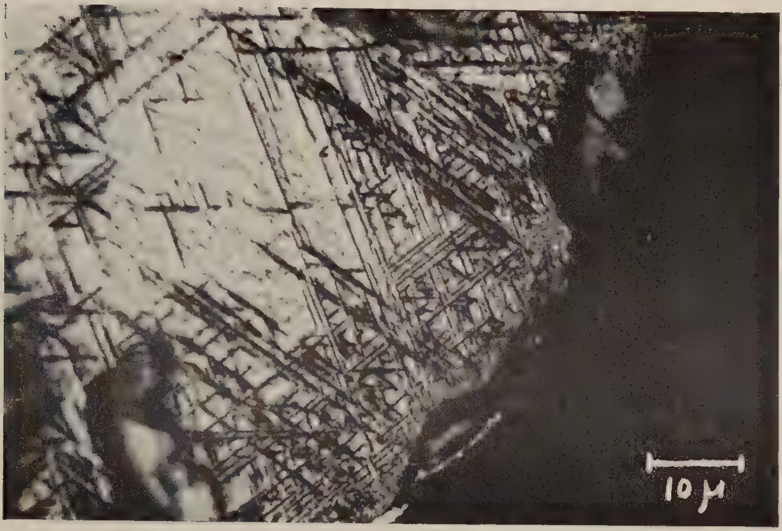

After heat treated at 550°c for 10 hours. The lamellae are the *H*-constituent.

Plate 12

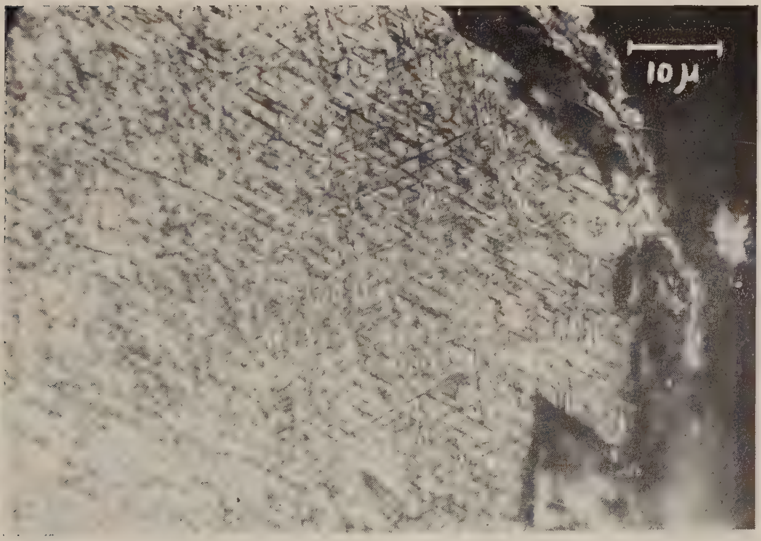

After heat treated at 550°c for 23 hours. The *H*-constituent is well developed.

Photomicrographs of the polished surfaces of the Niisima Ti–Mt sample.
The surfaces have been etched with HF for 6 seconds.

Fig. 1

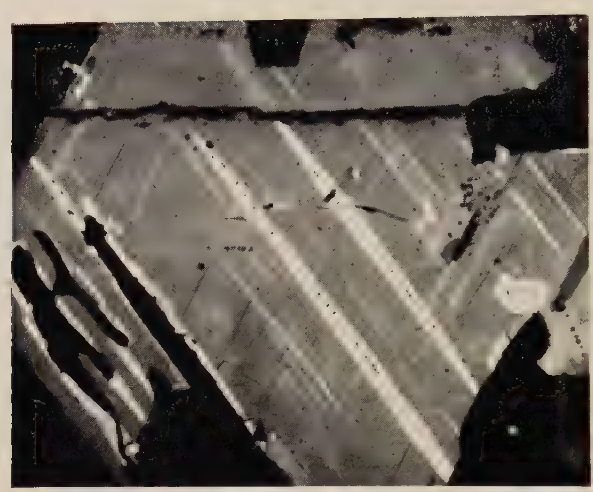

(*Photomicrograph by J. Gee, Esq.*)

×200. Crossed polars at 5°.

Basaltic lava, India.

Main part of field is titaniferous magnetite (med. grey) containing exsolution ilmenite lamellae in octahedral (111) planes. The anisotropism of the ilmenite shows in the photomicrograph as white (NW–SE), medium grey (E–W), and dark grey (NE–SW). There are also occasional thin titaniferous hematite lamellae also in the (111) planes. Small spinel crystallites (black) are present in the ilmenite lamellae. Traces of maghemite (pale grey) along minute curving cracks and ilmenite magnetite boundaries are formed by secondary alteration. Note corrosion of the outline of the magnetite crystal, especially along (111) directions, by the ferromagnesian constituents of the basalt.

Fig. 2

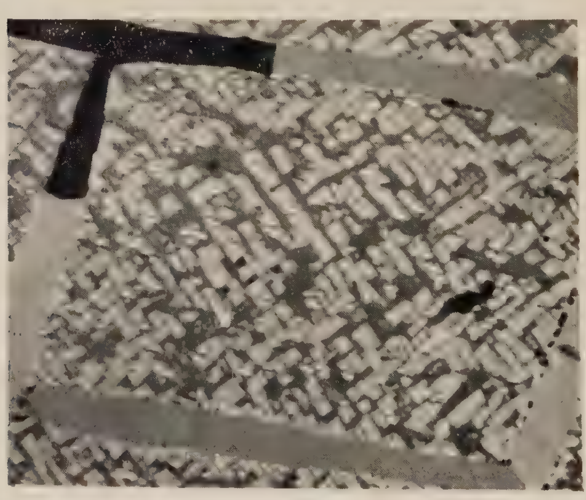

(*Photomicrograph by Miss P. Martin.*)

×1800, from ×1200 negative. Oil immersion with green filter. Carbon arc, polarized light.

Lac de la Blache, Saguenay Co., Quebec, Canada.

Characteristic ‘ petit-point ’ pattern of exsolution ulvospinel (med. grey) in titaniferous magnetite (pale grey). Note also long exsolution lamellae of ilmenite (pale grey) and spinel (black), both in octahedral planes in the magnetite.

Fig. 3

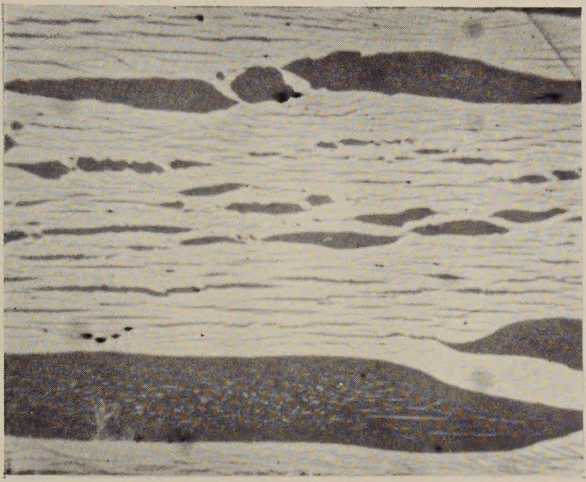

(*Photomicrograph by J. Gee, Esq.*)

×435. Oil immersion, tungsten light.

Metamorphosed basic igneous rock, Betty Hill, Scotland.

Exsolution bodies of ferriferous ilmenite (dark grey) in the (0001) basal plane directions of host titaniferous hematite (white). Note the seriate distribution of the exsolved ilmenite showing the impoverishment of the solid solution adjacent to the largest ilmenite bodies. A second generation of titaniferous hematite is also seen as exsolution spindles within the ilmenite.

Fig. 4

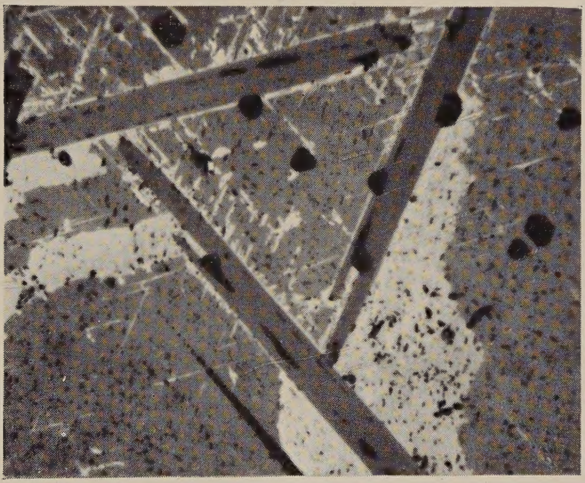

(*Photomicrograph by J. Gee, Esq.*)

×435. Oil immersion, tungsten light.

Metamorphosed peridotite, Co. Donegal, Ireland.

Secondary alteration of titaniferous magnetite (med. grey) to maghemite (white) along boundaries of exsolved ilmenite lamellae (dark grey), and along octahedral (111) partings. Note that exsolution of ilmenite followed after that of spinel (black).

Annals of Science

A QUARTERLY REVIEW OF THE HISTORY OF SCIENCE SINCE THE RENAISSANCE

EDITORS
D. McKIE, D.Sc., Ph.D.,
University College, London.
HARCOURT BROWN, M.A., Ph.D.,
Brown University, Providence, R.I., U.S.A.
H. W. ROBINSON,
Former Librarian,
Royal Society of London.
N. H. de V. HEATHCOTE, B.Sc., Ph.D.,
University College, London.

ANNUAL SUBSCRIPTION
£3 3s. 0d.
OR
18s. 0d.
PER PART
POST FREE

ALERE FLAMMAM

ALERE FLAMMAM

THE MATHEMATICAL WORKS OF JOHN WALLIS, D.D., F.R.S.

by

J. F. SCOTT, Ph.D., B.A.

"His work will be indispensable to those interested in the early history of The Royal Society. I commend to all students of the Seventeenth Century, whether scientific or humane, this learned and lucid book."—Extract from foreword by Prof. E. N. da C. Andrade, D.Sc., Ph.D., F.R.S.

Recommended for publication by University of London

12/6 net

Printed and Published by

TAYLOR & FRANCIS, LTD.
RED LION COURT, FLEET STREET, LONDON, E.C.4.

~~SEP 3 0 1957~~

Early Scientific Publications

ALERE FLAMMAM

DIARY OF ROBERT HOOKE, M.A., M.D., F.R.S.
1672-1680

25/-
net

Edited by **H. W. ROBINSON** and **W. ADAMS**
Recommended for publication by the Royal Society, London

"This vivid record of the scientific, artistic and social activities of a remarkable man during remarkable years has too long remained in obscurity."—Extract from foreword by Sir Frederick Gowland Hopkins, O.M., President of the Royal Society.

MATHEMATICAL WORK OF JOHN WALLIS, D.D., F.R.S.

12/6
net

By **J. F. SCOTT, Ph.D., B.A.**

"His work will be indispensable to those interested in the early history of The Royal Society. I commend to all students of the Seventeenth Century, whether scientific or humane, this learned and lucid book."—Extract from foreword by Prof. E. N. da C. Andrade, D.Sc., Ph.D., F.R.S.
Recommended for publication by University of London

CORRESPONDENCE AND PAPERS OF EDMOND HALLEY

21/-
net

Arranged and Edited by **EUGENE FAIRFIELD MACPIKE**

First published on behalf of The History of Science Society by Oxford University Press. Now re-issued by Taylor & Francis, Ltd.

MEMOIRS OF SIR ISAAC NEWTON'S LIFE

5/-
net

By **WILLIAM STUKELEY, M.D., F.R.S., 1752**
From an Original Manuscript
Now in the possession of the Royal Society, London

HEVELIUS, FLAMSTEED AND HALLEY

12/6
net

Three Contemporary Astronomers and their Mutual Relations
By **EUGENE FAIRFIELD MACPIKE**
Published by arrangement with The History of Science Society

Established over 150 years

TAYLOR & FRANCIS, LTD.
RED LION COURT, FLEET ST., LONDON E.C.
PRINTERS & PUBLISHERS OF SCIENTIFIC BOOKS